5-1997

Cenozoic Tectonic and Paleogeographic Evolution of the Horse Prairie Half-Graben, Southwest Montana

Colby J. VanDenburg
Utah State University

CENOZOIC TECTONIC AND PALEOGEOGRAPHIC EVOLUTION OF THE HORSE PRAIRIE HALF-GRABEN, SOUTHWEST MONTANA

by

Colby J. VanDenburg

A thesis submitted in partial fulfillment
of the requirements for the degree

of

MASTER OF SCIENCE

in

Geology

UTAH STATE UNIVERSITY
Logan, Utah

1997

ABSTRACT

Cenozoic Tectonic and Paleogeographic Evolution of the Horse Prairie Half-Graben, Southwest Montana

by

Colby J. VanDenburg, Master of Science

Utah State University, 1997

Major Professor: Dr. Susanne U. Janecke
Department: Geology

The Horse Prairie basin (HPB) of southwestern Montana is a complex, east-dipping half-graben that contains three angular unconformity-bounded sequences of Tertiary lacustrine, paludal, and fluvial sediments overlying middle Eocene volcanic rocks. The basin is near the eastern edge of the Cordilleran thrust belt, and represents the western half of a larger Paleogene rift basin. Geologic mapping within the Everson Creek and Bannock Pass 7.5 minute quadrangles indicates that five temporally and geometrically distinct episodes of extension characterize the late Mesozoic (?) to Cenozoic tectonic evolution of the upper HPB.

The first episode of extension occurred prior to emplacement of middle Eocene volcanic rocks on an enigmatic, low-angle, southeast-dipping fault. Pre-volcanic extension (?) may reflect gravitational collapse of the Sevier thrust belt beginning in the late Mesozoic. The second episode of extension occurred in middle Eocene time on northwest-dipping syn-volcanic normal faults. Syn-volcanic faults can be attributed to extension of the Challis volcanic arc, and typically accommodate less than 1 km of dip-slip separation. The third generation of normal faulting occurred on the low-angle, south-southwest- and west-dipping Lemhi Pass and Maiden Peak fault systems, respectively. Slip may have

initiated during the waning phases of Challis volcanism, but these late to post-volcanic normal faults probably reflect continued gravitational collapse of the Sevier thrust belt, because they generally parallel contractional structures in the region. Late to post-volcanic normal faults accommodate the bulk of extensional strain in the study area, and are responsible for the deposition and preservation of the majority of basin-fill deposits in the HPB. Two episodes of middle Miocene and younger extension also occur within the study area; however, structural and basin analysis indicates the HPB experienced only minor extension in the last 17 m.y.

Spatial and temporal relationships between magmatism and extension suggest that large magnitude extension in the HPB (episodes 1 and 3) was not associated with magmatism, and that extension in this portion of the Basin and Range province initiated due to gravitational instabilities imparted on the crust during the Sevier orogeny.

(152 pages)

ACKNOWLEDGMENTS

I would like to thank Donald Fiesinger and James Evans for serving as committee members and for providing helpful insights into the project. Anthony Barnosky (University of California, Berkeley, CA), Steve Good (West Chester University, West Chester, PA), Mortimer Hait, Jr. (USGS, retired, Green Valley, AZ), Karen Lund (USGS, Denver, CO), William McIntosh (New Mexico Bureau of Mines and Mineral Resources, Socorro, NM), John M'Gonigle (USGS, retired, Denver, CO), Ralph Nichols (Lazy Three S Ranch, Wise River, MT), Michael Perkins (University of Utah, Salt Lake City, UT), William Perry, Jr. (USGS, Denver, CO), Robert Thomas (Western Montana College, Dillon, MT), and Andrei Sarna-Wojicki (USGS, Menlo Park, CA) graciously shared their unpublished data. I thank the Bar Double T ranch, Roger Peters, Kenny Schira, and Elizabeth Brenner-Youngren, for allowing access to their land and the personnel of the Beaverhead National Forest and the Dillon district of the Bureau of Land Management for generously providing aerial photography of much of the study area. Discussions with Jim Blankenau, Eric Hetherington, Kelly Keighley, Siang-Joo Lim, Karen Lund, John M'Gonigle, Kim Robeson, Steve Schulz, Betty Skipp, and Robert Thomas were very helpful. I thank Elizabeth Blair, Elizabeth Brenner-Youngren, John M'Gonigle, James Sears, and Robert Thomas for their assistance in the field. Last, and certainly not least, I thank Susanne Janecke for her guidance, patience, and support throughout the entire process. This study was partially supported by the Tobacco Root Geological Society student fieldwork scholarship to Colby VanDenburg and by NSF grant EAR 93-17395 to Susanne Janecke.

Colby J. VanDenburg

CONTENTS

LIST OF TABLES

LIST OF FIGURES

LIST OF PLATES
(in pocket)

INTRODUCTION

The Horse Prairie basin is southwest of Dillon, Montana, northeast of the Montana-Idaho border (Fig. 1). The basin lies within the Rocky Mountain Basin and Range Province, north of the Snake River Plain near the eastern edge of the Cordilleran thrust belt. The Beaverhead Mountains border the basin to the west and south, the Maiden Peak spur of the Beaverhead Mountains lies to the east, and the Grasshopper basin borders the area to the northeast. The Medicine Lodge basin is located between the Maiden Peak spur and the Tendoy Range to the east, and is interpreted to be the eastern half of a larger Horse Prairie-Medicine Lodge protobasin that predates formation of the Maiden Peak spur (Flores and M'Gonigle, 1991). This study focuses on using detailed geologic mapping and basin analysis to reconstruct the structural and paleogeographic evolution of the Horse Prairie half-graben. In order to evaluate the significance of the findings herein, a discussion of the general tectonic evolution of the entire Basin and Range Province is required.

EXTENSION IN THE BASIN AND RANGE PROVINCE

The extensional history of the Basin and Range Province is dominated by late Paleogene and Neogene extension (Wernicke, 1992); however, several workers have documented late Cretaceous normal faults coeval with contractile deformation (Hodges and Walker, 1992; Taylor and Bartley, 1992; Applegate and Hodges, 1995; Camilleri and Chamberlain, 1997; Wells, 1997; this study). Extension coeval with contraction is thought to moderate topographic contrasts during lithospheric thickening (Burchfield and Royden, 1985), and may occur in areas that have accommodated significant shortening in the Mesozoic. Hodges and Walker (1992) hypothesized that extension occurred during the development of the Sevier foreland fold and thrust belt throughout the "internal zone"

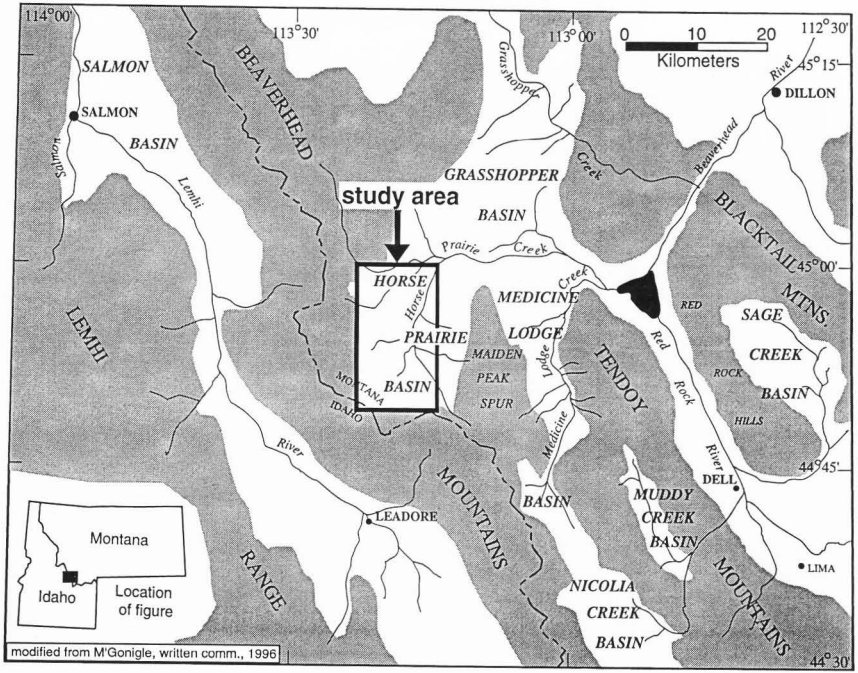

Figure 1. Location of study area. The study area is located within the Everson Creek, Bannock Pass, Lemhi Pass, and Goat Mountain 7.5 minute quadrangles of southwest Montana and east-central Idaho. Shaded areas represent topographic highs.

between the fold and thrust belt and the continental arc. More recent work in the Raft River Mountains, Utah (Wells, 1997), the Pequop Mountains-Wood Hills-East Humbolt Range region, northeast Nevada (Camilleri and Chamberlain, 1997), and in the Funeral Mountains, California (Applegate and Hodges, 1995), appears to confirm the presence of widespread late Cretaceous extension in the Basin and Range Province. Although some of the Basin and Range Province has experience pre-middle Eocene extension, this event was only recently documented in southwestern Montana (Janecke et al., *in review*).

In addition to late Cretaceous extension, most areas in the Basin and Range Province have undergone two major episodes of Cenozoic extension (Wernicke, 1992). The first episode extended from southern Canada to northwestern Mexico, within and west of the foreland fold and thrust belt (Coney and Harms, 1984; Wust, 1986; Constenius, 1996). Extension generally initiated in the Eocene north of the Snake River Plain, and in the Oligocene to early Miocene to the south (Coney and Harms, 1984). This event was characterized by large, shallowly dipping normal faults that locally juxtapose upper crustal rocks against mid-crustal metamorphic tectonites (Wust, 1986; Wernicke, 1992). Paleogene extension was localized and asymmetrical, and was broadly accompanied on a regional scale by intermediate to silicic magmatism and the formation of metamorphic core complexes (Gans et al., 1989; Wernicke, 1992; Axen et al., 1993).

In a study of Tertiary extension and magmatism in the Great Basin, Axen et al. (1993) described two narrow north-trending belts of Eocene to Oligocene extension. The western belt is characterized by west-directed extension similar to that found in the Horse Prairie basin area. Janecke (1994) expanded on the work of Axen et al. (1993) and hypothesized a north- to north-west trending, Eocene to Oligocene rift zone in east-central Idaho, that continues north into western Montana and British Columbia. Janecke (1994) correlated the narrow zone of Eocene to Oligocene extension north of the Snake River Plain to the western rift zone of Axen et al. (1993).

Other workers assert that initial extension in the Rocky Mountain Basin and Range Province was not confined to a narrow rift zone, and that Paleogene extension was more widespread and extended east of the Cordilleran foreland fold and thrust belt into the foreland province (Hanneman, 1989; Constenius, 1996). In a regional synthesis of work conducted from southern Canada to northern Utah, Constenius (1996) hypothesized that collapse of the Cordilleran foreland fold and thrust belt closely followed contractile deformation after a brief hiatus (1-5 m.y.), and that late Paleogene extensional collapse is distinctly different from middle Miocene and younger extension. Whether extension north of the Snake River Plain was widely distributed or confined to a narrow rift zone is controversial (compare Janecke, 1994 and Constenius, 1996), but most workers agree that late Paleogene extension and middle Miocene-Holocene extension represent two distinctly different extensional episodes (Miller, 1990; Wernicke, 1992; Janecke, 1994; Constenius, 1996).

The Miocene was a time of significant tectonic change from southeastern California to southeastern Washington (Davis, 1979). Physiographic, sedimentary, and structural features show that during the past 17 m.y. normal faulting has been active in the Basin and Range Province. In addition, extension in adjacent areas is indicated by Quaternary fault scarps, by numerous dikes and flood basalts of the High Lava Plains and the Columbia River Plateau (Christiansen and Yeats, 1992; Pezzopane and Weldon, 1993), and by relative plate motion studies of the Yellowstone hot spot track (Rodgers et al., 1990).

Three major changes occurred during this episode of middle Miocene-Holocene (Basin and Range) extension: 1) the area of extension widened, 2) extension was distributed more uniformly, and 3) widespread basaltic magmas were emplaced (Wernicke et al., 1987; Miller, 1990). Late Cenozoic extension was in part superimposed

on earlier extension, but also affected new regions, and was generally diachronous (Wernicke, 1992).

The initial phases of "Basin and Range" extension began around 17 Ma, and by 14 Ma extension was distributed across most of the region except the southwestern sector (Wernicke, 1992). In the southern Basin and Range Province, a correlation between late Cenozoic extension and the Pacific-North America transform faults is likely (Atwater, 1970), but the applicability of this correlation to the regions north of the Snake River Plain is not as obvious. Unlike the rest of the Basin and Range Province, the region north of the Snake River Plain contains evidence for two geometrically and temporally distinct episodes of Basin and Range normal faulting (Pierce and Morgan, 1992; Piety et al., 1992; Fritz and Sears, 1993).

Basin and Range extension in the Rocky Mountain Basin and Range is distributed between the Idaho batholith on the west, the Absaroka and Little Belt Mountains, with a basement of Archean crystalline rocks on the east, the Snake River Plain on the south, and the Lewis and Clark Line on the north (Reynolds, 1979). Northern regions within the province form a somewhat diffuse transition zone between major extension to the south, and relative late Cenozoic stability farther north (Christiansen and McKee, 1978). Reynolds (1979) calculated Late Cenozoic extension in the Rocky Mountain Basin and Range Province to be on the order of only 10 to 15 percent. Similarly, Janecke et al. (1991) and Anders et al. (1993a) calculated between 12 and 21 percent, respectively, of Basin and Range extension in east-central Idaho.

REGIONAL GEOLOGIC SETTING

Fields et al. (1985) were the first to synthesize the deformational history and paleogeography of the Cenozoic basins of western Montana and eastern Idaho. They inferred that during middle Eocene to Oligocene time, the early stages of basin development were locally characterized by high subsidence rates and internal drainage.

Beginning in the late-early Miocene, basins were dissected by listric normal faulting, most likely related to back-arc extension (Fields et al., 1985). Fields et al. (1985) also inferred that many of the basin-bounding faults have been active since middle Eocene time. Later studies (Flores and M'Gonigle, 1991; M'Gonigle and Dalrymple, 1993; Fritz and Sears, 1993; Janecke, 1994) question some of the conclusions of Fields et al. (1985) about the tectonic setting and deformational history of this region.

Hait and M'Gonigle (1988) and Flores and M'Gonigle (1991) hypothesized two major episodes of deformation in this region: compressional tectonism associated with the Sevier and Laramide orogenies, followed by late-early Miocene Basin and Range extension. They described the following sequence of events: 1) deposition of Eocene volcanic rocks on an erosional surface cut across a terrane previously deformed by Sevier thrust faults, 2) local uplift and erosion of the volcanic rocks during the latest phases of compression, 3) development of an asymmetrical basin ancestral to the Medicine Lodge and Horse Prairie structural basins, and 4) widespread late-early Miocene uplift and erosion associated with Basin and Range extension along a west-dipping detachment system in the Tendoy Range.

In contrast to single-phase extensional models (Hait and M'Gonigle, 1988; Flores and M'Gonigle, 1991), Janecke (1992) documented three superposed extensional systems for east central Idaho: 1) a 49-48 Ma episode of NW-SE extension, 2) a middle Eocene to Oligocene basin-forming event, and 3) Basin and Range extension. This three-phase extensional model will be shown to more adequately explain the relationships found in the Horse Prairie basin, but further modification is required.

Neogene extension is well documented in southwest Montana; however, the presence and distribution of Paleogene extension remains controversial. Whereas some previous workers have hypothesized that southwest Montana was tectonically quiescent in Eocene to Oligocene time (Thompson et al., 1981; Flores and M'Gonigle, 1991; Fritz

and Sears, 1993), others suggest that southwest Montana was actively extending in the Paleogene (Fields et al., 1985; Hanneman, 1989; Janecke, 1994; Constenius, 1996). Additional controversy exists over whether Paleogene extension was confined to a narrow region (Janecke, 1994) or broadly distributed (Hanneman, 1989; Constenius, 1996).

The location of the Horse Prairie basin is ideal for evaluation of several of these regional tectonic models. Janecke (1994) hypothesized that the Horse Prairie basin is located near the eastern margin of an Eocene to Oligocene rift zone, which is characterized by rapid subsidence, and dominated by coarse-grained basin-fill deposits. Alternatively, some models predict that the sedimentary rocks in the Horse Prairie basin accumulated in the broad Renova basin, which is dominated by fine-grained clastic and volcaniclastic siltstone and sandstone (Thompson et al., 1981; Fields et al., 1985; Fritz and Sears, 1993), and is generally thought to reflect tectonic quiescence in the Paleogene (Thompson et al., 1981). The Horse Prairie basin lies near the transition between these two temporally equivalent, yet tectonically different tectonic settings.

The purpose of this study is to determine the Cenozoic structural and paleogeographic evolution of the Horse Prairie basin in order to test the existing tectonic models for extension north of the Snake River Plain, and to evaluate general models for extension throughout the Basin and Range Province. This study also characterizes the spatial, temporal, and geometric attributes of extension in the Horse Prairie basin in order to place critical constraints on the boundary between extended and unextended terrain in the Paleogene. Seven $^{40}Ar/^{39}Ar$ age determinations and tephra correlation analyses were conducted on eight samples collected from the Challis volcanic rocks and from intercalated tuffs within the sedimentary sequence. These geochronological data, along with detailed geologic mapping and geophysical data (donated by ENSERCH CORP),

were used to determine the deformational history and geometry of Cenozoic extension in the Horse Prairie basin.

In addition, paleocurrent and provenance data were collected within the basin-fill deposits in order to reconstruct the paleogeography of the region throughout the Cenozoic. Once the extensional chronology and paleogeography have been deciphered, hypotheses concerning the location of the Horse Prairie basin relative to the Eocene to Oligocene rift zone of Janecke (1994) can be tested. Assuming the basin lies within the proposed rift, the migratory nature of extension along the rift can be used to test the gravitational collapse (Coney and Harms, 1984) and volcanically driven models of extension (Gans et al., 1989). An overall southward migration of extension along the proposed rift would support a strong relationship between volcanism and extension, whereas a lack of migration would be consistent with gravitational collapse of previously thickened crust (Janecke, 1994).

LOCAL GEOLOGIC SETTING

The Horse Prairie basin is a structurally complex, east-dipping half-graben that contains Tertiary lacustrine, paludal, and fluvial sediments, along with volcanic rocks temporally correlated to the Challis Volcanics of central Idaho (Fig. 2; M'Gonigle and Dalrymple, 1993). The Maiden Peak spur to the east is bounded on its western flank by a system of north-striking, west-dipping, low-angle normal faults (M'Gonigle, 1994). This basin-bounding fault system has exhumed Archean basement rocks overlain by east-tilted Paleozoic and Cenozoic strata. The Beaverhead Mountains to the west of the basin are made up mainly of Proterozoic metasedimentary rocks, but include some Paleozoic sedimentary rocks (Staatz, 1979; Skipp, 1988). The lack of Proterozoic rocks to the east of the basin, and the lack of significant amounts of basement rocks to the west, greatly simplifies provenance studies and will be used to discriminate between footwall and hanging wall-derived sedimentary rocks.

Figure 2. Simplified geologic map and cross-section of the Horse Prairie and Medicine Lodge basins. Pre-Cenozoic units include Archean gneiss (Ag), middle Proterozoic quartzite (Y), and Mesozoic and Paleozoic rocks (MPz). Tertiary units are divided into Challis volcanic rocks (Tcv), Sediment of Bear Creek and coeval units in the Medicine Lodge basin (Tbc), Sediment of Everson Creek (Tec), and the Sediment of Bannock Pass (Tbp). The Horse Prairie and Medicine Lodge basins are bounded on the east by the west-dipping Muddy Grasshopper fault, and are dissected further by the Maiden Peak and Lemhi Pass fault systems. Geologic map is compiled from numerous workers (this study; S. U. Janecke, unpublished mapping; M'Gonigle and Hait, in review; M'Gonigle, 1993, 1994; M'Gonigle et al., 1991; Skipp, 1988; Dubois, 1982; Hansen, 1983; Perry and Sando, 1983; Staatz, 1973, 1979; Scholten and Ramspott, 1968; Scholten et al., 1955). Cross-section between western and eastern splays of the Maiden Peak fault system based on mapping by M'Gonigle and Hait (in review); cross-section east of eastern Maiden Peak fault modified from M'Gonigle and Dalrymple (1993). Outline of study area, location of Figure 3, and approximate location of seismic lines are shown. MGF = Muddy - Grasshopper fault; LPF = Lemhi Pass fault; MPF = Maiden Peak fault; WMPF = Western Maiden Peak fault; EMPF = Eastern Maiden Peak fault; LECF = Little Eightmile Creek fault; BF = Beaverhead fault.

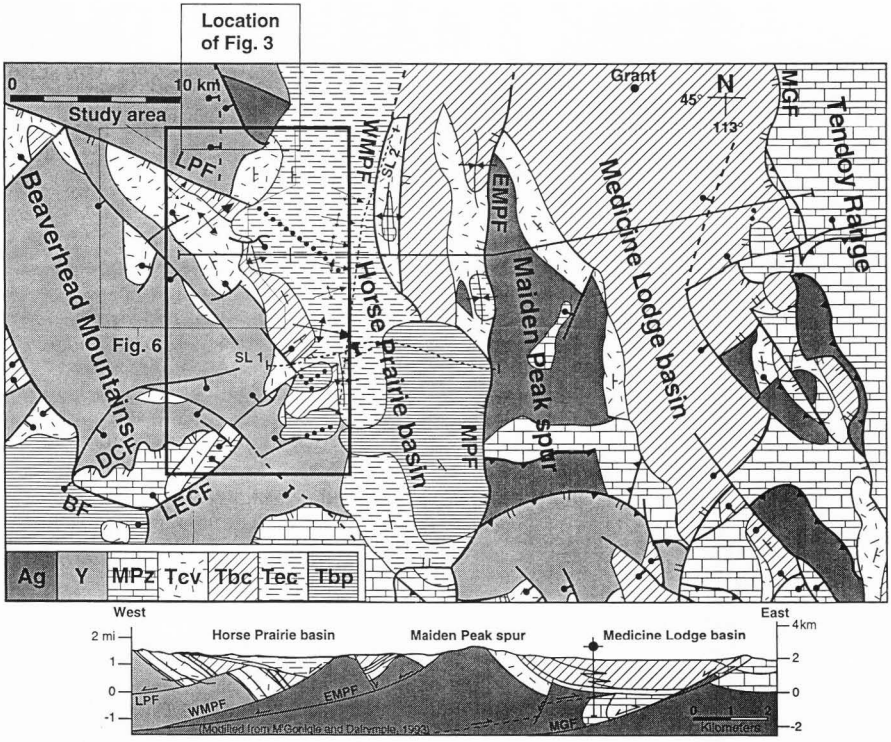
Location of Fig. 3
0
10 km
Study area
Grant
N
45°
113°
MGF
Tendoy Range
LPF
WMPF
SL 2
SL 1
EMPF
Medicine Lodge basin
Beaverhead Mountains
Fig. 6
Horse Prairie basin
Maiden Peak spur
MPF
DCF
BF
LECF
Ag
Y
MPz
Tcv
Tbc
Tec
Tbp
West
East
2 mi
1
0
-1
4km
2
0
-2
Horse Prairie basin
Maiden Peak spur
Medicine Lodge basin
LPF
WMPF
EMPF
MGF
0
1
2
Kilometers
(Modified from McGonigle and Dalrymple, 1993)

Archean, Proterozoic, Paleozoic, and Mesozoic units were cut by both low- and high-angle normal faults of uncertain age subsequent to contractile deformation associated with the Sevier orogeny (M'Gonigle and Dalrymple, 1993). Skipp (1985) hypothesized the presence of the Grasshopper and Cabin thrusts directly beneath the Horse Prairie basin, in addition to the north- to northwest-striking thrusts mapped to the east in the Tendoy Range (Fig. 3; Dubois, 1982; Perry et al., 1989). An east-west striking, south-dipping older-on-younger fault near the southern end of the Maiden Peak Spur may represent a segment of the Cabin thrust (M'Gonigle, 1993; M'Gonigle, 1994). These compressional structures may have had an effect on the orientation of the subsequent extensional deformation, as well as providing source rocks for Tertiary basin-fill deposits that are no longer present in the highlands surrounding the basin.

Northeast-striking, southeast-dipping, low-angle normal faults place Mississippian carbonates over Proterozoic strata southwest and southeast of the basin (Staatz, 1979; M'Gonigle et al., 1991). This Mississippian over Proterozoic relationship is also present farther south, just north of Hawley Creek (Lucchitta, 1966), and near the Nicholia Creek basin (Skipp, 1988). This system of low-angle normal faults may be the oldest extensional structures in the region (Janecke, pers. comm., 1995), but the critical cross-cutting relationships and kinematic indicators are not well documented.

A large, north northwest-striking, west-dipping, low-angle normal fault is present in the Tendoy Range along the east side of the Medicine Lodge basin, and may be responsible for the eastward tilt of the Horse Prairie-Medicine Lodge protobasin (Flores and M'Gonigle, 1991). Most of the slip on this low-angle structure predates a 27.4 ± 0.8 Ma basalt flow and dikes north of the Medicine Lodge basin (S. U. Janecke and W. C. McIntosh, unpublished data, 1996).

In addition to these low-angle normal faults, there are also many high-angle normal faults of various trends. Southwest of the basin a northeast-striking, high-angle

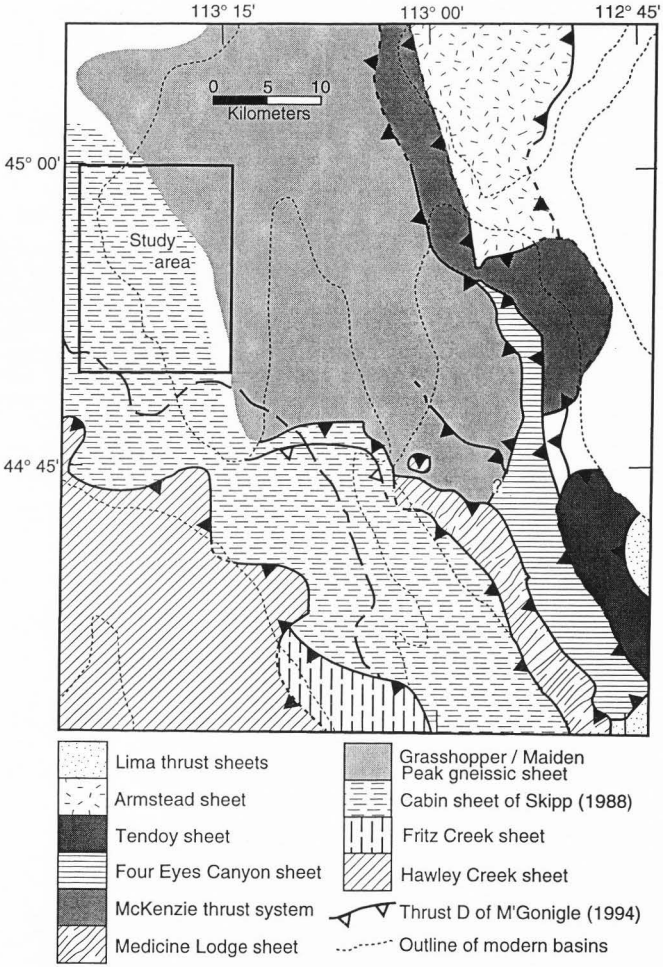

Figure 3. Simplified map of major thrust plates of southwestern Montana. Study area lies within the Grasshopper - Maiden Peak gneissic thrust plates and within the Cabin - Medicine Lodge thrust system of Skipp (1988). See M'Gonigle (1994) for a different interpretation of the Cabin plate. Modified from M'Gonigle et al. (1991), Skipp (1988), and S. U. Janecke (unpublished mapping).

fault appears to offset a northeast-striking low-angle fault down to the northwest. West of the study area, in the Lemhi Pass thorium district, both northeast- and northwest-striking normal faults of unknown age occur (Staatz, 1979). The chronological relationship between the two dominant sets is unclear. Northwest-striking faults appear to offset northeast-striking faults in some areas, whereas the opposite is the case in other locations. Staatz (1979) has also mapped a north-trending zone of deformation extending from the Agency Creek drainage southward to Yerian Creek, just east of the towns of Tendoy and Lemhi, Idaho. This zone is characterized by a series of cross-cutting northeast- and northwest-striking normal faults which are mostly covered with Quaternary sediments. With further study, the relative age of these different sets of normal faults may be decipherable.

STRATIGRAPHY

Four unconformity-bounded packages of Cenozoic volcanic rocks, and lacustrine, paludal, and fluvial sedimentary rocks are preserved in the Horse Prairie half-graben. The focus of this study is on Cenozoic structures and stratigraphy; therefore, unit descriptions of pre-Cenozoic rocks were not emphasized. Pre-Cenozoic rock descriptions were compiled from previous work in the adjacent quadrangles (Staatz, 1973, 1979; Hansen, 1983; M'Gonigle, 1994; M'Gonigle and Hait, 1997), and were modified little as a result of this study. Cenozoic unit descriptions are based largely on hand samples, although thin sections were examined where necessary.

PRE-CENOZOIC ROCKS

Archean (?) gneiss (Ag) Archean gneiss occurs in two separate blocks within the study area. The eastern block consists dominantly of granitic gneiss, and is exposed throughout the Maiden Peak spur between approximately 44° 45' and 45° N latitude. Rocks of the Maiden Peak spur consist mainly of coarse-grained, light grey to red-brown granite gneiss composed of 38 percent microcline, 25 percent quartz, 12 percent orthoclase, 11 percent plagioclase, and 12 percent hornblende and(or) biotite, with traces of apatite, zircon, ilmenite, and leucoxene (M'Gonigle, 1994). The western block consists dominantly of metasedimentary rocks, and is lithologically different from the gneisses of the eastern block. The western block is located in sections 4, 5, 8, and 9 of T 10 S, R 14 W in the Everson Creek quadrangle and sections 31, 32, and 33 of T 9 S, R 14 W of the Coyote Creek quadrangle, and consists of quartz-biotite gneisses and dark biotitic metasedimentary rocks (Hansen, 1983). Quartz, biotite, and plagioclase are abundant, with traces of garnet, amphiboles or pyroxenes, zircon, apatite, and magnetite (Coppinger, 1974).

The eastern block of granitic gneiss is exposed as far west as the immediate footwall of the western Maiden Peak fault, where it is unconformably overlain by Challis volcanic rocks (Plate 1). Locally, Paleozoic rocks are in depositional contact with the underlying granite gneiss, but Proterozoic rocks have never been shown to be in depositional contact with the eastern block of granite gneiss (M'Gonigle, 1993; M'Gonigle, 1994; M'Gonigle and Hait, 1997). East-dipping Challis volcanic rocks and basin-fill of the Medicine Lodge basin overlie the gneisses of the Maiden Peak spur to the east in the Medicine Lodge Peak, Hansen Ranch, and Jeff Davis Peak quadrangles (M'Gonigle et al., 1991; M'Gonigle, 1993; M'Gonigle and Hait, 1997).

Hansen (1983) concluded that the western block of gneiss is separated from Proterozoic rocks of the Big Creek Formation to the east and northeast by the Monument thrust, and from Big Creek quartzites to the southwest by the Bloody Dick Creek fault zone. Subsequently, Challis volcanic rocks and Tertiary sediments were deposited along the northeast and southern margins of the block of gneiss (Hansen, 1983). In contrast, new mapping (S. U. Janecke, unpublished mapping; this study) suggests the Monument thrust at this location is actually the north northeast-dipping depositional base of the Middle Proterozoic quartzites, and that the entire eastern and southern margins of the western block of gneiss are depositional contacts with younger Challis volcanic rocks and sediments of Everson Creek (Fig. 4).

The reinterpretation of the Monument thrust as the depositional base of the Proterozoic rocks has a number of possible implications. The base of the Belt Supergroup, and its equivalents, is not commonly exposed in this region. The area northeast of the Bloody Dick Creek fault may provide a unique location to study the stratigraphy at the base of the Proterozoic Belt basin, and the relationship between the quartzites and underlying Archean gneisses.

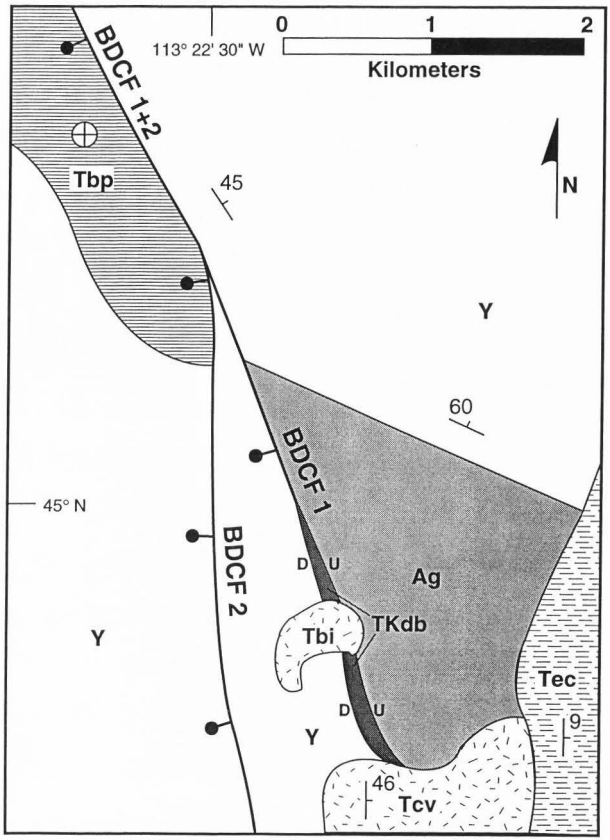

Figure 4. Geologic map of the Bloody Dick Creek fault system. The older strand of the Bloody Dick Creek fault zone (eastern splay, BDCF 1) is intruded by a 200-600 (?) Ma diabase (TKdb) and a 47.3 ± 0.2 Ma basalt (Tbi), and is lapped by middle Eocene Challis volcanic rocks (Tcv) to the south southeast. The younger strand (BDCF 2) contains middle Miocene (?) sediment in its hanging wall (Tbp), and reactivates the older strand to the northwest (BDCF 1+ 2). Proterozoic quartzites (Y) and Archean gneisses (Ag) exposed in the footwall of the fault system may represent the depositional base of Proterozoic rocks in the area (S. U. Janecke, unpublished mapping; this study).

The age of the western block of gneiss is not known, but a late Archean age has been assigned to the eastern block (M'Gonigle, 1993). U-Pb and Pb-Pb age determinations show late Archean crystallization with subsequent metamorphic overprints by various Proterozoic events (M'Gonigle, 1993).

Middle Proterozoic quartzite and siltite (Y) Middle Proterozoic quartzites and siltites underlie much of the western half of the study area. Hansen (1983) mapped the Middle Proterozoic rocks north of the Lemhi Pass fault as the Big Creek Formation of the Lemhi Group. Staatz (1973, 1979) referred to the Middle Proterozoic rocks south of the Lemhi Pass fault and north of the Peterson Creek thrust fault (Black Canyon) as Middle Proterozoic quartzites and siltites, but used traditional Salmon Supergroup stratigraphy south of the Peterson Creek thrust fault. Skipp (1988) classified the Middle Proterozoic rocks south of the Peterson Creek thrust fault as Lemhi Group and Swauger Formation undivided, but for the purpose of this study, all Middle Proterozoic quartzites and siltites are undifferentiated. Proterozoic clastic rocks in the study area are typically light-grey to red, fine- to medium-grained, micaceous and feldspathic quartzites with interbedded pale-green siltites. Thin- to thick-bedded quartzites dominate, but massive outcrops occur locally. The thickness of Middle Proterozoic rocks in the Beaverhead Mountains has been estimated to exceed 12000 meters (Hansen, 1983).

Middle Proterozoic rocks within the field area typically dip moderately west, but locally have a wide range of orientations. Northeast of the Bloody Dick Creek fault, in the Coyote Creek quadrangle, quartzites dip approximately 30° to the northeast (Hansen, 1983; S. U. Janecke, unpublished mapping), away from the depositional base of the Middle Proterozoic rocks. Middle Proterozoic rocks are generally separated from the overlying east- and northeast-dipping Tertiary volcanic rocks and basin-fill deposits by an angular unconformity, and locally the basal Tertiary contact is faulted (sect. 20, T 11 S, R 14 W and sect. 7, T 11 S, R 14 W). The southwesternmost exposures of Middle

Proterozoic rocks in the study area are faulted against Paleozoic carbonates along the Goat Mountain thrust of Staatz (1979). This gentle southeast-dipping younger-on-older fault has an uncertain origin (see Divide Creek fault discussion).

The Middle Proterozoic rocks in the Beaverhead Mountains temporally correlate with the Yellowjacket Formation, Lemhi Group and Swauger Formation of east-central Idaho and the Belt Supergroup of western Montana (Ruppel, 1975; Winston and Link, 1993). Although age determinations have not been conducted in the study area, previous work suggests a Middle Proterozoic age for the Precambrian quartzites and siltites.

Ordovician Summerhouse Formation (Os) Two small exposures of the Ordovician Summerhouse Formation occur in section 25 of T 10 S, R 14 W, and section 31 of T 10 S, R 13 W (Plate 1; M'Gonigle and Hait, 1997). This unit typically consists of very light grey to white, medium- to coarse-grained, cross-bedded, locally feldspathic conglomeratic quartzite (M'Gonigle, 1994). At least 10 m are preserved in the study area, but up to 68 m are exposed in the Medicine Lodge Peak and Deadman Pass quadrangles to the southeast (M'Gonigle, 1993, 1994). The Summerhouse Formation rests unconformably on Archean gneiss, and is overlain in angular unconformity by Challis volcanic rocks.

Mississippian limestone undivided (Mu) Light to medium grey, coarse-grained, thick- to massive-bedded limestone containing grey and black chert nodules occurs in the hanging wall of the Divide Creek fault in sections 5, 7, and 8 of T 17 N, R 26 E, and in the southwest corner of section 31, T 11 S, R 14 W (Plate 1). This unit has been mapped as Mississippian Madison Limestone (Staatz, 1973) and Mississippian Scott Peak Formation (K. Lund, oral communication, 1996), but will remain undivided for the purpose of this study. The base and top of the limestone are unexposed due to the underlying fault and overlying angular unconformity.

Diabase (TKdb) A dark green aphanitic to fine-crystalline diabase appears to intrude the west southwest-dipping Bloody Dick Creek fault zone, and Archean gneisses and Middle Proterozoic quartzites in its footwall and hanging wall, in sections 5 and 8 of T 10 S, R 14 W in the northwestern Everson Creek quadrangle. The diabase dominantly consists of plagioclase, augite, and hornblende, with lesser amounts of myrmekite, biotite, ilmenite, magnetite, and apatite (Coppinger, 1974). A whole-rock $^{40}Ar/^{39}Ar$ age determination of 47.3 ± 0.4 Ma from a mafic intrusion that intrudes the diabase south of Bloody Dick Creek (sections 5, 6, 7, 8, T 10 S, R 14 W) indicates a middle Eocene or older age for the diabase intrusion (sample 1, Plate 1; S. U. Janecke and W. C. McIntosh, unpublished data, 1996). Previous workers have suggested a variety of ages for the intrusion, including: "post-Laramide" (Coppinger, 1974), late Mesozoic or early Tertiary (Sharp and Cavender, 1962), and pre-Oligocene (Hansen, 1983). An $^{40}Ar/^{39}Ar$ whole-rock age of 200-600 Ma was determined for the diabase (sample 2, Plate 1); however, the disturbed nature of the spectrum prohibits a reliable age determination (S. U. Janecke and W. C. McIntosh, unpublished data, 1996).

CENOZOIC ROCKS

Geologic mapping and basin analysis reveal that over 4 km of Tertiary volcanic and sedimentary rocks have been preserved within the Horse Prairie basin. The study area is located on the western margin of this east-tilted half-graben, where four unconformity-bounded sequences are present in the Tertiary strata. Archean, Proterozoic, and Paleozoic basement rocks are overlain in angular unconformity by middle Eocene Challis volcanic rocks. Volcanic rocks dip approximately 50° to the north northeast, and are overlain in unconformity by 35° northeast-dipping coarse clastics and lacustrine limestones of the sediments of Bear Creek. Overlying the sediments of Bear Creek in angular unconformity are 11° east-dipping gravels and sands of the sediments of Everson Creek. The fine-grained sediments of Bannock Pass overlie the sediments of

Everson Creek in angular unconformity, and dip approximately 4° east in the study area (Fig. 5).

Challis Volcanic Group

Challis volcanic rocks are concentrated between 44° 53' and 44° 59' N latitude in the western Everson Creek and eastern Lemhi Pass quadrangles (Fig. 6; Plate 1). The maximum thickness of exposed volcanic rocks within this band locally exceeds 2 km (Fig. 6), but the original thickness is unknown due to the overlying angular unconformity (Fig. 5). Thick sequences of volcanic rocks also occur to the east in the northeastern Maiden Peak spur at the same latitude (M'Gonigle et al., 1991; M'Gonigle and Hait, 1997). Volcanic rocks pinch out abruptly to the north and south, but scattered outcrops can be found throughout the study area. Good exposures are relatively widespread, particularly surrounding Trail Creek in the northwestern Everson Creek quadrangle.

Challis volcanic rocks in the Horse Prairie basin consist of rhyolitic ash flow and ash-fall tuffs, andesitic lava flows and flow breccias, volcaniclastic sandstone and conglomerate, and interbedded gravels with well-rounded clasts. The volcanic stratigraphy varies dramatically across short distances with ash flow tuffs dominating the sequence north of Bear and Trail Creeks, and andesitic lava flows dominating to the south (Plate 1). Specific unit descriptions and their ages will be discussed in ascending chronologic order, starting with a discontinuous conglomerate at the base of the Challis Volcanic Group.

Basal conglomerate (Tcg1) The basal conglomerate is comprised of well-rounded pebbles and cobbles in a coarse sand and white tuffaceous matrix. Proterozoic quartzite clasts derived from the west dominate, with tuffaceous pebbles locally present in minor amounts. Exposures of the basal conglomerate are scattered and highly variable in thickness, but the unit is up to 45 m thick in the Lemhi Pass area (Staatz, 1979). Two

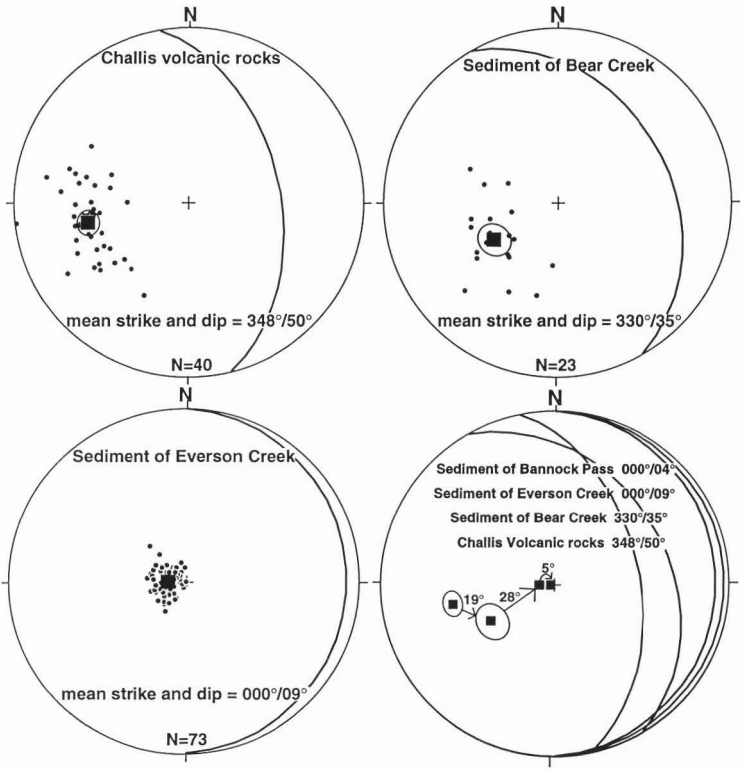

Figure 5. Equal area plots of poles to bedding for Tertiary rocks of the Horse Prairie basin. Mean poles to bedding show a 19° angular discordance between Challis volcanic rocks and the Sediment of Bear Creek, a 28° angular discordance between the Sediment of Bear Creek and the Sediment of Everson Creek, and 5° discordance between the Sediment of Everson Creek and the Sediment of Bannock Pass. All of these deposits are folded, so the discordance at a particular location will vary.

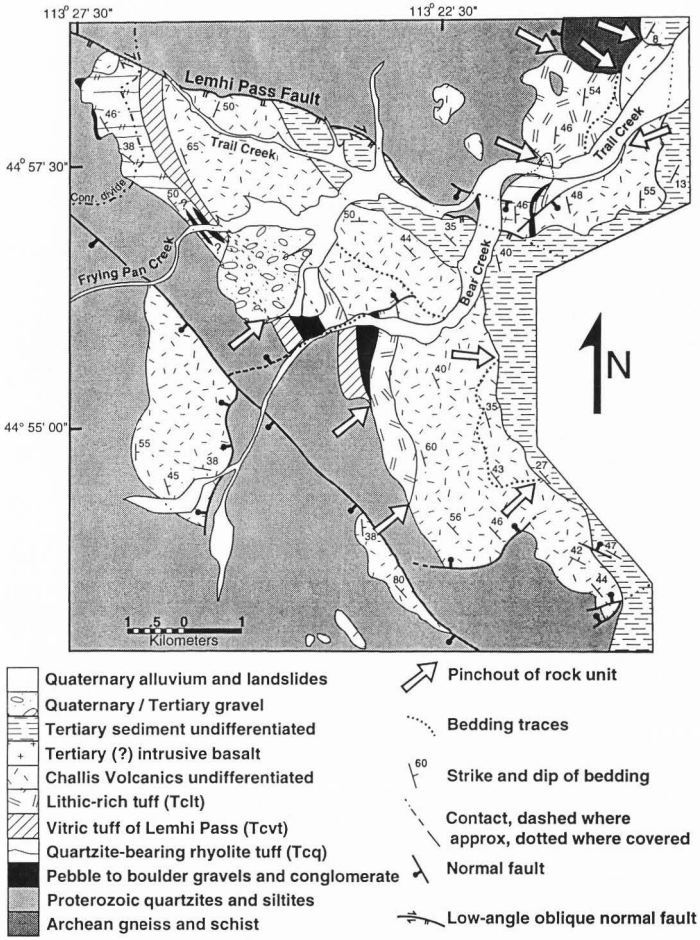

Figure 6. Geologic map of the Lemhi Pass area. The distribution of Challis volcanic rocks, and provenance data from interbedded gravels and conglomerates, define a significant middle Eocene east-sloping paleovalley through the Lemhi Pass area termed the Lemhi Pass paleovalley by Janecke et al. (*in review*). A basal ash flow tuff (unit Tcq) and bedding traces within lava flows pinch out against the margins of the paleovalley to the north and south. See map index of Plate 1 for sources. Location shown on Figure 2.

exposures of basal conglomerate occur in the study area; one is located at the confluence of Bear and Trail Creek in the northwest Everson Creek quadrangle, and the second overlies the Ordovician Summerhouse Formation in the footwall of the western Maiden Peak fault in section 25 of T 10 S, R 14 W (Plate 1). This unit appears to be confined to the Lemhi Pass paleovalley, and only occurs when an overlying quartzite-bearing ash flow tuff (Tcq) is present (Janecke et al., *in review*).

Quartzite-bearing rhyolite tuff (Tcq) The quartzite-bearing ash flow tuff is typically white, but can be pink, pinkish-brown, pinkish-grey, or light grey on fresh surfaces, and contains variable amounts of crystals, and lithic and vitric clasts. Lithics are dominantly dark grey or black angular micaceous quartzite clasts (< 30 mm), vitric clasts are typically tuff or glass (< 15 mm), and crystals (< 2 mm) consist of quartz and plagioclase, with lesser amounts of sanidine (Staatz, 1979; this study). The defining characteristic of the quartzite-bearing tuff is the stark contrast between universally present dark quartzite lithics and the typically light matrix. The tuff appears to be confined to locations where the thickest sections of Challis volcanic rocks are preserved, and is up to 440 m thick in the study area. Outcrops of the tuff can be found in sections 13, 19, 20, 24, and 25 of T 10 S, R 14 W, and sections 18 and 30 of T 10 S, R 13 W (Plate 1). M'Gonigle and Dalrymple (1993, 1996) performed $^{40}Ar/^{39}Ar$ age determinations on single sanidine crystals from the quartzite-bearing rhyolite tuff near Lemhi Pass (Tcq of Staatz, 1972), and found a mean age of 48.64 ± 0.33 Ma. The middle Eocene quartzite-bearing tuff represents the oldest member of the Challis Volcanic Group preserved in the Horse Prairie basin.

Conglomerate (Tcg2) Poorly sorted, well-rounded pebbles, cobbles, and boulders (< 3 m) are intercalated in and directly overlie the quartzite-bearing rhyolite tuff. Clasts consist dominantly of far-traveled quartzites derived from the west, with few volcanic and plutonic clasts, and are locally cemented with an ash matrix. This unit

correlates with the conglomerate of Flume Creek of Staatz (1979) at the Lemhi Pass locality. This middle Eocene conglomerate is preserved in sections 19, 20, 13, 24, and 25 of T 10 S, R 14 W, and in sections 18, 19, and 30 of T 10 S, R 13 W (Plate 1). Up to 50 m thick conglomerate lenses are present locally, with outcrops limited to the thickest sections of volcanic rocks coinciding with an east-west band at the latitude of Lemhi Pass (Fig. 6).

Lithic-rich tuff (Tclt) The lithic-rich ash flow tuff ranges from brown, tan, white, pink, to orange on fresh surfaces, and is typically densely welded. This dacite tuff contains abundant rhyolitic lithics with minor amounts of dark grey quartzite lithics (< 5 mm) in a glassy matrix. The lithic-rich tuff is comprised of up to 60 percent pumice fragments and rhyolitic lithics, which are typically less than 1.5 cm (fragments > 5 cm present locally). Crystals typically comprise less than 20 percent of the tuff, and consist of 40-50 percent plagioclase, 20-30 percent quartz, 10-20 percent sanidine, 5-15 percent biotite, with a trace of allanite. The lithic-rich tuff, like most of the ash flow tuffs in the study area, is confined to the thickest sections of the volcanic rocks, and is thickest north of Trail Creek where 1250 m is preserved (Plate 1). The lithic-rich tuff is at or very near the base of the lava flow sequence (Tcl), and up section from the quartzite-bearing ash flow tuff. The tuff pinches out abruptly against Middle Proterozoic quartzite and Archean gneiss in section 8 of 10 S, R 14 W to the north, and in section 36 of 10 S, R 15 W to the south, where it was incorrectly mapped as the basalt rhyodacite (Tcb) sequence by Staatz (1979).

Lava flow (Tcl) Dark grey to hematite-red aphanitic flows and flow-breccias with thin intercalated tuffs and small volcaniclastic deposits volumetrically dominate the Challis volcanic rocks in the study area. Flows range in composition from basalt to quartz latite, and correlate with the basalt-rhyodacite sequence of Staatz (1979). Up to

1100 m of lava flows are exposed at approximately 44° 55' N latitude, but scattered thin deposits occur throughout the study area (Plate 1). Lava flows may overlie Proterozoic basement rocks, the lithic-rich tuff (Tclt), or the quartzite-bearing rhyolite tuff (Tcq) depending on the geographic location. Ash flow tuffs typically underlie the lava flow sequence between 44° 55' and 44° 58' N latitude, whereas farther to the south the lava flows directly overlie Proterozoic quartzites in angular unconformity. A greenish-white rhyolite tuff directly down-section from the basalt-rhyodacite sequence of Staatz (1979) in the Lemhi Pass area has an $^{40}Ar/^{39}Ar$ single sanidine age of 48.04 ± 0.43 Ma (Staatz, 1972; M'Gonigle and Dalrymple, 1996).

Biotite tuff (Tcbt) The biotite tuff is generally a white to yellow andesitic ash-fall and ash flow tuff containing plagioclase, biotite, hornblende, pyroxene, sanidine and quartz crystals, and pumice shards in variable amounts. The biotite tuff is locally dominated by glass and pumice fragments, but typically contains 20-50 percent plagioclase, 5-10 percent biotite, 3-6 percent hornblende, 2-5 percent orthopyroxene and clinopyroxene, with lesser amounts of quartz and sanidine. Rhyolitic tuff lithics (< 2 cm) similar to those found in unit Tclt are locally present. This unit is only found north of approximately 44° 57' N latitude in sections 8, 9, 16, 17, 20, and 21 of T 10 S, R 14 W (Plate 1). The precise stratigraphic position of the biotite tuff is difficult to discern, but it appears to overlie or to be interbedded with the upper sections of both the lava flows (Tcl) and the lithic-rich tuff (Tclt) south and north of Trail Creek, respectively. The apparent thickness of the biotite tuff varies dramatically along strike, with a maximum thickness of approximately 670 m immediately south of Trail Creek. The extreme variability in thickness and the unusual outcrop pattern of the biotite tuff is likely the result of multiple intrusions (units Tci, Tcli, Tbi) in the vicinity. Significant paleotopography during emplacement of the tuff may have also affected its distribution resulting in considerable changes in thickness over short distances.

Sandstone (Tcs) Volcaniclastic sandstone and conglomerate occur intercalated with the lava flows (Tcl) in at least two locations. In the southern half of section 29, T 11 S, R 14 W, approximately 50 m of poorly sorted volcaniclastic sandstone and angular cobble conglomerate appear to be interbedded near the base of the lava flow sequence (Plate 1). In the west half of section 6, T 11 S, R 14 W, green volcaniclastic sandstone occur near the top of the lava flow sequence, immediately down section from the quartz-sanidine tuff (Tcqs). Volcaniclastic sandstone and conglomerate are usually poorly exposed and laterally discontinuous.

Tuff of Curtis Ranch (Tcr) The tuff of Curtis Ranch is typically a white to greenish-white or yellow, friable to moderately dense rhyolitic ash-fall and ash flow tuff containing plagioclase, quartz and biotite in an ash matrix. White pumice clasts are locally abundant, with small volcanic lithics (< 4 mm) present in lesser amounts. The tuff of Curtis Ranch is located up section from the lava flows (Tcl), and up to 340 m is preserved south of the Lemhi Pass fault and north of approximately 44° 54' N latitude (Plate 1). The tuff does not continue farther south due to nondeposition or subsequent erosion. Staatz (1979) determined an average age of 41.3 Ma using the K/Ar method on sanidine and biotite crystals from the middle of the tuff along Agency Creek in the Lemhi Pass quadrangle. However, more recent, and presumably more reliable $^{40}Ar/^{39}Ar$ age determinations from the tuff of Curtis Ranch along Trail Creek (sample 5, Plate 1) yield an age of 47.53 ± .06 from sanidine single crystals from the tuff (S. U. Janecke and W. C. McIntosh, unpublished data, 1996).

Dacite lava (Tcdl) Up to 560 m of dark grey to hematite-red, porphyritic lava flows with phenocrysts of augite, andesine, hornblende, biotite and olivine occur in the west-central Bannock Pass and east-central Goat Mountain quadrangles (Plate 1; Staatz, 1973). At this location, Staatz (1973) interpreted the basal contact of the dacite lava to be faulted; however, new mapping suggests that dacite lava flows overlie Proterozoic

quartzite, Mississippian carbonates, and the Divide Creek fault in angular unconformity, and overlie and underlie the quartz-sanidine welded tuff (Tcqs).

Quartz-sanidine welded tuff (Tcqs) A white, tan, or orange, densely welded, rhyolitic ash flow tuff containing chatoyant euhedral sanidine and smoky quartz crystals in a microcrystalline matrix occurs in scattered outcrops throughout the study area. Approximately 315 m of quartz-sanidine tuff is preserved in what appears to be a small paleovalley-fill in section 31 of T 10 S, R 14 W, and section 6 of T 11 S, R 14 W (Plate 1). Other exposures occur in the east-central Goat Mountain and west-central Bannock Pass quadrangles, and in section 14 of T 10 S, R 15 W. Eutaxitic foliations measured within the thickest exposure of the tuff show an approximate dip of 36° to the east northeast, whereas the underlying lava flows appear to dip more steeply. The relatively shallow dip of the tuff, and the fact that it appears to be confined to a paleovalley, suggests the presence of an angular unconformity under the quartz-sanidine tuff.

$^{40}Ar/^{39}Ar$ ages on single sanidine crystals from the sanidine-quartz welded tuff within the Everson Creek quadrangle show emplacement at approximately 46.01 ± 0.39 Ma (M'Gonigle and Dalrymple, 1993, 1996). The stratigraphic position of the quartz-sanidine tuff relative to the tuff of Curtis Ranch is unclear in the study area because the two tuffs are never in contact. However, a new $^{40}Ar/^{39}Ar$ age of 47.53 ± .06 from the tuff of Curtis Ranch indicates that the quart-sanidine welded tuff is distinctly younger than the tuff of Curtis Ranch (sample 5, Plate 1; S. U. Janecke and W. C. McIntosh, unpublished data, 1996).

Mafic intrusion (Tbi) Eight dark grey to black, aphanitic to porphyritic olivine pyroxene intrusions occur in the study area in sections 5, 6, 7, 8, 9, 17, and 18 of T 10 S, R 14 W, section 26 of T 10 S, R 15 W, and along the western edge of the Everson Creek quadrangle at approximately 44° 53' N latitude (Plate 1). These basaltic rocks appear to be intrusive based on typically irregular outcrop patterns and distributions,

although most exposures have an aphanitic texture. Mafic intrusions systematically intrude middle Eocene or older rocks, and are therefore assumed to be related to Challis volcanism. A whole-rock $^{40}Ar/^{39}Ar$ age determination of 47.3 ± 0.4 Ma from a matrix concentrate on a mafic intrusion that intrudes Proterozoic and Archean rocks south of Bloody Dick Creek (sections 5, 6, 7, 8, T 10 S, R 14 W) confirms a middle Eocene age for at least some of the mafic intrusions in the study area (sample 1, Plate 1; S. U. Janecke and W. C. McIntosh, unpublished data, 1996). In addition, a basaltic megabreccia within the sediment of Everson Creek in section 9 of T 10 S, R 14 W yielded an $^{40}Ar/^{39}Ar$ age of 46.1 ± 1.0 Ma from a matrix concentrate (S. U. Janecke and W. C. McIntosh, unpublished data, 1996).

Diorite (Td) Greenish-grey, medium-grained porphyritic biotite, augite, hornblende diorite occurs in small intrusive bodies and dikes in the southeastern Lemhi Pass quadrangle near the head of Bear Gulch and in section 7 of T 11 S, R 14 W (Plate 1). Diorite intrusions only occur within Proterozoic rocks, causing their age to be somewhat enigmatic. However, a diorite intrusion located 0.7 km north of North Fork Everson Creek at the western edge of the Everson Creek quadrangle appears to intrude a northeast-striking syn-Challis fault. These data suggest intrusion of the diorite sometime after initiation of Challis volcanism, and possibly associated with syn-Challis normal faulting.

Quartz latite (Tcd) Pink to purplish-brown, light grey, or brown, porphyritic quartz latite occurs in small intrusive bodies throughout the northwestern corner of the study area (Plate 1). Phenocrysts are dominantly quartz and plagioclase, with lesser amounts of potassium feldspar and biotite in an aphanitic matrix (Staatz, 1979). Quartz latite intrusions only occur within the Proterozoic rocks, but are assumed to be related to dominantly intermediate to siliceous Challis volcanism.

Intermediate intrusions (Tcli/Tci) Grey, dark grey, or hematitic red andesitic flows/intrusions occur within Challis volcanic rocks in sections 16, 17, 20, and 21 of T 10 S, R 14 W and in sections 25, 26, and 36 of T 10 S, R 15 W (Plate 1). Flows (Tcli) and intrusions (Tci) are lithologically similar, and tend to be aphanitic to porphyritic, and locally brecciated and very altered. **Tci** is used to classify igneous bodies whose outcrop morphology and distribution is suggestive of an intrusion rather than a flow, whereas **Tcli** is used where petrographic analysis and outcrop distribution are inconclusive in determining whether the bodies are intrusive or extrusive in nature. Both units are found interbedded with or intruding into Challis volcanic rocks, and are therefore assumed to be middle Eocene in age.

Challis undifferentiated (Tcu) The **Tcu** classification is used where exposures are insufficient to assign a specific lithology, or where the variations in lithology are too great to delineate separate units at a scale of 1:24,000. Undifferentiated Challis rocks can be found in sections 8 and 17 of T 10 S, R 14 W, and in section 36 of T 10 S, R 15 W (Plate 1).

Summary of Challis Stratigraphy

Over 2 km of Challis volcanic rocks accumulated in the Horse Prairie basin between 48.64 ± 0.33 Ma and 46.01 ± 0.39 Ma (M'Gonigle and Dalrymple, 1993, 1996). The distribution of the Challis volcanic rocks, and the thickness variations within the sequence, define the middle Eocene paleotopography of the western half of the study area. Stratigraphic differences, thickness variations along strike, and very coarse boulders (< 3m) interbedded with the quartzite-bearing rhyolite tuff suggest that the pre-Challis landscape was locally characterized by rugged topography, and significant east-sloping paleocanyons. This middle Eocene paleotopography enabled lava flows and ash flow tuffs to pinch out abruptly against valley walls resulting in dramatic thickness and stratigraphic variations over short distances (Plate 1; Fig. 6). In addition, syn-Challis

extension (see discussion of syn-Challis faults) facilitated abrupt changes in thickness and lithology across very short distances. Additional mapping in the region may help to clarify which stratigraphic variations are due to paleotopography and which are due to extension.

Sediment of Bear Creek

The sediment of Bear Creek reflects initiation of sedimentation and initial basin formation in the study area subsequent to Challis volcanism. The sediment of Bear Creek is approximately 1 km thick in the study area, and has been preserved in a discontinuous northwest-trending band between 44° 50 ' and 44° 57' 30" N latitude (Plate 1). The sediment is in the hanging wall of the Lemhi Pass fault, which bounds the sediment to the north, and does not appear in the footwall within the study area. Other exposures lie in the footwall of the western Maiden Peak fault to the east (M'Gonigle and Hait, 1997), but the position of these exposures relative to the Lemhi Pass fault is unclear. The sediments of Everson Creek and Bannock Pass overlie the Sediment of Bear Creek in angular unconformity, and conceal the original thickness of the unit; however, cross section D-D' shows a thickness of approximately 1900 m (Fig. 7; Plate 2). The underlying quartz-sanidine ash flow tuff (Tcqs), which represents the top of the Challis volcanic rocks, may be conformable with the sediment of Bear Creek. In contrast, the sediment of Bear Creek is separated from the older Challis volcanic rocks by an angular unconformity (19° discordance in attitude, Fig. 5). The sediment overlies the tuff of Curtis Ranch (Tcr), the quartz-sanidine ash flow tuff (Tcqs), lava flows (Tcl), and Middle Proterozoic quartzites (Y) from north to south.

The sediment of Bear Creek is dominanted by coarse clastic rocks with interbedded fine-grained sandstone, pebble conglomerate, and freshwater limestones. Siltstone and two gastropod-bearing limestones (often silicified) typically occur at the

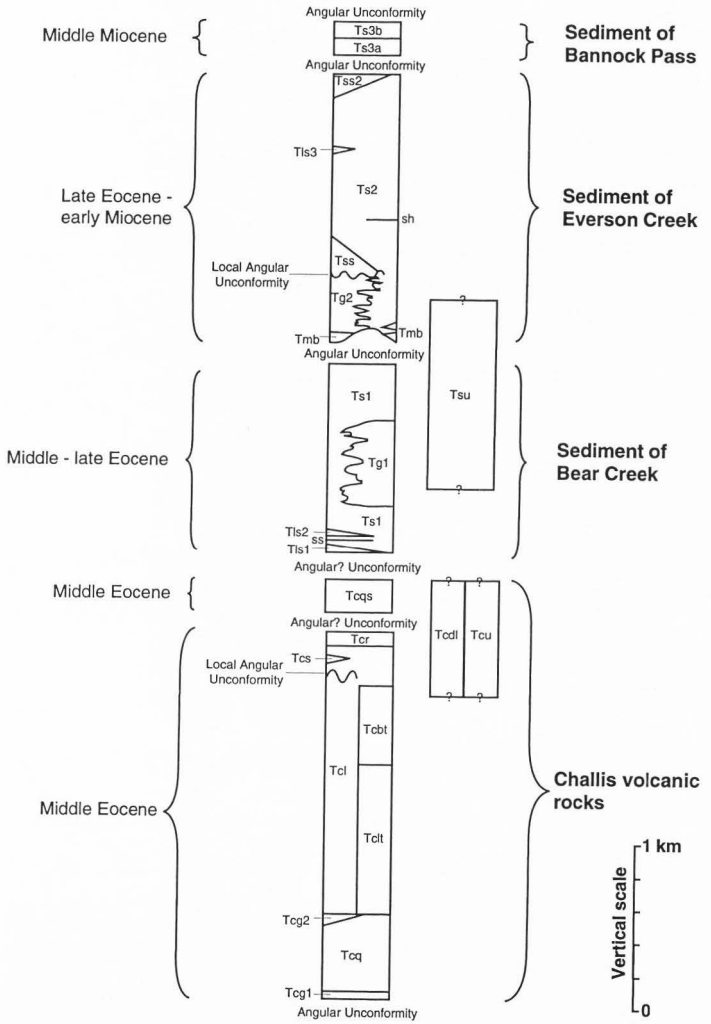

Figure 7. Simplified stratigraphic column of Tertiary basin-fill deposits in the Horse Prairie basin. Maximum thicknesses of exposed rock units are shown (thinner units are exaggerated). See Figure 9 for time-scaled stratigraphic column.

base of the sequence. Sandstone and pebble conglomerate are found up-section from the limestones, and are locally overlain by weakly consolidated, poorly sorted, well-rounded boulder to pebble gravels.

Basal limestone unit (Tls1) A light tan to light brown, thin to thickly bedded, sparry freshwater limestone marks the base of the sediment of Bear Creek (Plate 1). The basal limestone is exposed between Trail Creek and Black Canyon, and has a maximum thickness of 50 m. This unit is typically silicified, and weathers light tan to white. Middle Eocene gastropods (Gyraulus proceras) are locally abundant within the basal limestone, indicating initiation of sedimentation in the middle Eocene (Steve Good, written comm., 1996).

Sandstone unit (ss) Thin beds of poorly sorted volcaniclastic sandstone and pebble conglomerate are locally interbedded with the lacustrine limestones. This unit is less than 5 m thick, and is only mappable in section 19 of T 10 S, R 14 W, and section 24 of T 10 S, R 15 W (Plate 1).

Limestone unit (Tls2) The second occurrence of freshwater limestone is lithologically similar to the basal limestone, but appears to be thinner (< 40 m) and less continuous. This unit also locally contains abundant middle-late Eocene gastropods, and is typically silicified. A designation of **Tls** is used where exposures prohibit differentiating between the two limestones within the sediment of Bear Creek.

Older sediment unit (Ts1) Fine- to coarse-grained sandstone and pebble conglomerate occur throughout the sediment of Bear Creek interbedded with coarse gravels and lacustrine limestones. This unit is rarely cemented in outcrop, and typically weathers to a tan soil containing rounded pebbles. Pebble counts from cemented and noncemented pebble conglomerate show a dominance of volcanic clasts (20-90 percent) with lesser amounts of quartzite clasts (5-80 percent; Fig. 8). The presence of clasts

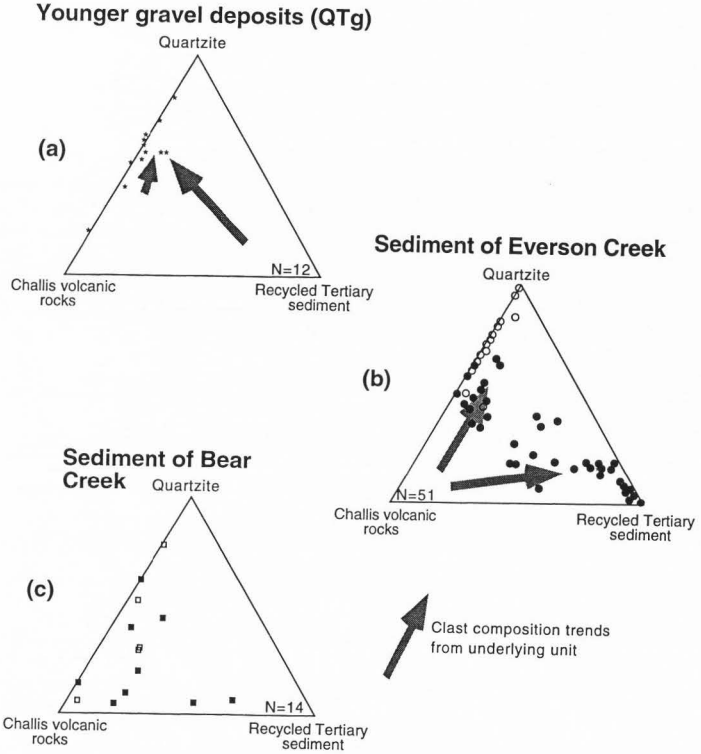

Figure 8. Ternary diagrams of pebble and boulder counts in Tertiary basin-fill deposits. A minimum of 50 clasts > 2 cm in diameter were counted for each data point. (a) Uncemented cobble and boulder counts from ridge-capping, younger gravel deposits (QTgo, QTgy). (b) Cemented (solid circles) and uncemented pebble to boulder counts from the sediment of Everson Creek. Note the low percentage of volcanic clasts and the two distinct subpopulations of gravel and conglomerate. (c) Cemented (solid squares) and uncemented pebble to boulder counts from the sediment of Bear Creek. Note the occurrence of clasts recycled from older Tertiary sediment within many beds of the sediment of Bear Creek. Solid black symbols represent cemented exposures. Raw data are in Table 3.

derived from the base of the sediment of Bear Creek in conglomerates 700 m from the base indicates syntectonic deposition. The original thickness of the older sediment unit is unknown, but approximately 900 m has been preserved under the overlying angular unconformity.

Older gravel unit (Tg1) Well-rounded, poorly sorted boulder to pebble gravel containing an abundance of volcanic clasts, with lesser amounts of quartzite clasts, can be found in sections 13, 14, and 24 of T 10 S, R 14 W, and sections 19, 30, and 31 of T 10 S, R 14 W (Plate 1). These gravels are concentrated in the immediate hanging wall of the Lemhi Pass fault where they are juxtaposed with Proterozoic quartzites. Volcanic clasts are typically dominant throughout the unit. The older gravel unit is 390 m thick and is locally overlain in angular unconformity by well-rounded gravels of the sediment of Everson Creek. The dominantly volcaniclastic older gravel unit is distinguished from the overlying quartzite gravels based on clast composition and attitude of bedding where possible.

Lava flow or intrusion (Tli / Ti) Typically brecciated and intensely weathered, grey, dark grey, or hematitic red andesitic flows and/or shallow intrusions occur throughout the sediment of Bear Creek, and appear to have been emplaced prior to deposition of the overlying sediment of Everson Creek. **Ti** is used when the outcrop pattern and distribution clearly indicate an intrusive contact, and **Tli** is used where petrographic analysis and outcrop distribution are inconclusive in determining whether the bodies are intrusive or extrusive. These lava flows or intrusions may correlate with intrusive rocks that intrude the basin-fill deposits in the Medicine Lodge basin (M'Gonigle and Hait, 1997). In the Jeff Davis Peak quadrangle, $^{40}Ar/^{39}Ar$ age determinations from an intrusion (Ti) near the top of the middle shale (Tsm) in section 12 of T 10 S, R 13 W yield a near plateau age of 47.2 ± 0.8 Ma (S. U. Janecke and W. C. McIntosh, unpublished data, 1996).

Summary of the Stratigraphy of the Sediment of Bear Creek

The relationship between the sediment of Bear Creek and the Lemhi Pass fault is equivocal for a number of reasons. First, the sediments are tilted to the northeast into the southwest-dipping Lemhi Pass fault, indicating deposition during or prior to movement along the fault. The temporal relationship between faulting and sedimentation cannot be adequately addressed due to non-deposition or subsequent erosion of the sediments of Bear Creek in the footwall of the fault in the study area.

Second, the older gravel unit (Tg1) in the hanging wall of the Lemhi Pass fault is dominated with volcanic clasts, despite being in fault contact with Proterozoic quartzites. This relationship might suggest movement along the Lemhi Pass fault after deposition of the gravel, but the lack of sediments preserved in the footwall fails to support or refute this interpretation. In addition, the older gravel unit is found at the same latitude as an east-flowing, pre- and syn-Challis paleovalley. The reestablishment of the paleovalley during deposition of the gravels would complicate any interpretations based on clast compositions within the gravels in the hanging wall of the Lemhi Pass fault.

Finally, if the lava / intrusions (Tli) into the sediment of Bear Creek in the field area correlate with the intrusion into the middle shale in the Jeff Davis Peak quadrangle (Ti, M'Gonigle and Hait, *in press*), then an age discrepancy exists for initiation of sedimentation in the Horse Prairie basin. The intrusion into the middle shale (Ti) has an $^{40}Ar/^{39}Ar$ near plateau whole-rock age of 47.2 ± 0.8 Ma, but intrudes units that overlie a rhyolite with an $^{40}Ar/^{39}Ar$ single sanidine age of 45.7 ± 0.14 Ma (Tr, Fig. 9). In addition, the sediment of Bear Creek in the Horse Prairie basin, which appears to correlate to the middle shale, postdates emplacement of the 46.01 ± 0.39 Ma quartz-sanidine ash flow tuff (Tcqs, Fig. 9). Age discrepancies between the anomalously old whole-rock age for the intrusion into the middle shale (Ti) and the presumably more

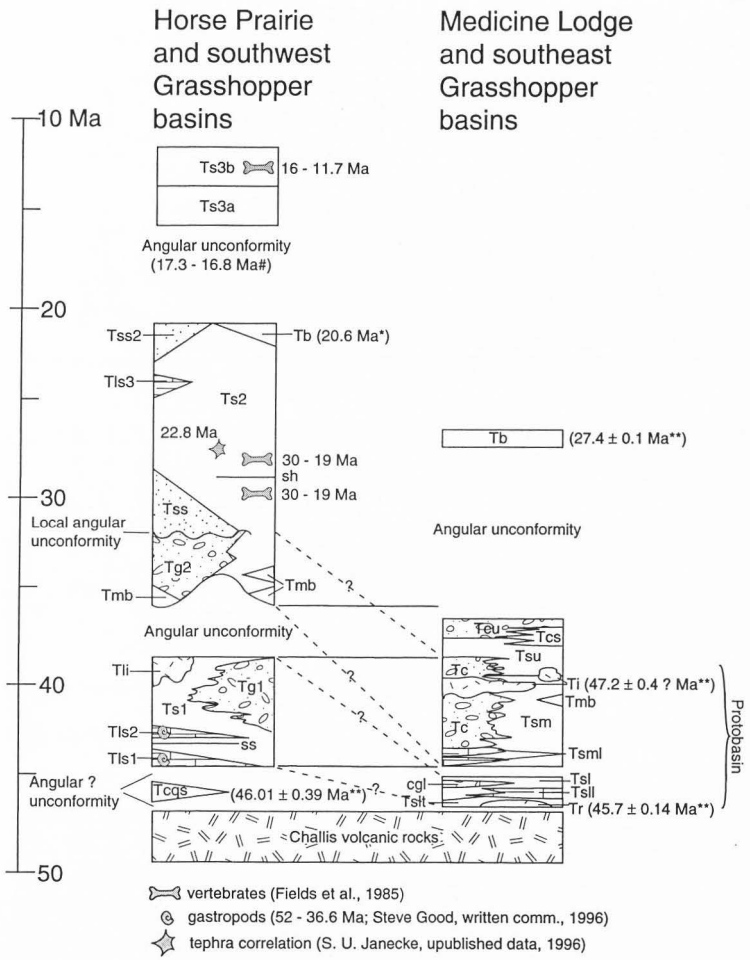
Horse Prairie and southwest Grasshopper basins
Medicine Lodge and southeast Grasshopper basins
10 Ma
20
30
40
50
Ts3b
Ts3a
16 - 11.7 Ma
Angular unconformity
(17.3 - 16.8 Ma#)
Tss2
Tb (20.6 Ma*)
Tls3
Ts2
22.8 Ma
30 - 19 Ma
sh
30 - 19 Ma
Tb
(27.4 ± 0.1 Ma**)
Local angular unconformity
Tss
Tg2
Tmb
Tmb
?
Angular unconformity
Angular unconformity
Teu
Tcs
Tsu
Tli
Tg1
Ts1
Tc
Ti (47.2 ± 0.4 ? Ma**)
Tmb
Tc
Tsm
Tls2
ss
Tls1
Tsml
Protobasin
Angular ? unconformity
Tcqs
(46.01 ± 0.39 Ma**)
?
cgl
Tsll
Tsl
Tsll
Tr (45.7 ± 0.14 Ma**)
Challis volcanic rocks
vertebrates (Fields et al., 1985)
gastropods (52 - 36.6 Ma; Steve Good, written comm., 1996)
tephra correlation (S. U. Janecke, upublished data, 1996)

accurate single sanidine ages for the underlying tuffs in the Horse Prairie and Medicine Lodge basins (Tcqs, Tr) suggest that the 47.2 ± 0.8 Ma intrusion age may be too old. Alternatively, the 47.2 ± 0.8 Ma date may be from a gravity emplaced rock slide of older volcanic or intrusive rock. Additional work is needed to resolve the apparent discrepacies with regards the timing of initial sedimentation in the Horse Prairie and Medicine Lodge basins.

Sediment of Everson Creek

The sediment of Everson Creek is the most widespread Tertiary deposit in the study area. The sediment is exposed throughout the Horse Prairie basin, and overlies Archean gneiss, Proterozoic quartzite, Challis volcanic rocks, and the sediment of Bear Creek in angular unconformity. In the study area, approximately 1.4 km of the sediment of Everson Creek are exposed beneath the overlying angular unconformity. The sediment conceals the older Lemhi Pass fault, and occupies the half-graben above the west-dipping Maiden Peak fault system. The sediment dips only 9° to the east in contrast to the underlying 35° northeast-dipping sediment of Bear Creek.

The sediment of Everson Creek is dominated by white to light tan, massive to thinly bedded tuffaceous siltstone, fine to coarse sandstone, and interbedded pebble conglomerate. Locally, the sediment contains lenses of megabreccia overlain by boulder and cobble gravels near the base of the section. In the northern half of the Everson Creek quadrangle, arkosic sandstone and conglomerate interfinger with finer-grained strata, including thin stringers of white to light tan, wood-bearing shales. Arkoses locally contain both biotite and muscovite, but muscovite does not appear to occur south of approximately 44° 56' 30" N latitude. Thin, laterally discontinuous lenses of thinly bedded, light to dark brown micritic limestone and calcareous sandstone occur locally near the top of the exposed section of the sediment of Everson Creek in the Everson Creek quadrangle. Mammalian fossil localities along Everson and Maiden Creeks contain

Arikareean and Hemingfordian vertebrates (samples 8, 11, Plate 1), suggesting a minimum age of early Miocene for the sediment of Everson Creek (Fields et al., 1985).

Megabreccia unit (Tmb) Multiple lenses of brecciated, white, tan, or orange densely welded quartz-sanidine ash flow tuff occur near the base of the sediment of Everson Creek in sections 4, 31, and 32 of T 10 S, R 14 W (Plate 1). This unit is lithologically identical to the quartz-sanidine tuff (Tcqs) of the Challis volcanic rocks, and is likely derived from the older tuff. The lenses of megabreccia are up to 35 m thick, and most likely reflect significant topographic relief in the hanging wall of the Maiden Peak fault system.

Middle gravel unit (Tg2) The middle gravel unit consists of up to 270 m of poorly sorted, weakly consolidated, well-rounded pebble to boulder gravels comprised dominantly of well-rounded Proterozoic quartzite clasts (50-90 percent) with lesser amounts of volcanic clasts (4-50 percent). With the exception of a thin lens in section 21 of T 11 S, R 14 W, the gravels appear to be confined to a paleovalley near the center of the Everson Creek quadrangle between approximately 44° 55' and 44° 58' N (Plate 1). This paleovalley is in the same area as the pre- to syn-Challis paleovalley and a possible paleovalley reestablished during deposition of the older gravel unit (Tg1). The middle gravel unit occurs at the base of the sediment of Everson Creek, and typically pinches out abruptly at the Lemhi Pass fault. This relationship may suggest the presence of remnant topography in the footwall of a recently dormant Lemhi Pass fault during deposition of the middle gravel unit.

Middle sediment unit (Ts2) The middle sediment unit is dominated by white to light tan, thick to thinly bedded tuffaceous siltstone and fine sandstone containing lenses of coarse sands and conglomerates. Pebble conglomerates often consist of over 70 percent well-rounded imbricated plates of tan to grey silicified Tertiary shale clasts, with lesser amounts of Proterozoic quartzite (0-85 percent) and volcanic clasts (0-50 percent;

Fig. 8). Thickly bedded, matrix-supported debris flow deposits containing subangular to rounded pebbles of quartzite and volcanic rocks are locally present. Risoliths, oscillatory ripple marks, and soft sediment deformation structures are common within finer-grained portions of this unit. The middle sediment unit occurs throughout the study area, and locally exceeds 950 m in thickness.

Sandstone unit (Tss) Two hundred meters of medium to thickly bedded, arkosic sandstone and conglomerate occur north of 44° 55' N latitude within the sediment of Everson Creek, and grade south into finer grained rocks within the middle sediment unit. Clasts range from coarse sand to cobbles in a quartz and feldspar sand and silt matrix. Proterozoic quartzite clasts are abundant (18-66 percent), with lesser amounts of volcanic rocks (16-52 percent) and grey to tan, recycled, platy Tertiary shale pebbles (0-46 percent). Muscovite and biotite grains (< 2 mm) are locally abundant, with the abundance of muscovite decreasing to the south. This unit is deposited directly on Archean gneiss in section 4 of T 10 S, R 14 W, on Challis volcanic rocks in sections 16 and 21 of T 10 S, R 14 W, and on the lower portions of the sediment of Everson Creek in sections 21 and 28 of T 10 S, R 14 W (Plate 1). Similar arkose and conglomeratic arkose occur stratigraphically higher in the sediment of Everson Creek in sections 1, 12, and 13 of T 11 S, R 14 W (M'Gonigle and Hait, 1997), and to the north in the Grasshopper basin (S. U. Janecke and J. W. M'Gonigle, unpublished data, 1995, 1996).

Shale unit (sh) A thin lense (3 m) of very thinly splitting, white to light tan, wood-bearing shales occurs along strike of the sandstone unit (Tss) in section 28 of T 10 S, R 14 W (Plate 1). Other shales occur locally throughout the sediment of Everson Creek, but are unmappable units.

Limestone unit (Tls3) Three exposures of thinly bedded, laterally discontinuous, dark to light brown micritic limestone and calcareous sandstone occur in

section 23 of T 10 S, R 14 W, and in section 15 of T 11 S, R 14 W in the upper half of the sediment of Everson Creek (Plate 1). This very localized unit is typically thin (< 12 m), and may be associated with localized hot springs or small internally drained ponds.

Sediment undifferentiated (Tsu) Poorly sorted, angular blocks of Mississippian limestone in a red mud and sand matrix occur in sections 8 and 9 of T 17 N, R 26 E (Plate 1). Quartzite clasts in the area of the exposures may be weathering from the undifferentiated sediment or may be float blocks from nearby exposures of Middle Proterozoic quartzite. The sediment appears to be restricted to the hanging wall of the Little Eightmile Creek fault. This unit rests on dacite lava flows (Tcdl), and is faulted against Middle Proterozoic quartzites in the footwall of the Little Eightmile Creek fault. The thickness of the sediment is uncertain, but approximately 1000 m appears to be preserved based on bedding traces and tonal changes on aerial photographs in the Little Eightmile Creek area. Because this unit is lithologically unlike any other sedimentary unit in the Horse Prairie basin, its age and stratigraphic equivalence are uncertain.

Summary of the Stratigraphy of the Sediment of Everson Creek

The sediment of Everson Creek represents the second unconformity-bounded package of sedimentary basin-fill in the Horse Prairie basin. Deposition of the sediment commenced after last motion on the Lemhi Pass fault, which is responsible for a 28° discordance in orientation between the sediment of Everson Creek and the underlying sediment of Bear Creek (Fig. 5). Orientation, lithology, provenance, and paleoflow data suggest that accumulation of the Oligocene to early Miocene sediment of Everson Creek was controlled by an active west-dipping Maiden Peak fault system (Fig. 10).

East-tilted megabreccias and coarse gravels show evidence for elevated topography in the hanging wall of the Maiden Peak fault system, and gneissic clasts derived from the footwall of the fault occur in conglomerates of the middle sediment unit

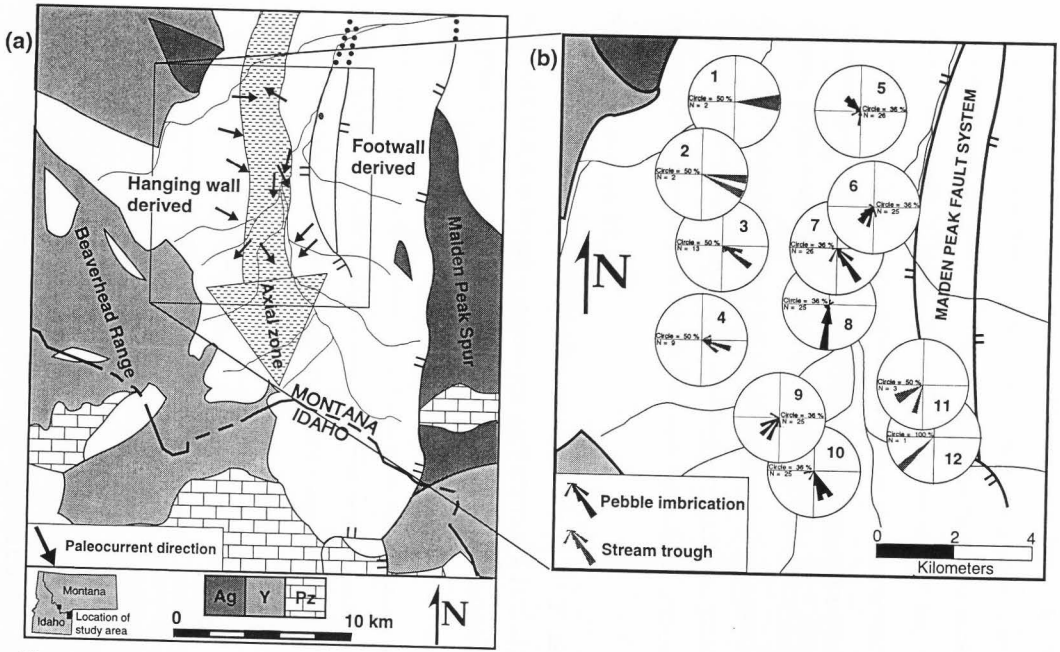

Figure 10. Interpretations of paleocurrent indicators from conglomerates of the sediment of Everson Creek. Rose diagrams (b) represent the direction of plunge for stream troughs where a flow direction could be determined, and the pole to the plane containing the long and intermediate axes of platy, well-rounded, imbricated pebbles. Mean paleocurrent vectors calculated from the rose diagrams in (b) have been included in Figure 17 for reference.

(Ts2) 1.2 km above the base of the section. Muscovite and biotite within the arkoses of the sediment of Everson Creek indicate that long axial drainage systems also persisted in the Oligocene and tapped sources 80 km to the north northwest in the northern Beaverhead Mountains (Thomas, 1995; S. U. Janecke, unpublished data, 1995, 1996; this study). This drainage system appears to have mixed with hanging wall and footwall drainages based on the occurrence of two-mica bearing arkosic debris, and Challis volcanic, Middle Proterozoic quartzite, and gneissic clasts within the same unit. Movement along the Maiden Peak fault system may have also been responsible for reestablishing an east-flowing paleoriver at the latitude of Lemhi Pass, which resulted in the accumulation of coarse gravels (Tg2) at the base of the sediment of Everson Creek.

Sediment of Bannock Pass

The sediment of Bannock Pass is exposed in sections 21, 22, 27, 28, 32, 33, 34, and 35 of T 11 S, R 14 W, and in sections 3, 4, and 5 of T 12 S, R 14 W within the field area (Plate 1). Other exposures can be found south and east of the field area in the Bannock Pass and Deadman Pass quadrangles (M'Gonigle, 1994). The sediment appears to be confined to the southern Horse Prairie basin, where a maximum thickness of 235 m is preserved, with the possible exception of two small accumulations in the hanging wall of the Bloody Dick Creek fault north of the study area and in the western Grasshopper basin in the southwest Coyote Creek and southeast Kitty Creek quadrangles (S. U. Janecke, unpublished mapping).

The sediment of Bannock Pass is dominated by tan to light brown, tuffaceous siltstone and sandstone. Scattered conglomerate lenses within the sediment contain pebbles and cobbles of Proterozoic quartzite and Archean gneiss on the west and east sides of the basin, respectively. The sediment dips gently (4°) to the east within the study area, and overlies the ~13° southeast-dipping sediment of Everson Creek in angular unconformity in the Bannock Pass quadrangle. Barstovian (middle Miocene) vertebrate

fossils found within the sediment of Bannock Pass indicate formation of this angular unconformity in early to middle Miocene time (sample 12, Plate 1; Fields et al., 1985).

Lower siltstone unit (Ts3a) The lower siltstone unit (lower mudstone unit, Tml of M'Gonigle, 1994) is poorly exposed in the study area. Mapping of the unit relied heavily on a characteristic dark tone on aerial photographs compared to the overlying upper siltstone (Ts3b). The lower siltstone unit is approximately 90 m thick in the study area, and likely contains conglomeratic lenses based on the abundance of subrounded to angular quartzite cobbles mantling its slopes.

Upper siltstone unit (Ts3b) Approximately 70 m of tan to light brown, massive to thinly bedded tuffaceous siltstone and fine-grained sandstone overlies the lower siltstone unit at the south end of the study area (Plate 1). Much of the original bedding appears to have been destroyed by intense bioturbation, but laminated bedding is preserved locally. This unit is typically poorly exposed, but contains pebble to cobble conglomerate lenses comprised of clasts of quartzite, volcanic rocks, and gneiss in the adjacent Deadman Pass quadrangle (M'Gonigle, 1994). This unit locally contains vertebrate fossils including horse, camel, and rhinoceros teeth and bones of Barstovian age in the Bannock Pass Quadrangle (sample 12, Plate 1; Fields et al., 1985).

Summary of the Stratigraphy of the Sediment of Bannock Pass

The dominantly fine-grained, nearly flat-lying sediment of Bannock Pass records minimal tilting associated with extensional deformation since middle Miocene time. Archean clasts found in exposures adjacent to the Maiden Peak spur, and quartzite clasts found on the west side of the basin show an approximately symmetric distribution of sediment derived from the east and west. The sediment of Bannock Pass likely represents passive infilling of a preexisting half-graben, given its distribution, orientation, lithology, and provenance. Similarly, exposures of the sediment of Bannock Pass north

of the study area, in the hanging wall of the Bloody Dick Creek fault, may reflect passive infilling of a preexisting half-graben that was later reactivated by latest motion on the younger strand of the Bloody Dick Creek fault (see discussion of Bloody Dick Creek fault).

Although the sediment of Bannock Pass appears to represent a period of tectonic quiescence, the underlying angular unconformity is the result of tilting in the hanging walls of both the Maiden Peak and Little Eightmile Creek faults. On average, a 5° discordance in dip exists between the east-dipping sediments of Bannock Pass and Everson Creek (Fig. 5), which is likely the result of the last phase of extension on the Maiden Peak fault system. Locally, however, a discordance in strike is also present, reflecting motion on the northwest-dipping Little Eightmile Creek fault.

Younger Gravel Deposits

Poorly sorted, well-rounded, unconsolidated boulders, cobbles, and sand cap ridges and hills throughout the Everson Creek and Bannock Pass quadrangles (Plate 1). These deposits are up to 30 m thick, and typically contain a variety of quartzite clasts derived from bedrock to the west and from gravels within underlying Tertiary deposits. The designation **QTgo** is given to gravels capping topographically high ridges and hills, which are typically expressed by a distinct break in slope at their base. Topographically lower gravels that do not exhibit a distinct break in slope are referred to as **QTgy**.

The basal contact of the younger gravel deposits appears to define a very subtle angular unconformity where they overlie the sediment of Bannock Pass, and a slightly more pronounced angular unconformity where they overlie the sediment of Everson Creek. Younger gravel deposits are found up to 230 m above current river level, showing considerable incision since deposition of the gravel in the late Pliocene (?) to Pleistocene (?). Deposition of the gravels may suggest renewed tectonism in the study area, or simple headward erosion at the headwaters of the Missouri River drainage basin.

Tectonic Significance of Basin-Fill Deposits

Basin-fill deposits preserved in the Horse Prairie basin provide important insights into the tectonic evolution of the basin, possible effects of multiple generations of extension on basin geometry, and sedimentation patterns within rift zones. Angular unconformities separating the Challis volcanic rocks, sediment of Bear Creek, sediment of Everson Creek, and sediment of Bannock Pass reflect distinct episodes of extension within the study area (Fig. 5). Discordances in both dip and strike show evidence for tilting into west-, southwest-, and northwest-dipping normal faults. In addition to evidence of tectonic activity, the sediments also indicate periods of tectonic quiescence. An overall lack of sediments preserved above the relatively flat-lying, fine-grained middle Miocene sediment of Bannock Pass suggests little Neogene extensional deformation in the Horse Prairie basin.

One consequence of multiple angular unconformity-bounded packages of basin-fill, and of the multiple generations of normal faulting that controlled them, is the superposition of depocenters with unique distributions and geometries. The result is a three-dimensionally complex compound basin containing deposits that thin abruptly along strike, down dip, and across normal faults of various ages. In areas that experience more than one episode of extension, structures controlling the present topographic basin do not necessarily control the distribution and thickness of basin-fill deposits.

STRUCTURAL GEOLOGY

The Horse Prairie basin is a complexly faulted and folded east-dipping half-graben that developed on the margins of the middle Eocene Challis volcanic field. The basin is located within the Sevier fold and thrust belt, and west of late Cretaceous to Eocene Laramide-style uplifts in the foreland. Much of the Cenozoic evolution of the Horse Prairie basin is characterized by a long (>47 m.y.) and complex period of crustal extension, subsequent to crustal contraction associated with the Sevier and Laramide orogenies.

Geologic mapping and basin analysis of the Horse Prairie basin indicate formation of vertically superposed depositional basins in response to multiple episodes of Cenozoic extension. At least five geometric and temporally distinct episodes of extension have affected the Horse Prairie basin in the late Mesozoic (?) to the Cenozoic, and basin-fill deposits are associated with three of these events. Five large (>2 km dip slip) southwest-, northwest-, and west-dipping normal faults have been mapped within the study area. In addition, at least three sets of extension-related folds deform the Tertiary basin-fill deposits at different stratigraphic levels. A discussion of the structures found in the study area will begin with a general overview of the thrust faults in the region, followed by a detailed discussion of the normal faults and extension-related folds.

FAULTS

Thrust Faults

Archean, Proterozoic, Paleozoic, and Mesozoic units within southwestern Montana were transported in several thrust plates during the Sevier orogeny, and were later dissected by both low- and high-angle normal faults of Mesozoic (?) to Cenozoic age (Scholten et al., 1955; Skipp, 1988; M'Gonigle and Dalrymple, 1993). Major thrust sheets in the region include (from structurally highest to lowest) the Hawley Creek, Fritz

Creek, Cabin, Medicine Lodge, Grasshopper, Maiden Peak gneissic, McKenzie, Four Eyes Canyon, Armstead, Tendoy, and Lima thrust sheets (Skipp, 1985, 1988; Perry et al., 1989; M'Gonigle, 1993; Fig. 3). The Cabin-Medicine Lodge thrust may be directly relevant to structures mapped within the study area, and will be discussed in slightly more detail.

The youngest thrust fault in the region, the Cabin, appears to be an out-of-sequence thrust within the Medicine Lodge thrust system (Skipp 1988). Skipp (1985) hypothesized the presence of the Cabin thrust directly beneath the Horse Prairie basin, linking the Cabin thrust of the southern Beaverhead Mountains to the Beaverhead Divide fault zone (Tucker, 1975) and the Miner Lake fault zone (MacKenzie, 1949) to the northwest. In addition, Skipp (1985, 1988) interpreted a south-dipping Proterozoic quartzite on Archean gneiss contact (Thrust D of M'Gonigle, 1993) in the immediate hanging wall of the Cabin thrust in the southern Maiden Peak Spur to be the original depositional margin of the Proterozoic Belt basin. If these interpretations are correct, the original margin of the Belt basin must lie under the Tertiary basin-fill deposits of the Horse Prairie basin, separating Proterozoic quartzites and siltites west of the basin from Archean gneisses to the east. Alternatively, M'Gonigle (1993) interpreted the Proterozoic on Archean contact in the southern Maiden Peak Spur as a younger-on-older thrust later reactivated as a low-angle normal fault. M'Gonigle (1993) did not hypothesize the presence of a thrust through the Horse Prairie basin, but instead showed the Cabin and Medicine Lodge thrusts terminating at the southeast margin of the Horse Prairie basin.

Other workers also differed in their interpretations of thrust faults in the Horse Prairie region. Coppinger (1974) correlated the Miner Lake fault to the Bloody Dick Creek fault zone northwest of the study area. And, whereas Coppinger (1974) did not hypothesize the continuation of this southwest-dipping thrust through the Horse Prairie basin, map relationships suggest that the thrust is simply concealed by younger Tertiary

basin-fill. Hansen (1983) appeared to agree with the correlation of Coppinger (1974), but terminated the Miner Lake-Bloody Dick Creek thrust fault at approximately 45° N latitude at the Horse Prairie fault zone of Scholten (1982). Ruppel and Lopez (1984) had a different interpretation, and correlated the Beaverhead Divide fault zone to the Medicine Lodge fault system to the southeast, but did not continue the structure under the basin-fill deposits. Neither M'Gonigle (1993), Ruppel and Lopez (1984), Hansen (1983), nor Coppinger (1974) explicitly stated that a thrust fault is required under the Tertiary basin-fill of the Horse Prairie basin, but their interpretations suggested it.

Critical evaluation of the various interpretations listed here is beyond the scope of this study, but the possible presence of the Cabin or Beaverhead Divide-Miner Lake-Bloody Dick Creek fault zones, and the original rifted margin of the Belt basin beneath the Horse Prairie half-graben may have influenced the geometry of the Cenozoic normal faults (Werkema and Young, 1983; Young, 1985). Inheritance from preexisting structures is well documented in this region (Schmidt et al., 1984; Schmidt et al., 1993; Kellogg et al., 1995; Janecke et al., 1996a; Schmidt, 1996; Harlan et al., 1996), and although no thrust faults were mapped in the actual study area, buried compressional structures may have had an effect on the orientation of the subsequent extensional deformation.

Major northeast-, northwest-, and north-striking normal faults have dissected the Horse Prairie basin throughout the Cenozoic, and possibly as early as the late Cretaceous. Five major temporally and geometrically distinct generations of normal faults occur within the study area, including pre-volcanic, syn-volcanic, and late to post-volcanic normal faults, as well as two generations of Neogene normal faults. The following discussion will progress in chronologic order from the oldest to the youngest younger-on-older fault in the study area, and will include the location, geometry, timing, and offset for each major normal fault. In addition, correlations to similar structures in the region, and

interpretations of mechanisms for the formation of each major generation of normal faulting will be discussed.

Pre-Middle Eocene Normal (?) Faults

Two large magnitude normal (?) faults in the Beaverhead Mountains predate the middle Eocene Challis Volcanic Group. Both faults dip southwest and both are in the footwall of thrust faults. These normal (?) faults are major structures, and may accommodate tens of kilometers of slip.

Divide Creek Fault

A northeast-striking, southeast-dipping, low-angle, younger-on-older fault places Mississippian carbonates over Proterozoic quartzite and siltite southwest of the basin (Staatz, 1973; VanDenburg et al., 1996; DCF, Fig. 2). This fault, first mapped by Staatz (1973) as the Goat Mountain thrust, was reinterpreted by Skipp (1988) as a low-angle normal fault. This Mississippian over Proterozoic relationship is also present farther south in the Beaverhead Mountains, in the Railroad Canyon area (Staatz, 1973; S. U. Janecke and C. J. VanDenburg, unpublished mapping), just north of Hawley Creek (Lucchitta, 1966), and south of the Nicholia Creek basin (Skipp, 1984; Scholten and Ramspott, 1968) where it has been termed the Divide Creek fault. Other segments of a gently southwest-dipping younger-on-older fault occur northwest of the study area, including segments in the northwest Lemhi Range and Salmon River Mountains (Soregaroli, 1961; Landreth, 1964; Tietbohl, 1981, 1986; Connor and Evans, 1986; Ekren, 1988; Evans and Zartman, 1990; Janecke et al., *in review*). I follow Janecke et al. (*in review*) and interpret the Mississippian over Proterozoic fault in the study area as a portion of the regionally extensive, southwest-dipping Divide Creek fault. The segment of the Divide Creek fault found in the study area is located approximately 1.5 miles northwest of Little Eightmile Creek in the south westernmost corner of the map area

(Plate 1). This segment juxtaposes Mississippian Scott Peak Formation (K. Lund, oral communication, 1996) in the hanging wall against Middle Proterozoic quartzites of the Lemhi Group in the footwall (Staatz, 1973), and omits approximately 3 km of stratigraphy.

The geometry of the segment of the Divide Creek fault in the study area is poorly constrained at depth. At the surface, three-point analysis of this fault yields a strike of 055° and a dip of 36° to the southeast (Table 1). The present orientation of the fault is not representative of its orientation during movement due to subsequent tilting to the southeast into the northwest-dipping Little Eightmile Creek fault (C_1-C_1'; Plate 2). Rotation of the Challis volcanic rocks that overlie the fault to horizontal results in a strike of 167° and a dip of 28° to the southwest for this segment of the Divide Creek fault (Table 1). Due to lack of subsurface data, the fault surface is assumed to be planar in the shallow subsurface for the purpose of cross section construction, except where the fault is gently folded into a rollover anticline in the immediate hanging wall of the Little Eightmile Creek fault. The Divide Creek fault omits approximately 3 km of stratigraphy, with both hanging wall and footwall rocks subparallel to the fault in a "flat on flat" relationship. Given the large stratigraphic omission, and low angle geometry of the Divide Creek fault, tens of kilometers of dip-slip separation is likely.

The Divide Creek fault cuts rocks as young as Permian in the southern Beaverhead Mountains (Skipp, 1984), and is lapped by middle Eocene volcanic rocks 2 km northwest of the headwaters of Little Eightmile Creek (Plate 1), permitting either a Mesozoic or Early Tertiary age. Other segments of the Divide Creek fault are also older than Challis volcanic rocks. On a more regional scale, the Divide Creek fault lies in the footwall of the Hawley Creek thrust, and is subparallel to the thrust for over 150 km (Janecke et al., *in review*; Fig. 11). The Divide Creek fault may slightly postdate the late Cretaceous (?) Hawley Creek thrust. Both structures ramp down-section in the hanging

TABLE 1. DESCRIPTION OF MAJOR LATE-MESOZOIC (?) AND CENOZOIC NORMAL FAULTS IN THE STUDY AREA

Episode of extension	Present geometry Restored geometry	Age	Name	~ Dip slip separation	Heave / Throw
Pre-middle Eocene	055° / 36° 167° / 28°	Post- Permian Pre- 49.5 Ma	Divide Creek fault	10's of km	heave >> throw
Pre-middle Eocene	161° / 51° 356° / 82° (?)	Post- Permian Pre- 49.5 Ma	Bloody Dick Creek fault (old strand)	unknown	unknown
Syn-volcanic	NE-striking / NW-dipping	Post- 48.0 Ma Pre- 46.0 Ma	Syn-Challis faults	0.9 km 1.3 km	0.4 km / 0.8 km 0.7 km / 1.1 km
Late to post-volcanic	102° / 24° 122° / 27°	Post- 48.6 Ma Pre- early Miocene	Lemhi Pass fault	2.4 km	2.2 km / 1.0 km
Late to post-volcanic	NNW / 20°-35° WSW	Post- 49.5 Ma Pre- late early Miocene	Maiden Peak fault system	11.7 km	9.6 km / 6.7 km
Basin and Range-1	212° / 34° (?)	Post-Early Miocene Pre-Middle Miocene	Little Eightmile Creek fault	3.0 - 1.0 km	1.5 km / 2.6 km - 0.5 km / 0.9 km
Basin and Range-2	NW-striking SW-dipping	Post-Middle Miocene	Basin and Range faults	1.1 km	0.6 km / 0.9 km

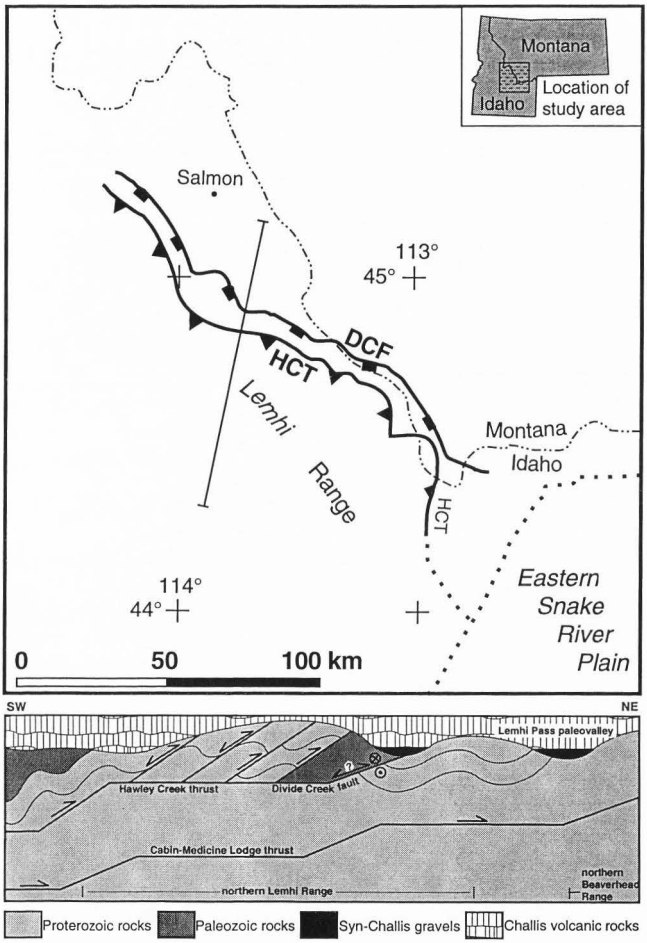

Figure 11. Location map and schematic cross-section of the Divide Creek normal (?) fault (DCF) and Hawley Creek thrust (HCT). The Divide Creek fault is located in the footwall of the Hawley Creek thrust, and may sole into the thrust at depth. Map and cross section modified from Janecke et al. (in review) to show southwest-dipping normal faults of Tysdal (1996a), Tysdal (1996b), and Tysdal and Moye (1996) in the hanging wall of the Hawley Creek thrust.

wall and footwall to the northwest, with the Hawley Creek thrust dipping about 15° steeper than the nearest segment of the Divide Creek fault (Janecke et al., *in review*). The Divide Creek fault may sole into the Hawley Creek thrust at depth (Fig. 11), and a genetic relationship between the two structures is likely. However, kinematic constraints on the Divide Creek fault are not available at this time.

Bloody Dick Creek Fault System

The northwest-striking, southwest-dipping Bloody Dick Creek fault is located between Bloody Dick Creek and Trail Creek in the northwestern corner of the Everson Creek quadrangle (Plate 1). The fault was first mapped by Coppinger (1974) as a thrust fault that places Proterozoic quartzites of the Yellowjacket Formation on the Wallace Formation. However, Hansen (1983) mapped the Bloody Dick Creek fault system as juxtaposing different sections of the Big Creek Formation in a younger-on-older relationship. Hansen (1983) concluded that the original thrust of Coppinger (1974) was reactivated by more recent normal slip, placing Big Creek Formation quartzites in the hanging wall on Archean gneissic rocks and Big Creek Formation quartzites in the footwall. The net normal slip on the Bloody Dick Creek fault zone is difficult to constrain because the correlation of Proterozoic rocks in the footwall and hanging wall is controversial (compare Coppinger, 1974; Hansen, 1983, and Ruppel et al., 1993), but exposure of Archean gneisses underlying the Proterozoic quartzites in the footwall of the southeasternmost segment of the fault suggests that normal dip-slip separation increases in that direction (Fig. 4).

The geometry of the Bloody Dick Creek fault is partially obscured by a diabase intrusion, but three-point analysis of the fault in the southwestern Coyote Creek quadrangle (Janecke, unpublished mapping) yields a strike of 341° and a dip of 51° to the southwest (Table 1). However, restoration for subsequent tilting changes the fault to a steeply east-dipping structure (356° / 82° E) in the northern Everson Creek quadrangle.

Geometric constraints are also complicated by the apparent reactivation of most of the Bloody Dick Creek fault by a younger north northwest-striking, west southwest-dipping normal fault (Fig. 4). Where the older and younger faults coincide (north of Bloody Dick Creek), subhorizontal tuffaceous Cenozoic sediments in the hanging wall appear lithologically identical to Barstovian (late-early Miocene) sediments found in the Bannock Pass quadrangle to the south (M'Gonigle, 1993; Janecke, unpublished mapping). The location of the younger strand of the Bloody Dick Creek fault south of Bloody Dick Creek is largely speculative, but exposures of brecciated quartzite suggest that the fault may continue at least to Bear Creek and coincide with a small west northwest-dipping normal fault in section 30 of T 10 S, R 14 W (Plate 1).

A dark-green aphanitic to fine-crystalline diabase (TKdb) commonly intrudes the older strand of the Bloody Dick Creek fault within the study area (Plate 1; Hansen, 1983). Middle Eocene lava flows and ash flow tuffs of the Challis volcanic rocks overlie both the older strand of the fault and the intruding diabase to the southeast (A-A'; Plate 2). North of Magpie Gulch, in sections 5, 6, 7, and 8 of T 10 S, R 15 W, the older strand of the fault and diabase are intruded by an aphanitic mafic intrusion (Plate 1). $^{40}Ar/^{39}Ar$ whole-rock analyses of the mafic intrusion, which postdates faulting and intrusion by the diabase, yield an age of 47.3 ± 0.4 Ma (sample 1, Plate 1; S. U. Janecke and W. C. McIntosh, unpublished data, 1996). These data are consistent with the preferred interpretation of Hansen (1983) of a Paleocene to Eocene age for the older strand of the Bloody Dick Creek fault zone; however, a very disturbed $^{40}Ar/^{39}Ar$ whole-rock age of 200-600 Ma for the diabase (sample 2, Plate 1) suggests an Early Jurassic or older age for initial slip along the Bloody Dick Creek fault zone (S. U. Janecke and W. C. McIntosh, unpublished data, 1996).

Discussion of Pre-Middle Eocene Normal (?) Faults

North- to northwest-striking pre-middle Eocene normal faults, like the Divide Creek and Bloody Dick Creek faults, were recently documented in the northern Lemhi Range in the hanging wall of the Hawley Creek thrust by Tysdal and Moye (1996), Tysdal (1996a), and Tysdal (1996b). Tysdal and Moye (1996) hypothesized reactivation of Mesozoic thrust faults by large displacement southwest-dipping normal faults before eruption of Eocene volcanic rocks.

Several striking similarities also exist between the Divide Creek fault as defined by Janecke et al. (*in review*) and the older strand of the Bloody Dick Creek fault. Both structures are parallel to, and lie in the footwall of thrust faults (the Hawley Creek thrust and the Beaverhead Divide thrust respectively), both faults are pre-Challis in age, and both strike northwest and dip southwest. Therefore, a common process may have produced these younger-on-older faults. The younger strand of the Bloody Dick Creek fault, however, parallels other northwest-striking late Cenozoic Basin and Range normal faults in the region (e.g. Beaverhead fault, Crone and Haller, 1991), contains Neogene sediments in the hanging wall, and is most likely related to other young Basin and Range faults in the region. If Hansen (1983) and Coppinger (1974) were correct to infer some early thrust slip along the Bloody Dick Creek fault, this fault was reactivated twice as a normal fault, once in pre-Challis time and again in the late Cenozoic.

The older Bloody Dick Creek and Divide Creek faults have at least three possible origins: they may be out-of-sequence thrust faults, strike-slip faults, or normal faults. The geometry and location of the Bloody Dick Creek and Divide Creek faults with respect to adjacent thrust faults (the Hawley Creek thrust and the Beaverhead Divide thrust respectively) might favor the out-of-sequence thrust interpretation. However, other out-of-sequence thrust faults documented in the region (Skipp, 1988; Haley et al., 1995; Horton, 1995) still retain an older-on-younger geometry.

In a study of the 30° southwest-dipping Lake Creek fault in south-central Idaho, Huerta and Rodgers (1996) concluded that slip was predominantly dextral strike-slip, with a 2° northwest-plunging slip vector. Huerta and Rodgers (1996) also concluded that the present-day gentle dip of the fault is representative of its initial orientation. A strike-slip origin is possible for the Bloody Dick Creek and Divide Creek faults, given the lack of kinematic data, and their parallelism to the Lake Creek fault farther to the southwest. But, based on the younger-on-older geometry, regional extent, and new data from the region, I favor the third interpretation that the Divide Creek and older Bloody Dick Creek faults reflect an episode of late Cretaceous (?) to early Tertiary crustal thinning. If the Bloody Dick Creek and Divide Creek faults are genetically related to the large normal faults recently identified in the northern Lemhi Range (Tysdal and Moye, 1996; Tysdal, 1996a; Tysdal, 1996b), they would have formed during a regional episode of late Mesozoic crustal collapse near structural culminations within the Sevier fold and thrust belt (Janecke et al., *in review*). If we are correct in interpreting the Divide Creek and Bloody Dick Creek faults, and three large younger-on-older faults in the northern Lemhi Range as normal faults, they are the oldest extensional structures in this region. Further work may show that these faults, like others in the Cordillera (Hodges and Walker, 1992) and the Himalayas (Royden and Burchfield, 1987), are coeval with the large thrust faults.

Syn-Volcanic Faults

Northeast-striking middle to late Eocene faults, which were active during to slightly after deposition of the Challis volcanic rocks, have been documented by previous workers in southwestern Montana and east-central Idaho (McIntyre et al., 1982; M'Gonigle et al., 1991; Janecke, 1992, 1995; Janecke et al., *in review*). Although northeast-striking syn-volcanic faults do not extend the upper Horse Prairie basin significantly, three such structures are located within the study area. Less than 0.5 km

northwest of North Fork Everson Creek in section 7 of T 11 S, R 14 W, a scoop-shaped (concave to the northwest) east northeast- to northeast-striking, northwest-dipping normal fault places lava flows at the base of the Challis volcanic rocks in the hanging wall against Middle Proterozoic quartzites in the footwall (Plate 1).

The geometry of the northeast-striking fault changes along strike, and is therefore difficult to characterize using standard three-point analysis. If an average dip on the fault plane of 60° is assumed, the dip slip separation of the base of the Challis volcanic rocks is approximately 1.3 km, with 0.7 km of heave and 1.1 km of throw (Table 1). However, these values should be considered a maximum offset due to the possibility of a pre-Challis paleohill in the footwall of the normal fault, which may be responsible for a portion of the apparent offset on the base of the lava flows.

The second northeast-striking, northwest-dipping syn-Challis fault is located in section 25 of T10 S, R15 W, and probably continues to the southwest along Bear Creek (Janecke, unpublished mapping; Plate 1). The continuation of the northwest-dipping fault southwest along Bear Creek also explains the abrupt termination of a thick sequence of Challis lava flows in and south of section 34, T 10 S, R 15 W against Proterozoic rocks in the footwall (Staatz, 1979). In section 25, the lithic-rich ash flow tuff and basal lava flows of the Challis volcanic rocks are displaced down to the northwest, but younger lava flows unconformably overly the fault. The fault has an approximate strike of 055°, but also appears to be nonplanar. Approximately 900 m of dip slip separation, 400 m of heave, and 800 m of throw occur on the fault, assuming pure dip slip on a 60° fault plane, and a dip of 44° northeast on the base of the lava flows (Staatz, 1979; Janecke, unpublished mapping). The northeast strike of both syn-Challis normal faults is retained even after restoration of the overlying northeast-dipping volcanic rocks to horizontal.

The third northwest-dipping syn-Challis fault is located in the east-central Goat Mountain and northwest Bannock Pass quadrangles, and is here referred to as the Little

Eightmile Creek fault. Most of the slip on this normal fault occurred in the Neogene, but changes in the thickness of volcanic rocks across the structure indicate syn-Challis movement. Approximately 450 m of volcanic rocks are preserved in the hanging wall of the Little Eightmile Creek fault, whereas only 140 m are preserved in the footwall (B-B'; Plate 2). The change in thickness across the fault indicates motion during or immediately following volcanism, prior to deposition of the overlying sediment of Bear Creek (see Basin and Range faults--Phase 1 for further discussion).

A middle Eocene age is assigned to these northeast-striking faults based on cross-cutting relationships and age control within the Challis volcanic rocks. All three structures offset the base of the Challis volcanic rocks, including a 48.04 ± 0.43 Ma lithic rich tuff (M'Gonigle and Dalrymple, 1993), and two of the three faults are lapped by lava flows that predate emplacement of a 46.01 ± 0.39 Ma sanidine-quartz ash flow tuff (M'Gonigle and Dalrymple, 1993). Given the geometric and age constraints for these structures, I correlate these faults to other northeast-striking syn-volcanic faults throughout the region that have extended the 49.5 to 45 Ma Challis arc (Janecke, 1992, 1995).

Syn-volcanic extension is likely the result of a brief reorientation of stresses during Challis volcanism, because northwest-southeast extension is anomalous and short-lived in the study area, and orthogonal to the dominant Paleogene extension direction. Northeast-striking, syn-volcanic normal faults may simply reflect a brief interruption in an overall east northeast-west-southwest extension of the crust.

Late to Post-Volcanic Faults

Two normal faults, the Lemhi Pass and Maiden Peak faults, were responsible for the formation of the Horse Prairie half-graben and the preservation of most of the Tertiary basin-fill deposits in the study area. The Lemhi Pass fault is the first normal fault associated with syn-rift sedimentary deposits, but it was the younger west-dipping

Maiden Peak fault system that blocked out the north-south trend of the Horse Prairie basin. Formation of the Lemhi Pass and Maiden Peak fault systems may have been roughly coeval, but the Maiden Peak fault system clearly outlasted the Lemhi Pass fault. Overall the two faults probably record continued gravitational collapse of the fold and thrust belt that began in pre-Challis time along the Divide Creek and related faults.

Lemhi Pass Fault

A west northwest-striking, south southwest-dipping, low-angle normal fault, which juxtaposes middle to late Eocene (?) coarse cobble to boulder gravels and Middle Proterozoic quartzites, is located south of the confluence of Bear Creek and Trail Creek (Plate 1). This structure continues to the northwest into the Lemhi Pass thorium district, and was named the Lemhi Pass fault by previous workers (Sharp and Cavender, 1962; Staatz, 1979; Hansen, 1983). Previous interpretations include a subvertical to steeply southwest-dipping, bifurcating fault zone that initiated prior to Challis volcanism and was reactivated sometime after deposition of post-Challis basin fill (Staatz, 1972, 1979; Hansen, 1983). This multiphase interpretation is permitted by the data collected in this study, but multiple episodes of slip on the Lemhi Pass fault zone are not required, and a single phase of deformation seems more likely.

The Lemhi Pass fault, contrary to previous interpretations, is a gently southwest-dipping structure within the field area, and may be low angle throughout its trace length (S. U. Janecke, and J. J. Blankenau, unpublished mapping). Three-point analysis of the fault contact in the Everson Creek quadrangle yields a strike of 282° and a dip of 24° to the south southwest. If the effects of subsequent tilting are corrected, by restoring the overlying sediment of Everson Creek to horizontal, the original orientation of the fault has a strike of 302° and a dip of 27° to the southwest. The apparent dextral strike-slip separation on the east- to northeast-dipping basal Tertiary contact is approximately 7.52 km (after elevation corrections), corresponding to a dip-slip separation of 18.6 km,

assuming pure dip slip and using an average east dip of 45° for the basal Tertiary contact. However, a cross section constructed near the easternmost exposures of the Lemhi Pass fault (A-A'; Plate 2) shows only 2.4 km of dip slip separation, leaving 6.55 km of the apparent strike-slip separation to dextral strike-slip motion. The strike-slip separation may greatly exceed the dip-slip separation if 1) the fault has a significant strike-slip component of deformation, 2) pure dip-slip separation diminishes to the east southeast, or 3) some combination of 1) and 2). Given that less than 8 km separate the line of cross section and the offset on the basal Tertiary contact, explanation 2) would result in an unreasonable slip gradient, and therefore, the Lemhi Pass fault is assumed to have at least some component of dextral strike-slip motion. This agrees with work in progress (J. J. Blankenau and S. U. Janecke) that suggests that the Lemhi Pass fault is the southeast continuation of a large southwest-dipping detachment fault along the northeast margin of the Salmon basin. The 75-km-long fault has southwest-plunging striae in the Salmon Basin (J. J. Blankenau and S. U. Janecke, unpublished data, 1996). If this slip vector applies to the west northwest-striking segment of the Lemhi Pass fault in the study area, a dextral componenet of slip is required.

In the west-central Everson Creek 7.5 minute quadrangle, the Lemhi Pass fault places gravels of the sediment of Bear Creek on the quartzite-bearing ash flow tuff (Tcq), and is overlain by gravels and fine-grained tuffaceous deposits of the sediment of Everson Creek (D-D'; Plate 2). This relationship suggests the Lemhi Pass fault initiated after deposition of the middle to late Eocene sediment of Bear Creek, and ceased before deposition of the Oligocene to early Miocene sediment of Everson Creek. In addition, a pronounced angular unconformity exists between the sediment of Bear Creek and the sediment of Everson Creek. This angular unconformity spans the entire study area, but is most pronounced in section 30 of T 10 S, 14 W in the immediate hanging wall of the Lemhi Pass fault. The sediment of Bear Creek, which unconformably overlies a 46.01 ±

0.39 Ma sanidine-quartz ash flow tuff (M'Gonigle and Dalrymple, 1993), strikes 330° and dip 35° northeast, on average, whereas the overlying sediment of Everson Creek, which contains Arikareean (29-20.5 Ma) vertebrates (sample 8, Plate 1; Fields et al., 1985), strikes 000° and dips 9° east (Fig. 5). We interpret the 26° discordance in dip, and the 30° discordance in strike between the sediments of Bear and Everson Creek (Fig. 5) as the result of tilting and folding of the sediment of Bear Creek in the hanging wall of the southwest-dipping Lemhi Pass fault prior to deposition of the sediment of Everson Creek. The ages of units that bracket the pronounced angular unconformity associated with tilting into the Lemhi Pass fault indicate a middle Eocene to early Oligocene age for the structure.

Geometric and kinematic data suggest that the Lemhi Pass fault is the same age as, and is probably genetically related to the Muddy-Grasshopper fault, another large north northwest-striking, west-dipping, low-angle normal fault present in the Tendoy Range along the east side of the Medicine Lodge and Grasshopper half-grabens (Janecke et al., 1996a; Fig. 2). The majority of slip on this low-angle structure predates a 27.4 ± 0.8 Ma basalt flow and associated intrusions of the Grasshopper basin (S. U. Janecke and W. C. McIntosh, unpublished data, 1996). A genetic relationship between the Muddy Grasshopper and Lemhi Pass faults is likely, given their geometric and temporal similarities. Mechanisms involved in the down-to-the-west and southwest displacement along these structures will be discussed later.

Maiden Peak Fault System

The north- to north northwest-striking, west-dipping Maiden Peak fault system separates the Tertiary sediments and volcanic rocks of the Horse Prairie basin in its hanging wall from Archean gneisses and Paleozoic rocks in the footwall (M'Gonigle, 1994; Fig. 2). The Maiden Peak fault system consists of a single west-dipping fault where it bounds the southeastern Horse Prairie basin in the Deadman Pass quadrangle,

but it bifurcates into a number of east-, west-, and southwest-dipping faults north of the north fork of Maiden Creek (M'Gonigle, 1994; M'Gonigle and Hait, *in press*; Fig. 2). Three-point analysis of the westernmost splay of the Maiden Peak fault system between Shenon and Jeff Davis Creeks (M'Gonigle and Hait, *in press*) results in a strike of 002° and a dip of 20° west. Based on map patterns of relatively poorly exposed rocks, the Maiden Peak fault system appears to be low- to moderate-angle throughout its trace length. Unmigrated industry reflection seismic data also suggest a shallow dip for the southern strand of the fault along North Fork Maiden Creek (Fig. 12). An average dip of 35° was calculated for the fault using the depth to the fault plane at 0.6 seconds (2-way travel time) on a reflection seismic profile (Fig. 12), a velocity of 9300 ft/s, and the mapped surface trace of the fault 1.5 km south of Chinatown (M'Gonigle, 1994). A lack of substantial post-Early Miocene extension and tilting in the vicinity of the Maiden Peak fault suggests that its current low-angle dip is representative of its attitude during the latest phases of slip.

The amount of displacement on the Maiden Peak fault system is difficult to constrain accurately due to erosion of the Tertiary rocks in the footwall, but a total dip-slip separation of 11.7 km, with 9.6 km of heave and 6.7 km of throw, is estimated across the three splays of the fault system using the base of the Challis volcanic rocks along an east-west transect at 45° 55' N latitude (D-D'; Plate 2). The eastern and western splays of the fault system account for 5.2 km and 4.8 km of the total 11.7 km of dip-slip separation, respectively. The east-dipping central splay appears to be a smaller antithetic fault to an overall west-dipping fault system, and only accounts for 1.7 of the 11.7 km of dip-slip separation.

Cross-cutting relationships can be used to loosely bracket the timing of extension on the Maiden Peak fault system between middle Eocene and early Miocene time. The fault system cuts Challis volcanic rocks, the sediments of Everson Creek, and may cut the

Figure 12. Unmigrated industry reflection seismic profile through the Maiden Peak fault system (SL 1 shown in Figure 2 and Plate 1). West-dipping reflections correspond to mapped traces of the western and eastern splays of the Maiden Peak fault system. The Maiden Peak fault system is lapped by subhorizontal reflections corresponding to mapped traces of the middle Miocene sediment of Bannock Pass. Antiformal reflection in the hanging wall of the western Maiden Peak fault may correlate to a southeast plunging anticline (Fold D). Synformal reflections within the sediment overlying the Maiden Peak fault systems correlates to a gentle north-south trending syncline within the sediment of Bannock Pass (Fold G).

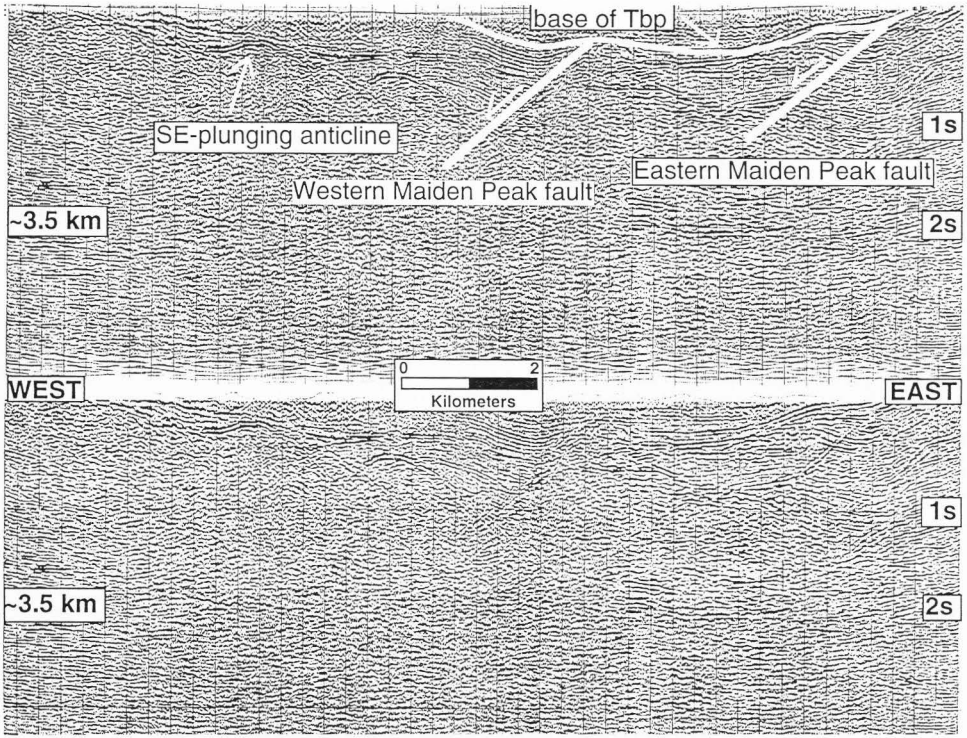
base of Tbp
SE-plunging anticline
Western Maiden Peak fault
Eastern Maiden Peak fault
1s
2s
~3.5 km
WEST
0
2
Kilometers
EAST
1s
2s
~3.5 km

late-early Miocene sediments of Bannock Pass, but the latest slip ended before deposition of younger gravel deposits (QTg; M'Gonigle, 1993; M'Gonigle and Hait, 1997). Although the age of last motion on the fault system is poorly constrained, several lines of evidence suggest that initial slip may be middle Eocene. First, the eastern Maiden Peak fault is intruded by rhyolites in sections 3 and 10 of T 11 S, R 13 W (M'Gonigle and Hait, 1997; S. U. Janecke, pers. comm., 1996). These rhyolite intrusions have not been dated, but they are lithologically similar to middle Eocene rhyolites associated with the Challis Volcanic Group. Secondly, several lines of sedimentological data suggest that the Maiden Peak fault system bounded the Horse Prairie half-graben on the east while the sediment of Everson Creek was being deposited in the Oligocene to Early Miocene: 1) The sediment of Everson Creek dips toward the west-dipping fault system; 2) an angular unconformity is located near the base of the sediment; 3) provenance and paleocurrent data from the upper sediment of Everson Creek show sediment shed from the footwall of the Maiden Peak Fault system; 4) paleocurrents show north to south transport of sediment along the axis of the half-graben, parallel to the Maiden Peak fault; and 5) coarse gravels and megabreccia deposits are intercalated in the base of the sediment of Everson Creek. Lastly, the western splay of the Maiden Peak fault system cuts a 20.6 Ma basalt flow northwest of Red Butte in the Bachelor Mountain quadrangle (S. U. Janecke, unpublished mapping). Therefore, slip on the Maiden Peak fault system may have begun as early as middle Eocene time during Challis volcanism, but a younger Oligocene onset in also consistent with the data. $^{40}Ar/^{39}Ar$ dating of the rhyolite intrusions, in progress, will further constrain the age of initial deformation.

The geometry and location of the Maiden Peak fault system suggest a possible correlation with the Lemhi Pass and Muddy-Grasshopper faults during its early phases of movement. Unlike the Lemhi Pass and Muddy-Grasshopper faults, slip on the Maiden Peak fault system continued into the Miocene.

Discussion of Late to Post-Volcanic Faults

In an examination of sedimentary basins in east-central Idaho, Janecke (1994) documented an episode of late middle Eocene to Oligocene extension north of the eastern Snake River Plain. This Paleogene event was confined to a narrow (100 ± 25 km) north- to north-northwest-trending rift zone in east-central Idaho, western Montana, and southern British Columbia. The Horse Prairie basin was hypothesized to lie in the rift zone near its eastern margin (Janecke, 1994). This study confirms that the Horse Prairie compound half-graben developed in the late Eocene to Oligocene due to slip on the Muddy-Grasshopper, Maiden Peak, and Lemhi Pass fault systems. However, the Horse Prairie half-graben is more temporally and geometrically complex than first envisioned in Janecke (1994). Formation of the basin in the Paleogene was due to slip on three low-angle normal faults that extended the crust in an overall east northeast --west southwest direction, but in detail the Muddy-Grasshopper, Lemhi Pass, and Maiden Peak fault systems differ enough in their strike and age to produce a composite half-graben with internal angular unconformities. If the Horse Prairie basin is representative, the Paleogene episode of extension produced approximately 63 percent east-west crustal extension. If uniform extension throughout the crust and a present crustal thickness of 33 km are assumed, the pre-Paleogene thickness of the crust exceeded 68 km. If additional extension on pre- and syn-Challis faults, and on Basin and Range faults is considered, even greater original crustal thicknesses are implied.

The Paleogene rift zone, as defined by Janecke (1994), probably collapsed due to gravitational instabilities in late middle Eocene to early Miocene time. Similarly, the Horse Prairie basin experienced west to southwest-directed extension between middle Eocene and late-early Miocene (?) time on the Lemhi Pass and Maiden Peak fault systems, as well as on the Muddy-Grasshopper fault system in the Tendoy Range to the east (Janecke et al., 1996a). In addition, synorogenic sediments representing the

initiation of rift sedimentation in the Horse Prairie basin contain middle to late Eocene gastropods (Gyraulus proceras; Steve Good, written comm., 1996) identical to species found in the Kishenehn Formation, which has been shown to be a synorogenic deposit of a middle Eocene to Oligocene half-graben located within the hypothesized rift zone in northwestern Montana (Constenius, 1981, 1982, 1988, 1995; McMechan and Price, 1980; McMechan, 1981; Janecke, 1994). Thus, extension was approximately synchronous in the Horse Prairie and Kishenehn half-grabens, despite being separated by 4° of latitude. Throughout east-central Idaho, Janecke (1994) found evidence for the initiation of extension within the rift zone during the waning phases of Challis volcanism (47-45 Ma). Thus, the age of Paleogene extension in the Horse Prairie basin and nearby Tendoy Range supports the interpretation of Janecke (1994) that extension along the rift zone was largely synchronous, and did not monotonically migrate southward as previously thought. Janecke (1994) appears to have been correct with regards to the Paleogene basin forming event, but evidence for the Divide Creek, Bloody Dick Creek, and related faults suggests that gravitational collapse of the fold and thrust belt initiatied earlier, before Challis volcanism. Challis volcanism may have acted as a thermal trigger for the Paleogene basin-forming event, but it was not a major factor driving the earliest extension in the region. Extension both predated and long outlasted volcanism throughout east-central Idaho and western Montana.

Inheritance from preexisting structures is likely to have affected the geometry of subsequent normal faults within the Horse Prairie basin. As previously mentioned, the Cabin thrust, the Beaverhead Divide-Miner Lake-Bloody Dick Creek fault zone, and the original rifted margin of the Belt basin may be located beneath the Horse Prairie half-graben. The Lemhi Pass fault lies in the hanging wall and roughly parallels the northwest-striking Beaverhead Divide-Miner Lake-Bloody Dick Creek fault zone throughout much of its trace. Similarly, the original faulted margin of the Belt Basin may

coincide with the western splay of the west-dipping Maiden Peak fault system. Although both the Lemhi Pass and Maiden Peak fault systems cut Tertiary volcanic rocks that postdate the older inherited structures, the younger phase of faulting may reactivate the preexisting structures at depth. More detailed mapping and reflection seismic data may help to better constrain the subsurface geometry of the Beaverhead Divide-Miner Lake-Bloody Dick Creek fault zone, and the original rifted margin of the Belt basin, and lead to a more robust interpretation of the role of inheritance in the development of the Lemhi Pass and Maiden Peak fault systems.

Basin and Range Faults--Phase 1

While Paleogene normal faulting appears to have dominated the extensional history of the Horse Prairie basin, evidence also exists for two episodes of Neogene extension. The first of these episodes occurs on the northeast-striking Little Eightmile Creek fault. With the exception of syn-Challis faults, northeast-striking normal faults are anomalous within the study area. Northeast-striking normal faults appear to be relatively common throughout southwest Montana in late-early Miocene time (e.g. Ruby and Beaverhead half-grabens; Fields et al., 1985; Fritz and Sears, 1993), but only one such structure was identified in the Horse Prairie basin.

Little Eightmile Creek Fault

Staatz (1973) mapped a northeast-striking, down-to-the-northwest normal fault just northwest of Little Eightmile Creek in the Goat Mountain quadrangle (Plate 1). This fault continues to the northeast into the Bannock Pass quadrangle, where some of its trace is concealed by younger deposits. In the Goat Mountain quadrangle, the Little Eightmile Creek fault juxtaposes Mississippian carbonates and Challis volcanic rocks in the hanging wall against Middle Proterozoic quartzites in the footwall (Staatz, 1973). Farther to the northeast, in the Bannock Pass quadrangle, the fault is approximately located where it

contains quartzites in both the footwall and hanging wall. Still farther to the northeast, two splays of the fault contain Challis volcanic rocks in the hanging wall.

Although the Little Eightmile Creek fault has been offset by at least one younger normal fault, it appears to retain its original geometry throughout most of the trace. The limiting factors in quantifying the initial orientation of the fault are the limited exposure and curvilinear trace, not the presence of younger deformation. Cemented outcrops of brecciated fault rocks found in section 29 of T11S, R14W trend 032°, and three-point analysis of an approximately located fault contact show a 34° northwest-dipping fault plane. However, the dip of the fault plane calculated by three-point analysis may be inaccurate due to the nonplanar nature of the fault, poor constraints on the exact location of the contact, and the presence of two splays of the fault system in the vicinity. The presence of a rollover anticline in the hanging wall of the Little Eightmile Creek fault indicates a steeper dip near the surface than at depth. A 60° surface dip was assumed for cross section C_1-C_1' in the absence of reliable three-dimensional data, and a listric subsurface geometry was extrapolated using an assumed 75° cutoff angle with Tertiary strata in the hanging wall (C_1-C_1'; Plate 2).

In the Bannock Pass quadrangle, separation on the basal Tertiary contact across both strands of the Little Eightmile Creek fault can be resolved into 1.0 km of dip-slip separation, 0.5 km of heave and 0.9 km of throw, assuming pure dip-slip motion on a listric fault with a 60° dip at the surface (Table 1). The amount of slip appears to increase to the southwest, and in the eastern portion of the Goat Mountain quadrangle, along cross section C_1-C_1', the fault shows 3.0 km of dip-slip separation, 1.5 km of heave, and 2.6 km of throw (Table 1). These values should be considered a minimum because there is considerable uncertainty about the subsurface geometry of the fault.

The age of the Little Eightmile Creek fault is well constrained at approximately 0.5 km south of Black Canyon, where the fault contains southeast-dipping sediment of

Everson Creek in the hanging wall, and is lapped by 4° east-dipping sediment of Bannock Pass (Plate 1). These relationships bracket the timing of extension on the Little Eightmile Creek fault to postdate deposition of the sediment of Everson Creek (early Miocene), and pre-date deposition of the sediment of Bannock Pass (late-early Miocene). The Little Eightmile Creek fault thus has the same age as a regionally extensive mid-Tertiary unconformity found throughout the Rocky Mountain Basin and Range Province (e.g. Kuenzi and Fields, 1971; Fields, 1972; Rasmussen, 1973, 1977; Fields et al., 1985; Fig. 5).

The Little Eightmile Creek fault is the only northeast-striking Neogene structure within the study area, but other normal faults with similar orientation and timing constraints have been documented in the Rocky Mountain Basin and Range Province. Fritz and Sears (1993) concluded that initial Basin-and-Range-style faulting in southwestern Montana occurred on northeast-striking, late-early Miocene faults, based on their study of the Ruby and Beaverhead half-grabens. The Little Eightmile Creek fault is most likely the result of the same tectonic processes responsible for the formation of its temporal and geometric equivalents to the northeast.

In a regional summary of previous work in western Montana and eastern Idaho, Fields et al. (1985) listed evidence for a regional mid-Tertiary unconformity. This ubiquitous unconformity is typically angular, although in some basins only a disconformity is present (e.g. Jefferson Basin; Kuenzi and Fields, 1971). The mid-Tertiary unconformity is thought to represent the initiation of "Basin and Range" extension, and may also reflect a regional climate change (Fields et al., 1985). The mid-Tertiary unconformity is present in the southern third of the Horse Prairie basin, and has been bracketed using magnetochronology and paleontologic control at 16.8-17.3 Ma (A. D. Barnosky, pers. comm., 1996). The unconformity is most evident in the northern Bannock Pass quadrangle, where Oligocene to early Miocene sediment of Everson Creek

dips approximately 12° to the southeast into the northwest-dipping Little Eightmile Creek fault. Overlying the fault, and the sediment of Everson Creek in its hanging wall, is the 4° east-dipping late-early Miocene sediment of Bannock Pass. In the study area, the mid-Tertiary unconformity is clearly the result of extensional tectonism, but whether this event represents the initiation of "Basin and Range" extension or simply the waning phases of Paleogene extension is not as clear.

Models for Basin and Range Extension

Several extensional models have been proposed for "Basin and Range" extension in the western U. S., including gravitational collapse, active and passive models, and models related to the Yellowstone hot spot. The limiting factor in the applicability of one or more of these models to late-early Miocene extension in the study area (represented by the Little Eightmile Creek fault) appears to be the northwest-southeast direction of extension. A valid extensional model must account for the interruption in the west southwest-directed extension that appears to have dominated the Cenozoic tectonic evolution of the Horse Prairie basin.

Gravitational collapse models typically predict extension parallel to the direction of maximum shortening. Paleogene west southwest-directed extension is parallel to the shortening direction for the fold and thrust belt in the region, and is likely the result of gravitational collapse of overthickened crust. The late-early Miocene event, in contrast, is northwest-directed, perpendicular to the Mesozoic shortening direction. In addition, gravitational collapse models only predict extension when lithospheric thickness is maintained at levels above normal (Coney and Harms, 1984). This seems unlikely given the magnitude of extension on the Bloody Dick Creek-Divide Creek and Muddy-Grasshopper-Lemhi Pass-Maiden Peak fault systems prior to initiation of extension on the late-early Miocene Little Eightmile Creek fault, and the length of time between late Mesozoic shortening and late-early Miocene extension.

Active models for Basin and Range extension are also problematic. The driving mechanism for extension in an active model is flow of the underlying asthenosphere due to mantle disturbances or associated with subduction (Gans et al., 1989). One prediction associated with this model is early magmatism, possibly preceding extension. The prediction of early magmatism, and of a general correlation between extension and magmatism, does not seem to be universally applicable throughout the Basin and Range Province. While bimodal and fundamentally basaltic magmatism is present within the Basin and Range during the Miocene and Pliocene, many areas experienced magmatism and no extension, extension before magmatism, or extension without magmatism, suggesting a poor correlation at best (Miller, 1990).

Extension in the passive model is driven solely by lithospheric forces associated with interactions at the plate margins (Atwater, 1970). Predictions of the passive model include: 1) early subsidence, 2) late magmatism, and 3) a spatial and temporal association with a change in plate motions. Evidence to suggest early subsidence or widespread magmatism is not apparent in the northeastern Great Basin and Rocky Mountain Basin and Range. However, extension in the southern Great Basin does correlate to the inception of a transform boundary to the west, and the northward migration of the Mendocino triple junction (Glazner and Bartley, 1984; Dokka and Ross, 1995). While this model may be somewhat applicable to regions east of the transform, the effects of these plate reorganizations should not have affected extension within the study area due to continued subduction of the Juan de Fuca plate at the Cascadia subduction zone.

The three traditional extensional models do not seem to adequately explain the initiation of late-early Miocene "Basin and Range" extension in the study area. Similarly, Yellowstone hot spot models are not consistent with data throughout the region. Rodgers et al. (1990) proposed a model relating extension in the northeast Great Basin and Rocky Mountain Basin and Range to the southwestward migration of the North American

continent relative to the Yellowstone hot spot. This model predicts a northeastward younging of extension throughout the region. But, if the distribution of extension within the entire Rocky Mountain Basin and Range is examined, evidence for mid-Miocene extension far removed from the outbreak point of the hot spot is apparent, suggesting extension in the province prior to the predicted effects of the hot spot.

A second model relating the Yellowstone hot spot to Basin and Range extension proposes that the outbreak of the hot spot produced a radial pattern of deformation throughout the entire Basin and Range Province during the mid-Miocene (Sears, 1995). Evidence for this radial pattern is found in southwestern Montana, and in several well-documented mid-Miocene structures elsewhere in the province (Sears, 1995). Superimposed on the initial province-wide radial pattern are smaller radial patterns associated with the relative northeastward migration of the hot spot subsequent to its initial outbreak. Evidence for these smaller radial pattern is sparse, except in southwest Montana where older northeast-striking faults radial to the outbreak point are displaced by a series of younger, northwest-striking faults radial to the hot spot located in the Island Park-Yellowstone area (Sears et al., 1995). The Sears (1995) model has not been described in detail as of yet, but the simplified version is inadequate. First, the model predicts a continuum of smaller radial patterns superimposed on the larger pattern, and onto each other. But, no more than two orthogonal trends of uplifts have been documented. Evidence for the predicted chaotic pattern of deformation has yet to be found. Secondly, the model is applied to the entire Basin and Range Province, and yet extension continues in the southern Basin and Range despite the significant separation between the predicted smaller radial pattern and the rest of the province.

No single extensional model adequately explains the time-space patterns of Miocene and younger extension in the Basin and Range Province. It seems likely that a combination of models, or an entirely new extensional model is required to resolve the

controversy. Mechanisms responsible for producing the regional mid-Tertiary unconformity and northeast-striking mid-Miocene normal faults in the region are enigmatic, but must have been widespread and short lived to interrupt what appears to be protracted east northeast-west southwest extension in the study area.

Basin and Range Faults--Phase 2

The second phase of Neogene extension in the Horse Prairie basin occurs on a series of northwest-striking normal faults. Northwest-striking Basin and Range faults tend to have small displacements in the study area (typically < 1 km dip slip separation), and do not appear to preserve syntectonic sediments. The second episode of Neogene extension does not extend the study area significantly; however, major northwest-striking Basin and Range faults are common throughout the region (Rodgers et al., 1990; Crone and Haller, 1991; Janecke, 1992; Anders et al., 1993b; Fritz and Sears, 1993).

Five northwest-striking, southwest- and northeast-dipping normal faults occur in the southern half of the study area (Plate 1). Although the age of deformation on four of the five structures is uncertain, one southwest-dipping fault offsets the northeast-striking Little Eightmile Creek fault along the western border of the Bannock Pass quadrangle (Plate 1). Because the relatively well-exposed fault trace does not define a planar fault, three-point analysis of the contact is impossible. A 60° southwest dip was assumed for the fault in the absence of reliable constraints on the geometry of the fault plane. Assuming a 60° dip yields dip-slip separations up to 1.1 km, 0.6 km of heave, and 0.9 km of throw across the northwest-striking normal fault (C_2-C_2', C_3-C_3'; Plate 2).

Northwest-striking faults with evidence for slip in the Quaternary and recent seismicity have been documented throughout the Rocky Mountain Basin and Range Province (Stickney and Bartholomew, 1987; Crone and Haller, 1991; Janecke, 1992). In a study of paleovalley deposits of southwest Montana, including the Timber Hill basalt flow (6 Ma), Fritz and Sears (1993) documented at least 2 km of offset along northwest-

striking faults that displace the Timber Hill basalt and northeast-striking late-early Miocene normal faults. Although the timing of the northwest-striking faults in the Horse Prairie basin is poorly constrained, their parallelism to nearby active normal faults (e.g. Beaverhead fault, Red Rocks fault), and the fact that they offset late-early Miocene faults, suggests a strong temporal and genetic correlation between the faults in the study area and other northwest-striking Basin and Range faults in the region.

Previous workers have attributed late Cenozoic southwest-northeast extension surrounding the Snake River Plain to passage of the Yellowstone hot spot (Rodgers et al., 1990; Pierce and Morgan, 1992; Anders et al., 1993a; Sears, 1995). Although problems exist with applying hot spot-related models to the entire northeastern Great Basin and Rocky Mountain Basin and Range Provinces (see discussion of Little Eightmile Creek fault), the effects of the Yellowstone hot spot are difficult to dismiss. In a study of several basins immediately south of the Snake River Plain, Rodgers et al. (1990) documented a northeastward younging of extensional basins, tracking the migration of the hot spot. I infer that Neogene northwest-striking faults within the study area are associated with effects of the passage of the Yellowstone hot spot, and are unrelated to mechanisms responsible for Paleogene west southwest-directed extension in the region.

FOLDS

Middle Eocene to Miocene volcanic rocks and sediments have been folded about a variety of fold axes within the upper Horse Prairie basin (Fig. 13). Because there are no known thrust or reverse faults of this age in the region, the folds are most likely related to extension. Seven mesoscopic- to macroscopic-scale folds found in the study area deform the Tertiary basin-fill at different stratigraphic levels. Angular disordances between stratigraphic units of different ages indicate multiple generations of folding. At least three generations of folding have affected the Horse Prairie basin, and three geometric sets of

folds are present: northeast-trending, east southeast-trending, and north-trending folds. A discussion of the three generations of folds will progress in chronologic order, and the nearest normal fault will be identified were possible.

First Generation

The first generation of folding is indicated by a macroscopic fold plunging 46° in the direction 052°, located along Bear Creek at the western edge of the Everson Creek quadrangle (Fold B, Table 2, Fig. 13, Fig. 14; Plate 1). Both Challis volcanic rocks and lacustrine limestones and gravels of the sediment of Bear Creek are folded into a gentle anticline with an interlimb angle of 162°, and an amplitude of approximately 1.5 km (Fold B, Table 2). The fold axis was determined using orientation data from the Challis volcanic rocksdue to poor exposure of the overlying sediment of Bear Creek. The overlying gravels and fine-grained tuffaceous sands of the sediment of Everson Creek are not folded, and dip approximately 9° to the east. Thus, this northeast-plunging fold formed after deposition of the middle to late Eocene sediment of Bear Creek, but before deposition of the Oligocene to early Miocene sediment of Everson Creek. Other northeast-plunging folds occur to the northwest in the Lemhi Pass, Agency Creek, Goldstone Mountain, Tendoy, and Baker quadrangles (J. J. Blankenau, S. U. Janecke, unpublished mapping). This northeast-trending fold train contains at least 13 anticlines and synclines with fold spacing ranging from 0.9 km to 5.6 km, and averaging 4.0 km.

The northeast-plunging anticline in the study area, as well as other northeast-striking folds, is located in the immediate hanging wall of the southwest-dipping Lemhi Pass fault (F_2-F_2'; Plate 2). The trend of the fold axis forms an angle of approximately 60° to the strike of the Lemhi Pass fault. On a more regional basis, however, northeast-plunging folds are perpendicular to the dominant northwest strike of the Lemhi Pass fault (J. J. Blankenau, S. U. Janecke, unpublished mapping). I infer a genetic relationship

TABLE 2. DESCRIPTION OF CENOZOIC EXTENSIONAL FOLDS IN THE HORSE PRAIRIE BASIN

Fold names	Orientation P/T	Orientation of axial surface	Interlimb angle	Mean fold spacing	Type	Age	Associated normal fault	Angle between axial plane and fault plane	Angle between trend of fold and strike of fault
A	23° / 081°	079° / 85°	51°	isolated	syncline	Post- 46.0 Ma Pre-late middle Eocene	unknown	NA	NA
B	46° / 052° (38° / 058°)	234° / 87° (053° / 88°)	162°	4.0 km	anticline	Post- 46.0 Ma Pre- early Miocene	Lemhi Pass fault	88° (80°)	50° (64°)
C	07° / 106°	106° / 90°	168°	0.7 km	anticline	Post- early Miocene Pre- late early Miocene	Maiden Peak fault system	78°	~60°
D	26° / 106°	105° / 88°	131°	isolated(?) or related to C	anticline	Post- early Miocene	Little Eightmile Creek fault Maiden Peak fault system	53° 79°	74° ~60°
E	22° / 079°	260° / 84°	147°	isolated	anticline	Post- early Miocene	Little Eightmile Creek fault	37°	47°
F	01°/ 173°	172° / 88°	175°	isolated	anticline	Post- middle Eocene	E-W-striking fault	~90°	~90°
G	01°/ 164°	344° / 88°	168°	isolated	syncline	Post- late early Miocene	Maiden Peak fault system(?) Beaverhead fault(?)	~32° ~64°	~10° ~18°

Notes: Folds are named on Figure 13 and shown in Plate 1. Equal area plots of folds A-F are shown in Figure 14. Restored orientations are shown in parentheses.

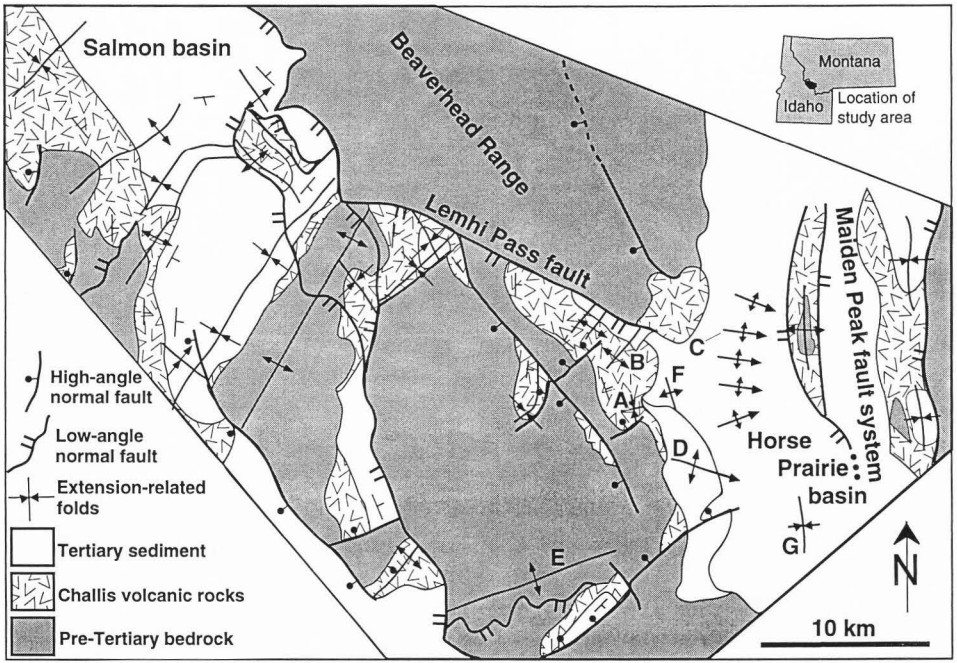

Figure 13. Location map for Cenozoic extensional folds in the Salmon basin, Beaverhead Range, and Horse Prairie basin. Geometric data and fold names (A-G) are in Table 2. Compiled in part from unpublished mapping by S. U. Janecke and J. J. Blankenau. Modified from Janecke et al. (*in prep.*).

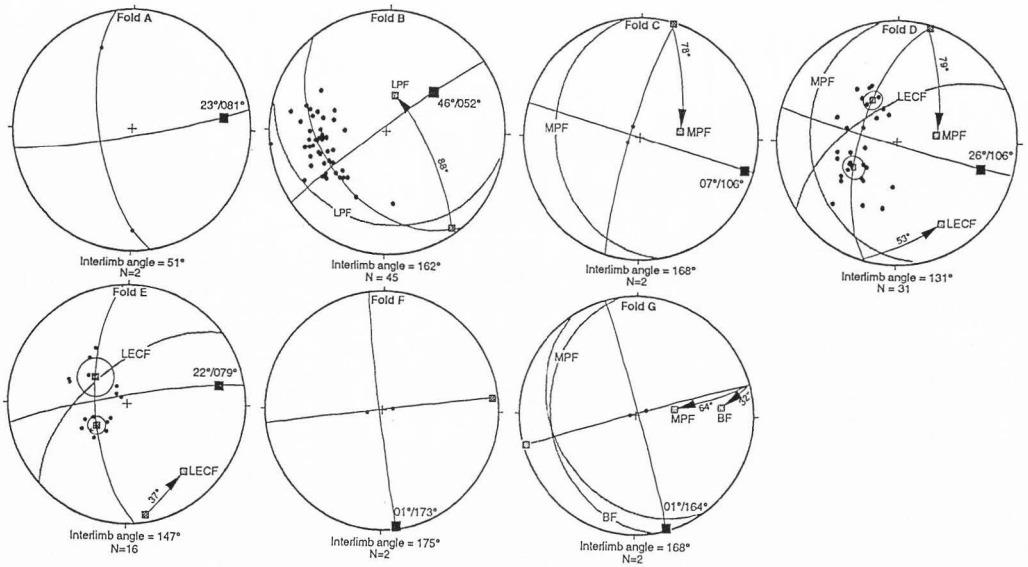

Figure 14. Stereograms of poles to bedding for extensional folds in the Horse Prairie basin. Fold axes (dark squares) are defined by cylindrical best fit π great circles through poles to bedding within Proterozoic quartzites (Fold E), Challis volcanic rocks (Folds A, B), sediment of Bear Creek (Fold D), sediment of Everson Creek (Folds C, F), and the sediment of Bannock Pass (Fold G). Axial surfaces and associated normal faults are shown where applicable. Arrows indicate angular distance between poles to the axial surface and associated normal fault. Mean vectors and 95% confidence interval cones were calculated for individual limbs where possible. N = number of data points; LPF = Lemhi Pass fault; MPF = Maiden Peak fault; LECF = Little Eightmile Creek fault; BF = Beaverhead fault. See Table 2 for a complete description of folds.

between the two structures based on their geographic location and their apparent temporal correlation.

Northeast-trending folds within the fold train are generally oriented at a relatively high angle to the Lemhi Pass fault (64°, Fold B, Table 2), but technically should be classified as oblique folds (see Schlische, 1995) because the fold is greater than 22.5° from perpendicular to the strike of the Lemhi Pass fault (Janecke et al., *in prep.*). The mechanisms responsible for this fold train are difficult to identify, but a combination of mechanisms seems likely to have produced these folds. The Lemhi Pass fault appears to have a significant component of dextral strike-slip motion (see discussion of Lemhi Pass fault), which may have reoriented an initial transverse fold train to the observed oblique orientation. If so, then a mechanism capable of forming transverse fold trains must be identified. Three common types of transverse folds have been documented in an extensional setting: 1) fault-bend folds, 2) displacement-gradient folds, and 3) constrictional folds (Schlische, 1995; Janecke et al., 1996c). Displacement-gradient and constrictional folds predict folding in the footwall of the associated normal fault, but folding in the footwall of the Lemhi Pass fault has not be documented. Similarly, evidence of fault corrogations corresponding to individual fold axes is unavailable. A unique solution is difficult to discern without additional detailed structural analysis of the fault plane and rocks in the immediate footwall and hanging wall.

Second Generation

Along the western bank of Horse Prairie Creek, in section 26 of T10S, R14W, a gentle east southeast-trending anticline is present in the upper portion of the sediment of Everson Creek (Plate 1; Fold C, Table 2, Fig. 13, Fig. 14). This particular fold can be seen west of the highway between Grant and Bannock Pass, and several other similar anticlines and synclines, with an average spacing of 0.7 km, appear on north-south-trending reflection seismic profile (Fig. 15) and are evident in strikes and dips in the

sediment of Everson Creek. There is evidence for nine east southeast-plunging anticlines and synclines in this area. Although no overlying unfolded units are present to bracket the timing of folding, the location of these folds suggests an association with the western splay of the Maiden Peak fault system, 2 to 3 km to the east. All folds lie in the immediate hanging wall of the Maiden Peak fault, die out to the west, and deform the same units cut by the fault. These data suggest that extension-related folding occurred in the Oligocene and early Miocene.

Although the trend of the east southeast-trending folds in the hanging wall of the Maiden Peak fault system are at a relatively high angle to the strike of the fault (~ 60°), similar to the fold train of generation one, strike-slip motion has not be observed on the Maiden Peak fault system (Fold C, Table 2, Fig. 13, Fig. 14). Oblique extension-related folds in a purely dip-slip fault system can be the result of fault-bend folding, or compound mechanisms (Schlische, 1995; Janecke et al., 1996c; Janecke et al., *in prep.*). Individual mechanisms responsible for the folding are difficult to identify, but effects of corrugations in the fault surface are likely to be a significant factor given a lack of transverse folding in the footwall of the Maiden Peak fault system.

Northeast and east southeast-trending folds farther to the southwest also appear to represent this generation of folding. In the south-central Everson Creek quadrangle and north-central Bannock Pass quadrangle, units within the sediment of Bear Creek and the sediment of Everson Creek are folded about an anticlinal axis plunging 26° toward 106°, with an interlimb angle of 131°, and an amplitude of approximately 2 km (Fold D, Table 2, Fig. 14). The orientation of this anticline was determined using the attitude of bedding in the sediment of Bear Creek north of Black Canyon, which may have been modified by three northwest-striking normal faults in the immediate vicinity (Fold D, Fig. 13, Fig. 14; Plate 1). The anticline also appears on two separate unmigrated, industry reflection

Figure 15. Unmigrated industry reflection seismic profile through the western Maiden Peak fault. Labeled as SL 2 in Figure 2 and Plate 1. South-dipping reflection correlates to mapped traces of the western Maiden Peak fault. Antiformal and synformal reflections south of the Maiden Peak fault may represent east southeast plunging folds of generation 2. Antiformal reflection farther south may correlate to Fold D.

SE-plunging folds
SE-plunging anticline
Western Malden Peak fault
0.5 s
1 s
~1.5 km
SOUTH
NORTH
0
2
Kilometers

seismic profiles. Antiformal reflections on reflection seismic profiles (Fig. 12; Fig. 15) coincide with the projection of this southeast-plunging fold, and confirm the trend of the fold calculated from surface data. Nearly flat-lying mudstones, siltstones, and gravels of the Barstovian sediment of Bannock Pass are located along trend of the fold axis, but are not folded (B-B'; Plate 2). These cross-cutting relationships, in addition to the location of the fold in the hanging wall of the late-early Miocene Little Eightmile Creek fault, suggest that this particular east southeast-plunging fold was formed in the early to late-early Miocene, during and/or after deposition of the sediment of Everson Creek and before deposition of the sediments of Bannock Pass.

The trend of this east southeast-trending anticline is oriented approximately 74° to the strike of the Little Eightmile Creek fault and 60° to the strike of the Maiden Peak fault system. This obliquity may be the result of rollover in the hanging wall of two oblique listric normal faults. Eastward tilt into the Maiden Peak fault coupled with southeastward tilt into the Little Eightmile Creek fault could result in an east southeast-trending fold axis oblique to both the Maiden Peak and Little Eightmile Creek faults. If this mechanism produced the large anticline north of Black Canyon, the parallelism between it and the subtle fold train to the north would be coincidental.

An isolated northeast-trending anticline exposed to the southwest appears to be of the same generation as the southeast-plunging anticline in the Black Canyon area. This fold is located in the Goat Mountain quadrangle, southwest of the continental divide, but unlike the east southeast-trending fold along Black Canyon, this anticline trends northeast (Plate 1). The fold is defined by a southeastward progressive steepening in the dip of the Mississippian limestones in the hanging wall of the Little Eightmile Creek fault (Staatz, 1973; C_1-C_1', Plate 2). Tertiary volcanic rocks are preserved on only one limb of the fold, but a plot of poles to bedding for the underlying Proterozoic quartzites (Staatz, 1973) shows a fold axis plunging 22° toward 079°, with an interlimb angle of 147°, and

an amplitude of approximately 1 km (Fold E, Table 2, Fig. 13, Fig. 14; Plate 1). The small angle between the trend of the fold and the strike of the Little Eightmile Creek fault (22°), and the location of the fold in the immediate hanging wall of the fault are characteristics indicative of a longitudinal fault-bend fold or "rollover fold."

Several north-south-trending folds occur within middle Eocene to middle Miocene basin-fill deposits east of the study area, in the Jeff Davis Peak (M'Gonigle and Hait, 1997) and Deadman Pass (M'Gonigle, 1993) quadrangles (Fig. 13). In the Jeff Davis Peak quadrangle, M'Gonigle and Hait (1997) identified four synclines and anticlines parallel to strands of the northern Maiden Peak fault system. These folds trend north northwest, and probably formed during slip on the west-dipping fault system. These longitudinal folds could be due to drag, fault propogation, or fault bend folding.

Third Generation

A north northwest-trending syncline in the Jeff Davis Peak and Deadman Pass quadrangles (Fold G, Table 2, Fig. 13, Fig. 14) shows evidence for folding into Barstovian (middle Miocene) time. This syncline is located in the western Deadman Pass quadrangle (Fig. 13), and coincides with the axis of the modern Horse Prairie basin. This fold trends approximately 344°, has an interlimb angle of 168°, and the trend forms an angle of 10° to the strike of the Maiden Peak fault system (Fold G, Table 2, Fig. 14). The syncline is poorly defined using surface data, but can be seen on reflection seismic profile SL-1 (Fig. 12), which cross the fold at an angle of ~30° to the trend of the syncline. Cross section D-D' through the Bannock Pass and Deadman Pass quadrangles also illustrates the gentle form and small amplitude (< 0.8 km) of the north northwest-trending syncline (D-D'; Plate 2). This syncline deforms the sediments of Bannock Pass, but does not appear to deform the overlying gravel caps of unknown age. The orientation and location of the fold with respect to the Maiden Peak fault system might suggest a

genetic relationship, but flexure in the footwall of the Beaverhead fault to the southwest could explain this structure.

Small Folds of Uncertain Age

An isolated mesoscopic syncline located within section 6 of T11S, R14W plunges 23° to the east northeast (081°), and has an interlimb angle of 51° (Fold A; Table 2). At this location, the youngest unit involved in the folding is the middle Eocene quartz-sanidine ash flow tuff (Tcqs). The basal lacustrine limestone (Tls1) directly overlying the fold is not folded, suggesting the folding took place between eruption of the tuff (46.01± 0.39 Ma, M'Gonigle, 1993) and deposition of the middle to late Eocene limestone.

Two normal faults are located within close proximity to the east northeast-plunging syncline: a northwest-dipping syn-Challis fault discussed previously, and a northwest-striking, southwest-dipping normal fault which offsets the base of the quartz-sanidine tuff (Plate 1). The northeast-striking fault appears to have been inactive by the time the quartz-sanidine tuff was emplaced, so a genetic correlation between the two structures is unlikely. The northwest-striking fault, in constrast, has similar age constraints to the fold and projects along strike to its location. These data may suggest a genetic correlation between the northwest-striking fault and the east northeast-plunging fold, but other northwest-striking faults of this age have not been identified in the study area. Alternatively, the small amount of offset on the northwest-striking fault suggests that it may die out before reaching exposures of the limestone, may not predate deposition of the middle Eocene carbonate, and may belong to the generation of northwest-striking Basin and Range structures discussed previously. If the northwest-striking normal fault represents Neogene extension, age relations between the fault and the east northeast-plunging fold are inconsistent. Presently, no nearby normal faults can explain the observed fold, but the presence of unidentified structures concealed by younger basin fill deposits or a nontectonic origin cannot be ruled out.

Another fold occurs in the study area, but the timing of its formation is not well constrained. In sections 31 and 32 of T10S, R14W (Plate 1), gravels of the base of the sediment of Everson Creek have been folded into a gentle anticline plunging 01° to the south (173°), with an interlimb angle of 175° (Fold F; Table 2). It is unclear whether adjacent or overlying units have been folded, so the only age control on this isolated anticline is poor. The base of the sediment of Everson Creek is undated, so we can therefore only assign a post-middle Eocene age for this structure. This northwest-trending fold is located in the hanging wall of an east-west striking, south-dipping non-planar normal fault (D-D'; Plate 2), and while several possible origins exist for this particular fold, it is likely related to slip on the nearby fault. Strata in the footwall of the associated nonplanar normal fault are unfolded, suggesting that the present curvilinear trace of the fault is original, and that folding of the hanging wall rocks is the result of transverse fault-bend folding.

Summary of Extensional Folds

At least three generations of folds deform the Tertiary basin-fill deposits of the Horse Prairie basin. Folds are typically gentle, occur in fold trains of similar age and orientation, have spacings ranging from 0.5 to 5.6 km, and have amplitudes ranging from tens of meters to up to 2 km. Folds are commonly oblique to, and plunge gently (20°-30°) towards the associated normal fault. Locally, however, isolated folds are open to close, and can be orthogonal to a fold train of similar age. For example, the second generation of folds is characterized by an east southeast-plunging fold train, a large east southeast-plunging anticline, and an isolated northeast-plunging anticline. All folds appear to be coeval, and may be the result of different mechanisms.

Folds related to extension may not account for a significant portion of the overall strain, but they do reflect the presence of shortening throughout an extensional strain field. Extension-related folds are widespread and important structural elements within

extending regions, affecting sediment dispersal patterns, and the geometry and distribution of basin-fill deposits (Janecke et al., *in prep.*). Further detailed study is needed to better quantify the geometry, occurrence, and mechanisms producing folds related to extension.

DISCUSSION OF FAULTS AND FOLDS

Although much of the Basin and Range Province has experienced more than one episode of extension, multiple temporally and geometrically distinct events like those in the Horse Prairie basin have yet to be well documented. The extension direction in the study area has changed from NE-SW to NW-SE to ENE-WSW to NW-SE to NE-SW. This change in extension direction can be characterized by a relatively systematic 360° counterclockwise rotation, in which the regional stress/strain field rotates as the result of a singular, gradational rotating mechanism. Alternatively, the pattern of extension directions may be more erratic, with each individual episode resulting from a distinctly different mechanism. I prefer a combination of the two end members, in which four discrete mechanisms produced the observed pattern of extension through time.

The first episode of NE-SW extension in pre-Challis time may reflect the beginning of a protracted episode of crustal collapse associated with thickened crust in the fold and thrust belt. Gravitational collapse likely commenced in the late Mesozoic, and continued into the early Miocene within this segment of the fold and thrust belt. In middle Eocene time, however, NE-SW extension was briefly interrupted by an episode of NW-SE syn-volcanic extension of the Challis volcanic arc. ENE-WSW gravitational collapse probably reestablished itself near the end of Challis volcanism (~45 Ma) and continued until another brief interruption in the late-early Miocene. NW-SE late-early Miocene extension across the Little Eightmile Creek fault may reflect the initiation of Basin and Range style extension in the study area, but the mechanisms responsible for this short-lived episode are enigmatic. NE-SW extension again reestablished itself after

the late-early Miocene, and continues to the present in this region. Although active normal faults in this region may be in part the result of processes affecting extension in the entire Basin and Range Province, the effects of the passage of the Yellowstone hot spot have likely dominated the stress/strain field since the late-early Miocene.

The Horse Prairie basin has experienced multiple episodes of extension and extension-related folding subsequent to shortening associated with the Sevier orogeny. Orientations of Cenozoic normal faults and extension-related fold axes are highly variable within the study area, producing bulk three-dimensional strain. Late to post-Challis and younger extension calculated along an east-west transect through the Lemhi Pass and Maiden Peak fault systems (D-D'; Plate2) yields a net extension of approximately 63 percent. In contrast, only 20 percent extension was calculated for a NNW-SSE transect through the southern half of the study area (B-B'; Plate2), and 32 percent extension for a NNE-SSW transect through the northwestern corner of the study area (A-A'; Plate 2; Fig. 16). Extension across the Divide Creek and Bloody Dick Creek faults is difficult to quantify due to poor stratigraphic control, but would greatly increase the NE-SW component of extension. The result of this temporally and geometrically complex deformation is a series of superposed depositional basins and a structurally complex half-graben.

Southwestern Montana experienced a long and complex history of tectonism starting in the early Proterozoic. Previous workers have documented the effects of preexisting structures on the geometry of subsequent deformation (Werkema and Young, 1983; Young, 1985), particularly in western Montana (Schmidt et al., 1984; Schmidt et al., 1993; Kellogg et al., 1995; Janecke et al., 1996a; Schmidt, 1996; Harlan et al., 1996). Although the Bloody Dick Creek and Little Eightmile Creek faults are the only reactivated faults in the study area, preexisting crustal anisotropies likely affected

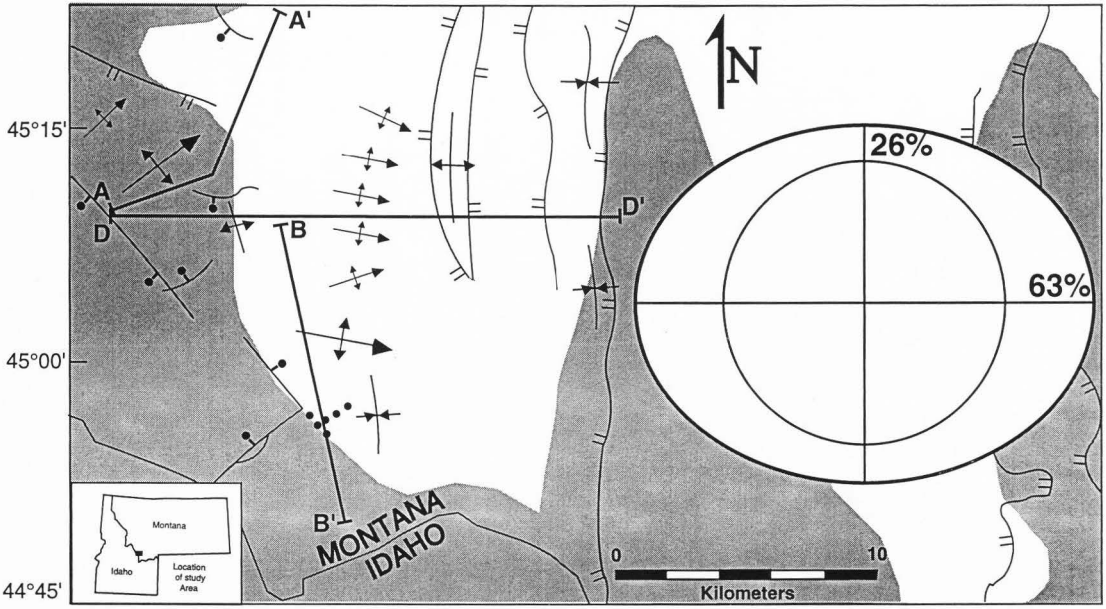

Figure 16. Post-middle Eocene strain ellipse for the Horse Prairie half-graben. Sixty-three percent east-west extension was calculated using the base of the Challis volcanic rocks along cross-section D-D'. Twenty-six percent north-south extension was calculated using the base of the Challis volcanic rocks along cross-sections A-A' and B-B'.

subsequent episodes of extension. In short, inheritance seems to have been an important process involved in the development of the Horse Prairie half-graben.

BASIN EVOLUTION AND PALEOGEOGRAPHY

The four unconformity-bounded Tertiary sequences preserved in the Horse Prairie basin, and the structures that control them, provide a unique opportunity to reconstruct the basin evolution. Structural and geochronological data from basin-fill deposits allow correlations to be made between individual unconformity-bounded sequences and the structures active during their deposition. These data enable the evolution of the Horse Prairie compound half-graben to be described in terms of individual vertically superposed depocenters. These individual depocenters are here referred to as the Little Eightmile Creek basin, Medicine Lodge/Horse Prairie protobasin, and the Maiden Peak fault basin (in chronologic order). In addition, data pertaining to pre- to syn-Challis topography, Neogene passive infilling, and Quaternary (?) incision will be presented.

METHODS

Provenance, clast size, and paleocurrent data were collected from gravel and conglomerate within the Challis volcanic rocks, the sediments of Bear Creek, Everson Creek, and Bannock Pass, and from younger gravel deposits in order to reconstruct the Cenozoic paleogeographic evolution of the Horse Prairie basin. These data, along with basic lithologic descriptions, were also used to identify the typical depositional environments for each unit, and to relate these environments to the tectonic and paleogeographic setting at the time of their deposition, where possible.

Provenance and clast size data were collected from both cemented and uncemented exposures of pebble- to boulder-sized clasts greater than 2 cm in diameter. A minimum of 50 clasts was examined at each station, and the composition, rounding, and maximum clast size was recorded (Appendix). Provenance studies were facilitated by the distribution of source rocks. Proterozoic quartzites of the Beaverhead Mountains comprise the bulk of pre-Tertiary bedrock west of the western splay of the Maiden Peak

fault system, whereas Archean gneisses of the Maiden Peak spur lie east of the fault, making sediment derived from the west and east readily distinguishable (Fig. 17).

Paleocurrents were determined using stream trough orientations and pebble imbrications, dominantly from within the sediment of Everson Creek. Adequate three-dimensional exposures were rarely available within the other sedimentary sequences. The trend and plunge of individual stream troughs were measured and corrected for subsequent tilting. In addition, foresets and clast compositions were examined in order to evaluate the validity of the flow direction denoted by trough attitude. Pebble imbrications were measured on three dimensional exposures of platy, well-rounded pebble conglomerate. Strikes and dips of the plane containing the long and intermediate axes of at least 25 clasts were measured within a single exposure, and later restored to their original orientation. Rose diagrams of the poles to the planes indicate the paleoflow directions. Clast composition data were also collected at each locality for comparison.

DATA

Data collected from coarse clastics within the Challis volcanic rocks, the sediments of Bear Creek, Everson Creek, and Bannock Pass, and from younger gravel deposits will be described in chronologic order. Depositional environments will also be discussed, followed by a regional correlation of units and interpretations of the overall basin evolution.

Challis Volcanic Rocks

Conglomerate and gravel comprise less than 5 percent of the total thickness of the Challis volcanic rocks. Consequently, imbricated pebbles and three-dimensional stream troughs were not found, and only two clast counts were conducted, one from the basal conglomerate (Tcg1) and one from the gravel at the top of the quartzite-bearing

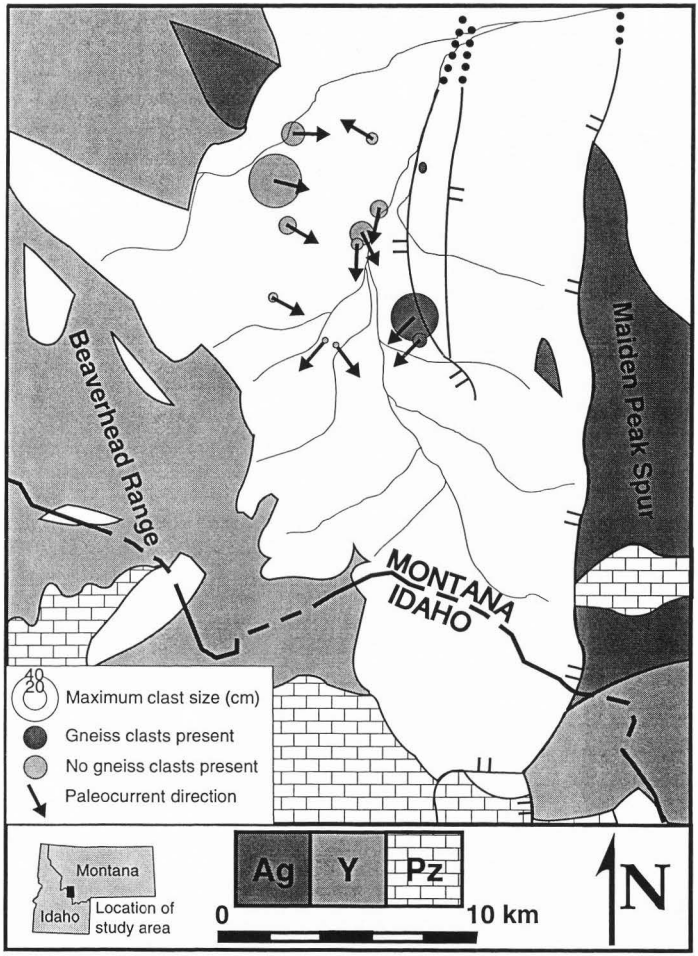

Figure 17. Provenance map showing source areas, maximum clast size, clast composition, and mean paleocurrent vectors from the sediment of Everson Creek. The distribution of bedrock represents the current location of probable source rocks for the basin-fill, subsequent to extensional deformation. Raw data are in Figure 10 and Table 3 (Appendix).

ash flow tuff (Tcg2) (Plate 1). The basal conglomerate consists of 100 percent well-rounded quartzite clasts less than 35 cm in diameter. No diagnostic rock types were found, but the presence of quartzite suggests a source to the north, west, or southwest.

The gravel at the top of the quartzite-bearing ash flow tuff is comprised of well-rounded cobbles and boulders (< 3 m), 92 percent of which are quartzite, 4 percent volcanic, and 4 percent plutonic. A dominance of Middle Proterozoic quartzite clasts and an absence of gneissic clasts indicates a westerly source for the gravel at the top of the quartzite-bearing ash flow tuff. In addition, distinctive rapakivi granite boulders found within the gravel at the top of the quartzite-bearing ash flow tuff show that the paleodrainage originally flowed across Proterozoic granites exposed west and northwest of Salmon Idaho (Evans and Zartman, 1990; Schmidt et al., 1994; Janecke et al., *in review*). The maximum clast size (< 3 m) and well-rounded texture suggest deposition of the quartzite-clast conglomerates within a stream system of considerable competence. This stream system, termed the Lemhi Pass paleoriver by Janecke et al. (*in review*), appears to have been responsible for the formation of a deep and long-lived paleovalley through the northern half of the study area. These data are consistent with a wet climate in the Eocene (Fields et al., 1985).

Sediment of Bear Creek

The sediment of Bear Creek consists of approximately 90 percent well-rounded gravels and pebble to cobble conglomerate, with thin freshwater limestones and finer-grained sediment at or near the base. Adequate exposures of imbricated pebbles and stream troughs were not found, but 18 pebble counts were conducted. Clast composition trends within the sediment of Bear Creek show an abundance of volcanic clasts (20-90 percent), with high concentrations of quartzite (5-80 percent) and clasts recycled from underlying Tertiary sediment (0-65 percent) present locally (Fig. 8). All clast types within the sediment of Bear Creek had sources on the west side of the Horse Prairie

basin, and Archean clasts derived from the east are completely absent. The presence of clasts recycled from underlying Tertiary sediment indicates exhumation of the lower units within the sediment of Bear Creek during deposition of the upper parts of the section, and implies the presence of a subtle progressive unconformity within the unit. Clast composition trends within the sediment of Bear Creek show a southward increase in clasts recycled from underlying Tertiary sediment in the southern Everson Creek quadrangle.

Maximum clast size data from the sediment of Bear Creek show coarse clasts (> 20 cm) within one kilometer of the Lemhi Pass fault. Coarse clasts are also present south of the north fork of Everson Creek, but appear to be restricted to the base of the sediment. At this location, maximum clast size decreases abruptly up-section from 1-2 m near the base of the sediment to an average maximum clast size of 5 cm immediately up section.

The depositional environment of the sediment of Bear Creek appears to have been dominated by high energy fluvial systems, although lacustrine or paludal facies are present locally. Gastropod (*Gyraulus proceras, Biomphalaria aequalis, Biomphalaria pseudoammonius*, Steve Good, written comm., 1996), ostracod, and stromatolite-bearing freshwater limestones at the base of the sediment can be traced continuously for at least 7 km along the western margin of the Horse Prairie basin (Plate 1). Similar limestones have been documented in the Medicine Lodge basin to the east, where they were interpreted to have been deposited in a littoral or shallow freshwater lake environment (Flores and M'Gonigle, 1991). Gravels overlying the limestones locally contain very well-rounded clasts up to 2 m in diameter, indicating deposition within a fluvial system of significant discharge and gradient. Gravels within the sediment of Bear Creek may correlate to those described by Flores and M'Gonigle (1991) in the Medicine Lodge basin; however, correlations are tenuous because exposures lack continuity, and are typically uncemented in the Horse Prairie basin.

Sediment of Everson Creek

Well-rounded pebble to boulder gravels occur at the base of the sediment of Everson Creek between 44° 55' and 44° 57' 30" N latitude in the west-central Everson Creek quadrangle (Plate 1). Conglomeratic arkose, tuffaceous siltstone and sandstone, and well-rounded pebble to cobble conglomerate containing three-dimensional exposures of imbricated pebbles and stream troughs overlie the gravels along an angular unconformity. Fifty-eight pebble counts within the sediment of Everson Creek show two populations of clast compositions (Fig. 8). Both populations contain less than 55 percent volcanic clasts, and range from nearly 100 percent quartzite clasts to 100 percent clasts recycled from the underlying sediment of Bear Creek (Fig. 8). The basal gravels (Tg2) are dominated by quartzite clasts, with little or no recycled Tertiary clasts. However, exposures of the gravels are typically uncemented, and may be biased towards more resistent clast types. The proportion of recycled Tertiary sediment clasts appears to increase up-section to as high as 100 percent along Horse Prairie Creek near the top of the upper sediment of Everson Creek. Further trends in clast composition are difficult to discern, due to a high variability within individual outcrops. Clast size and composition vary significantly within very short distances (< 1 m).

Maximum clast size trends within the sediment of Everson Creek are also difficult to interpret. With the exception of gravels at the base of the section (Tg2), which contain clasts as large as 1 m in diameter, clast diameters greater than 15 cm are rare. In general, clast size appears to decrease up section within the 1.4 km thick unit, with an average maximum clast size of 30 cm for the gravels at the base of the section (Tg2), 15 cm for the conglomeratic arkose (Tss), and 10 cm for the overlying sediments (Ts2; Plate 1; Fig. 7). In addition, the gravels at the base of the section interfinger with finer-grained sediments to the south.

Paleocurrent indicators were also measured in the conglomeratic arkose (Tss) and the overlying unit (Ts2) within the sediment of Everson Creek. Four pebble-imbrication and stream-trough localities in the conglomeratic arkoses show flow from the west and northwest, and contain quartzite clasts derived from the west (samples 1-4, Fig. 10). Immediately to the east, and approximately 450 m up-section, five pebble-imbrication localities show southward paleoflow, ranging from southeast to southwest (samples 6-10, Fig. 10). Farther to the southeast, and 500 m up-section, two stream-trough attitudes show flow from the northeast, and contain gneissic clasts derived from the east or northeast (samples 11,12, Fig. 10). These data appear to define a south-flowing Oligocene to early Miocene drainage system fed by streams draining highlands to the west and east.

The location and orientation of this south-flowing drainage system is less certain to the north. In a study of Eocene to Oligocene two-mica-bearing arkoses, some of which may correlate to similar two-mica sandstone found within the conglomeratic arkose (Tss) of the sediment of Everson Creek, Thomas (1995) hypothesized that sands derived from a two-mica granitic source in the Idaho Batholith were transported to the east and southeast. Thomas et al. (1995) stated that the two-mica-bearing arkoses are located within the Renova Formation and its equivalents, with limited age control between 27 and 40 Ma. Thomas (1995) concluded that an extensive east- and southeast-flowing braided stream system drained highlands to the west prior to the development of most of the present topography in southwestern Montana. These conclusions were based on a reduction in grain size and an increase in compositional maturity from west to east within "correlative" sandstone deposits. However, age control for individual deposits is poor, and some of Thomas's localities lack the muscovite and biotite that is diagnostic of these arkoses (e.g. Sage Creek basin, Upper Ruby basin, Medicine Lodge basin; R. Thomas, pers. comm., 1996).

More recent work in the region suggests that two-mica-bearing arkoses occur in at least three distinct stratigraphic levels, and are not everywhere coeval (S. U. Janecke, unpublished mapping; this study). $^{40}Ar/^{39}Ar$ single crystal age determinations from muscovite and potassium feldspar grains within two-mica-bearing arkose at the base and top of the Tertiary sediments in the Grasshopper basin yield ages ranging from latest Cretaceous to middle Eocene (70-47 Ma; S. U. Janecke and W. McIntosh, unpublished data, 1996), and substantiate correlations made by Thomas (1995) to a large two-mica granodiorite suite in the Bitterroot lobe of the Idaho batholith exposed in the ranges northwest of the Big Hole valley, which has a poorly constrained intrusion age of about 58 Ma (Desmarais, 1983). $^{40}Ar/^{39}Ar$ whole-rock age determinations on matrix concentrates from basaltic rocks that intrude and overlie two-mica-bearing arkoses at the top of the sediments in the Grasshopper basin yield ages of 27.4 ± 0.8 Ma and 27.4 ± 0.2 Ma, respectively (S. U. Janecke and W. C. McIntosh, unpublished data, 1996). These data suggest that both two-mica-bearing arkoses in the Grasshopper basin are older than two-mica-bearing arkoses within the Horse Prairie basin, which are along strike of and possibly correlative with units bearing Arikareean and Hemingfordian vertebrates (~30-16 Ma; samples 8, 11, Plate 1; Fields et al., 1985).

If the two-mica-bearing arkoses within the sediment of Everson Creek were derived from the two-mica granodiorite suite of Desmarais (1983), the point source in the western Big Hole basin may be a very long-lived source that coincided with the headwaters or a large tributary of an Oligocene to early Miocene south-flowing drainage within the Horse Prairie basin. This south-flowing drainage system may have been axial to the hypothesized rift zone of Janecke (1994) for a relatively long period of time. This is a surprising conclusion given the complex nature of Paleogene extension in the Horse Prairie basin, a system where drainage patterns are likely to change over relatively short periods of time. Without further age control, correlations between coeval two-mica-

bearing arkose deposits and inferences regarding drainage patterns are tenuous. In addition, the two-mica-bearing arkoses in the sediment of Everson Creek often contain pebbles recycled from older Tertiary basin-fill deposits. The arkoses may themselves be recycled from older deposits. This possibility needs to be addressed in order to accurately correlate coeval deposits, and to reconstruct the paleogeographic evolution of a tectonically active region.

Deposition of the sediment of Everson Creek was dominated by fluvial systems. Well-rounded coarse quartzite-clast gravels at the base of the section show evidence for a large stream system of considerable length and competence. These gravels are not laterally continuous to the south, and probably reflect deposition within a large fluvial system. Fluvial and floodplain deposits overlie the gravels, and typically include lenticular sand and pebble conglomerate beds, trough cross-bedding, ripple marks, and thinly bedded to laminated siltstone and sandstone containing risoliths and soft sediment deformation structures. Thin, discontinuous calcareous sandstone and limestone occur locally, indicating the presence of ponds or small shallow lakes, possibly in the adjacent floodplain.

Tertiary Sediment Undifferentiated (Tsu)

Undifferentiated sediment lies in the hanging wall of the Little Eightmile Creek fault in the east-central Goat Mountain and west-central Bannock Pass quadrangles. No pebble counts or paleocurrent data were collected within the unit, but poorly sorted, angular blocks of Mississippian limestone are abundant. One contiguous block of Mississippian limestone several tens of meters across may represent a paleolandslide deposit associated with oversteepened topography in the hanging wall of the Little Eightmile Creek fault. Exposures of Mississippian limestone beneath volcanic rocks to the northwest may be the source of limestone clasts within the sediment, but the apparent absence of volcanic clasts is more consistent with a source in the footwall. The sediment

appears to be restricted to the hanging wall of the fault, and may have been deposited during slip on the northwest-dipping structure in the middle Eocene or late-early Miocene. The age of this proximal deposit is uncertain; however, the lack of volcanic glass in the matrix may suggest the sediment is not coeval with other late-early Miocene tuffaceous sediments in the study area, and that a middle Eocene age is more likely.

Sediment of Bannock Pass

Approximately 160 m of dominantly fine-grained, thin-bedded to massive siltstone and fine sandstone overlie the mid-Tertiary unconformity in the Horse Prairie basin (Plate 1). Locally the contact appears conformable; elsewhere it is an angular unconformity. Bioturbation appears to have destroyed much of the original bedding and laminations within the sediment of Bannock Pass resulting in a massive thick-bedded unit. Where remnants of original bedding can be found, the unit is dominantly well laminated. Thin clast and matrix-supported conglomerate lenses, which yield the only provenance information available in the sediment of Bannock Pass, can also be found locally. The sediment of Bannock Pass contains pebble-to-cobble conglomerate lenses comprised of clasts of quartzite, volcanic rocks, and gneiss in the Deadman Pass quadrangle (M'Gonigle, 1994), but limited exposures prohibit determining their relative abundance within the unit in the study area. Three pebble counts of uncemented exposures in the Bannock Pass quadrangle show maximum clast size ranging from 30 to 50 cm, with abundant quartzite (19-75 percent) and volcanic (13-42 percent) clasts, and lesser amount of clasts recycled from older Tertiary sediment (0-36 percent, Fig. 8; samples 89, 93, 94, Appendix). Clasts within the sediment of Bannock Pass are subrounded to angular, and have sources to the northwest, west and south.

The depositional environment of the sediment of Bannock Pass is unclear. Scattered conglomerate lenses show periodic fluvial deposition, but the sequence is dominated by finer-grained deposits. Locally these fine-grained sections are intensely

burrowed, suggesting deposition in a subaqueous, near shore, or floodplain environment. Matrix-supported debris flow deposits are also present locally, and may reflect subaerial or subaqeous mass flows. Deposition in a fluvial / floodplain setting seems likely, although the presence of a small lake or pond cannot be ruled out.

Younger Gravel Deposits

Poorly sorted, well-rounded to subangular, unconsolidated boulders, cobbles, and sand can be found capping ridges and hills throughout the Everson Creek and Bannock Pass quadrangles (Plate 1). Twelve clast counts within the younger gravel deposits typically show a dominance of quartzite (51-70 percent) and volcanic (13-77 percent) clasts (Fig. 8). All clasts found in the younger gravels have sources in the pre-Tertiary and Tertiary bedrock exposed to the west. West-to-east transport is also indicated by a direct correlation between bedrock exposed to the west of younger gravel deposits and clast compositions within those deposits. Two ridge-capping younger gravel deposits occur in the north-central Bannock Pass quadrangle, immediately to the north and south of Nip and Tuck Creek. Thick accumulations of volcanic rocks are exposed west of the northern gravel deposit, which contains 77 percent volcanic clasts. Proterozoic quartzites and a thin band of volcanic rocks lie to the west of the southern gravel deposit, which contains 55 percent quartzite clasts, 33 percent volcanic clasts, and 12 percent chert.

The average of the maximum-clast-size data within the younger gravel deposits is approximately 70 cm. Maximum-clast-size trends, however, are difficult to interpret because individual deposits may represent separate stream systems, and may not directly correlate to adjacent deposits. Two clast counts from a single gravel deposit north of Nip and Tuck Creek show a decrease in maximum clast size to the northeast, but applying this trend to all deposits may not be valid.

Ridge-capping gravels are locally up to 30 m thick, and appear to grade into the Beaverhead Mountains to the west, possibly defining a poorly preserved, gently east-dipping, pediment-like surface. However, the thickness of the deposits, and the roundness of clasts is more consistent with the deposits being remnants of alluvial fans or a bajada. The original thickness and geomorphic form of the younger gravel deposits is unknown, but most, if not all of the gravels were likely transported in a powerful stream-dominated alluvial fan setting.

Correlation of Units

Flores and M'Gonigle (1991) hypothesized the presence of a large protobasin encompassing the modern Horse Prairie and Medicine Lodge basins that predates formation of the Maiden Peak spur. They also inferred that the protobasin developed in response to Laramide deformation, and that normal faults east of the basin are distinctly younger than the sediments preserved in the protobasin (Flores and M'Gonigle, 1991). In contrast, Janecke et al. (1996a) identified a west-dipping, low-angle Eocene-Oligocene detachment fault in the Tendoy Range of southwestern Montana, which bounds the Medicine Lodge/Horse Prairie supra-detachment basins, and hypothesized that the Paleogene sediments within the Horse Prairie/Medicine Lodge protobasin were deposited during slip on the basin-bounding normal fault (Janecke et al., 1996b). Both hypotheses imply that some units in the Paleogene basin-fill should correlate between the two adjacent basins. These hypotheses were tested by comparing stratigraphic units in the Horse Prairie basin, described here, to stratigraphic units within the Medicine Lodge basin (Flores and M'Gonigle, 1991; M'Gonigle et al., 1991; M'Gonigle, 1993; M'Gonigle and Dalrymple, 1993; M'Gonigle and Hait, 1997). Correlations between unconformity-bounded sequences in the Horse Prairie and Medicine Lodge basins are hampered by the limited age control, absence of region-wide marker units, and the occurence of similar lithofacies in different parts of the stratigraphy.

As much as 5.4 km of Eocene to early Oligocene lacustrine, swamp, floodplain, and alluvial fan deposits are preserved in the Medicine Lodge basin (M'Gonigle et al., 1991; S. U. Janecke and W. McIntosh, unpublished data, 1996). These Eocene to early Oligocene basin-fill deposits have a general eastward tilt, and overlie middle Eocene Challis volcanic rocks (M'Gonigle et al., 1991). In general, the Paleogene sediments in the Medicine Lodge basin can be divided into four sequences: the lower shale unit, the middle shale unit with interbedded conglomerates, the upper shale unit with interbedded conglomerates, and the upper conglomerate unit (Fig. 9; M'Gonigle et al., 1991). Age control is lacking for most of the units in the Medicine Lodge basin, but all the units were deposited between 45.7 ± 0.14 and 27.4 ± 0.1 Ma (Fig. 9). Geochronologic constraints allow correlation of the sediment of Bear Creek and the gravel member of the sediment of Everson Creek (Tg2) in the Horse Prairie basin to any or all of the four sequences in the Medicine Lodge basin. Basin-fill preserved above the gravel member of the sediment of Everson Creek appears to be younger than all the units in the Medicine Lodge basin, and probably postdates dissection of the Horse Prairie/Medicine Lodge protobasin.

In the Medicine Lodge basin, the lower shale unit contains shale, limestone, carbonaceous shale, and conglomeratic sandstone containing Middle Proterozoic quartzite and Challis volcanic clasts (M'Gonigle et al., 1991). $^{40}Ar/^{39}Ar$ age determinations from sanidine crystals within a tuffaceous zone at the base of the lower shale in the Medicine Lodge Peak quadrangle yield an age of 45.72 ± 0.16 Ma (M'Gonigle and Dalrymple, 1993; M'Gonigle, 1993). A zone of limestone occurs locally at the base of the lower shale, stratigraphically below a conglomeratic zone (M'Gonigle, 1993).

The middle shale unit overlies the lower shale unit in angular unconformity, and dominantly consists of shale with interbedded pebble, cobble, and boulder conglomerate and gravel (M'Gonigle et al., 1991). Lacustrine limestone, carbonaceous shale, and coal beds also occur in the middle shale unit locally (M'Gonigle et al., 1991). Gravel and

conglomerate dominate the middle shale in the Hansen Ranch quadrangle, but thin to the south in the Medicine Lodge Peak quadrangle (M'Gonigle et al., 1991; M'Gonigle, 1993). Clast types found in the gravel and conglomerate of the middle shale include Middle Proterozoic quartzite, Challis volcanic rocks, and minor Tertiary shale, and Tertiary sandstone (M'Gonigle et al., 1991). All clast types have a westerly source, with the nearest exposure of Middle Proterozoic quartzite located west of the western Maiden Peak fault (presently > 9 km). Two limestones occur under the conglomerate and gravel, near the base of the unit between 44° 57' and 44° 59' 30" N latitude in the Jeff Davis Peak quadrangle (M'Gonigle and Hait, 1997). Megabreccias of Middle Proterozoic quartzite and intrusions also occur locally, typically near the top of the gravel and conglomerate (M'Gonigle et al., 1991; M'Gonigle and Hait, 1997).

The upper shale unit is dominated by tuffaceous shale, but thin conglomeratic sandstone containing clasts of Archean granite gneiss, Middle Proterozoic quartzite, Paleozoic limestone, and Tertiary lava and tuff occur locally (M'Gonigle et al., 1991). Similar units do not occur in the Horse Prairie basin, suggesting that this unit does not continue across the Maiden Peak spur. The upper shale is the oldest unit in the Medicine Lodge basin that could postdate the Horse Prairie/Medicine Lodge protobasin because it is the first sequence containing Archean gneissic clasts (M'Gonigle et al., 1991).

A variety of correlations between the lower and middle shale units in the Medicine Lodge basin and the sediments of Bear Creek and Everson Creek in the Horse Prairie basin is permissible. The limestone zone at the base of the lower shale unit may be related to the limestones at the base of the sediment of Bear Creek. This correlation would imply that the overlying members of the sediment of Bear Creek and the basal gravel of the sediment of Everson Creek (Tg2) correspond to the lower and or middle shale units and interbedded gravel and conglomerate. However, my preferred interpretation is that the sediment of Bear Creek is genetically related to the middle shale,

and that the lower shale reflects sedimentation in the Medicine Lodge basin that either did not occur or was not preserved in the Horse Prairie basin (Fig. 9).

The sediment of Bear Creek and the middle shale are thought to be genetically related for a number of reasons: 1) Both units contain two lacustrine limestones near their base at the same latitude; 2) gravel derived from the west occurs in both units at approximately the same latitude; 3) both conglomerate units interfinger with finer-grained sediment to the south; 4) both units contain andesitic intrusions at similar latitudes; and 5) both units contain some clasts recycled from underlying Tertiary sediment (Flores and M'Gonigle, 1991; M'Gonigle et al., 1991; M'Gonigle, 1993; M'Gonigle and Dalrymple, 1993; M'Gonigle and Hait, 1997; this study). Gravels at the base of the sediment of Everson Creek may also correlate with the conglomerate unit within the middle shale (Fig. 9). This correlation requires 1) the pronounced angular unconformity that separates the gravel of the sediment of Bear Creek and Everson Creek in the study to be subtle or absent in the Medicine Lodge basin, or 2) for the angular unconformity in the Horse Prairie basin to coincide with deposition of the upper shale and upper conglomerate unit in the Medicine Lodge basin. These interpretations seem reasonable given the distance between the structure that produced the angular discordance in the Horse Prairie basin (Lemhi Pass fault) and exposures of the middle shale in the Medicine Lodge basin (> 16 km).

INTERPRETATIONS

While no detailed studies of the basin fill have been conducted in the upper Horse Prairie basin prior to this study, several workers have included the Horse Prairie basin in their regional Cenozoic tectonic and paleogeographic models. Fields et al. (1985) concluded that pre-late Eocene intra-arc extension in western Montana and eastern Idaho resulted in high subsidence rates and internal drainage during the early stages of basin development. Beginning in the late-early Miocene, these basins were dissected by listric

normal faulting, but some of the original basin-bounding normal faults remained active since middle Eocene time (Fields et al., 1985).

Flores and M'Gonigle (1991) concluded that middle Eocene volcanic rocks were deposited on an erosional surface cut across a terrane previously deformed by Sevier thrust faults, but extensional basin formation did not occur until the late-early Miocene in the Horse Prairie and Medicine Lodge basins. Hanneman and Wideman (1991) discuss five unconformity-bounded sequences of basin fill in the Jefferson, Beaverhead, Melrose and Divide valleys of southwestern Montana, beginning with middle Eocene to Oligocene volcanic rocks and sediments, but do not discuss any specific basin-forming events.

Janecke (1992), in contrast, documented extension dating back to middle Eocene time in east-central Idaho, approximately 60 km to the southwest. More recently, a west-dipping low-angle normal fault has been described along the western flank of the northern Tendoy Mountains (Perry and M'Gonigle, 1995), and has been interpreted to be the breakaway fault for an Eocene to Oligocene rift zone (Janecke, 1994; Janecke et al., 1996a). This fault bounds the eastern margin of the Medicine Lodge/Horse Prairie protobasin, and is likely reponsible for initial basin development (Janecke et al., 1996a; Janecke et al., 1996b). These data, and the results of this study, suggest that initial basin development occured in response to extension, and not during Laramide contraction as hypothesized by Flores and M'Gonigle (1991).

Most previous workers have hypothesized, or at least implied, initial basin formation sometime in middle Eocene to Oligocene time, followed by an episode of normal faulting and basin modification in the Miocene. Alternatively, I propose a slightly more complicated interpretation of multiple superposed Paleogene and Neogene depositional basins formed by four generations of normal faulting.

Pre-Challis Topography

Thick accumulations of ash flow tuffs, lava flows, intrusive rocks, and interbedded gravels and conglomerates of the Challis volcanic rocks occur in the study area, but no major volcanic centers have been documented in the Horse Prairie basin. The nearest possible source caldera for the volcanic rocks is located approximately 30 km west northwest of the western margin of the study area south of the Salmon basin (Ruppel et al., 1993; Janecke et al., *in review*). The paleorelief required to transport the Challis volcanic rocks into the Horse Prairie and Medicine Lodge appears to have been significant both in magnitude and duration. The distribution of the Challis Volcanic rocks, and thickness variations within the sequence, reveal significant middle Eocene (48.64 ± 0.33 - 46.01 ± 0.39 Ma; M'Gonigle and Dalrymple, 1993, 1996) paleorelief of the western half of the study area.

Although extension appears to have initiated in the middle Eocene along northeast-striking normal faults (Fig. 6; Plate 1), the Challis volcanic rocks do not appear to have accumulated in a fault-bounded depositional basin. Instead, the volcanic rocks reflect significant paleotopography, including a west-to-east-sloping paleovalley through the Lemhi Pass area, termed the Lemhi Pass paleovalley by Janecke et al. (*in review*) (Fig. 6). In the trough of the Lemhi Pass paleovalley, the volcanic rocks exceed 2 km in thickness, but thin very rapidly to the north and south (Fig. 6). The volcanic rocks thin to less than 500 m 8 km to the south, and are apparently absent at 9 km (Janecke et al., *in review*; Plate 1). To the north, the volcanic rocks terminate abruptly 3 km north of the trough of Lemhi Pass paleovalley. The location of the probable source caldera for the quartzite-bearing ash flow tuff, and the occurrence of interbedded west-derived gravels indicate flow from west to east within the Lemhi Pass paleovalley (Janecke et al., *in review*). These data suggest that despite the great thickness of the volcanic rocks within

the study area (> 2 km), no local source calderas or fault-controlled basins are required for such accumulations to be preserved in the rock record.

Ash flow tuffs and andesitic lava flows directly overlying the quartzite-bearing ash flow tuff appear to show "cut and fill" relationships within the Lemhi Pass paleovalley (Janecke et al., *in review*; Fig. 6). In section 20 of T 10 S, R 14 W, lava flows strike into a thick sequence of ash flow tuff (Plate 1; A-A', Plate 2). The ashfow tuff appears to have been emplaced prior to eruption of the lava flows, and subsequently eroded into a steep canyon, which was then backfilled by the lava flows. However, this interpretation is complicated by the presence of intrusions in the vicinity (units Tci, Tcli, and Tcu; Plate 1). The river that occupied the Lemhi Pass paleovalley must have had substantial discharge in order to reestablish itself during rapid accumulation of volcanic flows. Given a wet climate in the Eocene, gravels containing clasts up to 3 m in diameter interbedded with volcanic rocks (Janecke et al., *in review*), the amount of time since the probable inception of the Lemhi Pass drainage system (late Cretaceous (?), Janecke et al., *in review*), and the apparent length of the paleoriver (200-350 km, Janecke et al., *in review*), it seems plausible for paleotopography similar to that associated with the modern Snake River to have existed in the middle Eocene, and for that paleoriver to have reestablished itself between intermittent eruptions of ash flow tuffs and lava flows.

Little Eightmile Creek Basin

The northwest-dipping Little Eightmile Creek fault, which bounds the Little Eightmile Creek basin, was active during Challis volcanism, and again in the late-early to middle Miocene (Plate 1). The geometry of the basin is defined by the distribution of undifferentiated sediment (Tsu) found southwest of the continental divide, as little or no syntectonic sediments are preserved in the hanging wall of the fault to the northeast. The lack of Little Eightmile Creek basin-fill deposits northeast of the divide may reflect a

deeper structural level of the exposure, or a lack of syn-tectonic sedimentation. Insufficient data prohibit further evaluation of the hypotheses.

Southwest of the divide, up to 1000 m of sediment (Tsu) may have accumulated in the basin, but poor stratigraphic control and limited exposures limit quantitative analyses of the timing and character of the depositional environment. One outcrop located on the border of Montana and Idaho, near the uppermost headwaters of the Little Eightmile Creek drainage (Plate 1), consists of angular blocks (> 2 m) of Paleozoic limestone and chert in a red sand and clay matrix. This particular exposure is directly adjacent to the Little Eightmile Creek fault, and suggests significant topography during deposition of the sediment (Plate 1). Two km to the southwest, a 100-m-long block of Paleozoic limestone (mapped as Madison Limestone by Staatz (1973)) occurs interbedded with red clay (Plate 1). Local hematite staining within the block of Paleozoic limestone, and similarities to the Paleozoic limestone and red matrix found to the northwest suggest this exposure may be a slide block within the synrift sediments. In addition, air photo interpretations show the sediment striking parallel to the fault, and dipping moderately southeast into the fault. The size and angularity of clasts within the sediment, the location of the sediment with respect to the fault, and the orientation of the sediment seem to suggest sedimentation coeval with movement on the Little Eightmile Creek fault.

Poor age control within the undifferentiated sediment prohibits determining whether the sediment accumulated during the middle Eocene or late-early Miocene phase of slip on the Little Eightmile Creek fault. Lithologically, the sediment is unlike any other Tertiary basin-fill preserved in the study area. If the sediment accumulated in the late-early Miocene, one might expect to see tuffaceous sediment similar to the Oligocene to early Miocene sediment of Everson Creek. If the undifferentiated sediment accumulated during the middle Eocene phase of slip, it would be the first documented sedimentary half-graben-fill deposit on the margins of the Challis volcanic field (Janecke et al., *in*

review; Allen and Hahn, 1994). Additional data are required to elucidate the relationship between the unit Tsu and the two episodes of slip on the Little Eightmile Creek fault.

Medicine Lodge/Horse Prairie Protobasin

The Medicine Lodge/Horse Prairie protobasin refers to the depocenter that accumulated Paleogene basin-fill deposits (sediment of Bear Creek, lower shale and middle shale of M'Gonigle et al., 1991) prior to exposure of Archean gneisses of the Maiden Peak spur (Flores and M'Gonigle, 1991; M'Gonigle 1993; M'Gonigle and Dalrymple 1993, 1996). The structure that bounded the east-tilted protobasin is probably the low-angle, west-dipping Muddy-Grasshopper fault system in the Tendoy Range (Perry and M'Gonigle, 1995; Janecke et al., 1996a; Fig. 2; Fig. 18). As much as 3.4 km for Eocene to Oligocene sediments preserved within the Medicine Lodge part of the protobasin (Flores and M'Gonigle, 1991; S. U. Janecke and W. McIntosh, unpublished data, 1996) supports the interpretation of deposition within a rift-basin setting (Fig. 7; Fig. 9). Flores and M'Gonigle (1991) describe thick accumulations of coarse fan-delta sequences within the Medicine Lodge basin. In addition, freshwater limestones within the protobasin-fill deposits in the Horse Prairie basin, which are preserved in the hanging wall of the Lemhi Pass fault, contain middle to late Eocene gastropods (*Gyraulus proceras*) identical to endemic gastropods found in the Eocene to Oligocene Kishenehn half-graben (Steve Good, written comm., 1996; Constenius, 1981, 1982, 1988, 1995; McMechan and Price, 1980; McMechan, 1981; Janecke, 1994).

The original geographic extent of the Paleogene Medicine Lodge/Horse Prairie protobasin is unclear due to deposition of younger basin-fill deposits, and subsequent extension and erosion. However, exposures of protobasin deposits in the Medicine Lodge and Horse Prairie basins (Fig. 9; Plate 1) suggest that the protobasin was quite broad, and may have extended from the Muddy-Grasshopper fault system as far west as the confluence of Frying Pan and Trail Creeks in the eastern Lemhi Pass quadrangle (Fig.

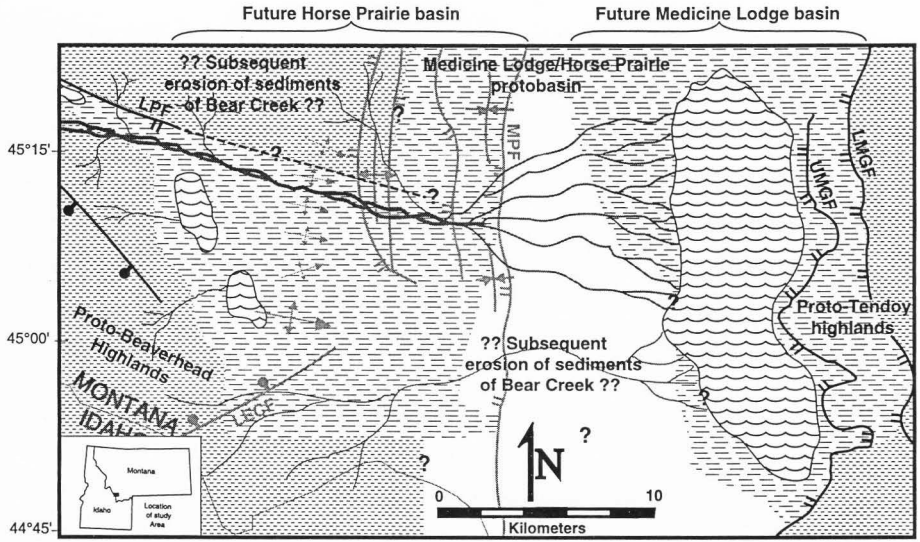

Figure 18. Middle to late Eocene paleogeographic map of the Horse Prairie/Medicine Lodge protobasin. Short horizontal dashes represent highlands; long horizontal dashes represent depocenters based on mapped exposures. Structures in black were active in middle to late Eocene time; structures in grey formed later or are inactive and are shown for reference only. Sediments that accumulated in the protobasin include the sediment of Bear Creek in the Horse Prairie basin, and the lower and middle shale units of M'Gonigle et al. (1991) in the Medicine Lodge basin. Map represents a slice in time immediately after initiation of slip on the Lemhi Pass fault, during deposition of coarse quartzite-clast conglomerate east of the Maiden Peak spur (unit Tc on Figure 9).

18). When subsequent extension on the Maiden Peak fault system is removed, this results in an original basin approximately 25 km wide.

Evidence within the sediment of Everson Creek also suggests that the underlying sediment of Bear Creek and its lateral equivalents were more widespread in the Eocene and Oligocene than the current distribution of exposures indicates. Well-rounded, platy, imbricated pebbles in the sediment of Everson Creek, which appear to be recycled from shale within protobasin deposits, show flow from the west and northwest (Fig. 10), suggesting the protobasin extended west and northwest of outcrops of the sediment of Everson Creek. The apparent lack of source rocks for the sediment of Everson Creek conglomerates may be the result of subsequent erosion and/or burial of the older protobasin deposits.

Despite tentative stratigraphic correlations made between the sediment of Bear Creek and the middle shale unit in the Medicine Lodge basin, the possibility exists that the sediment of Bear Creek accumulated in a separate basin bounded by the south southwest-dipping Lemhi Pass fault. This interpretation, however, is inconsistent with a number of observations that suggest the Lemhi Pass fault is distinctly younger than sediments that accumulated in Medicine Lodge/Horse Prairie protobasin, including: 1) Lithologic and geochronologic correlations can be made between the sediment of Bear Creek and the middle shale unit in the Medicine Lodge basin; 2) the sediment of Bear Creek or its lateral equivalents must have been present in the footwall of the Lemhi Pass fault to supply clasts to conglomerates in the overlying sediment of Everson Creek; and 3) freshwater limestone and interbedded fine-grained units of the sediment of Bear Creek can be traced to within 240 m of the Lemhi Pass fault with certainty, and may be offset by the fault. Thus, the preferred interpretation is that the Lemhi Pass fault postdates deposition of the sediment of Bear Creek and its lateral equivalents. Slip on the Lemhi Pass fault appears to have initiated after extension on the Muddy-Grasshopper fault, which bordered the

Medicine Lodge/Horse Prairie basin in Eocene to Oligocene time. The sediment of Bear Creek likely accumulated in the Paleogene protobasin, and has simply been denuded from the footwall of the Lemhi Pass fault. However, the data are permissive of either the Lemhi Pass fault-controlled basin or protobasin hypotheses.

The Medicine Lodge/Horse Prairie protobasin hypothesis of Flores and M'Gonigle (1991) differs from the protobasin described in this study. First, Flores and M'Gonigle (1991) hypothesized the development of the protobasin in response to Laramide contraction. New data (Perry and M'Gonigle, 1995; Janecke et al., 1996a; Janecke et al., 1996b; S. U. Janecke and W. McIntosh, unpublished data, 1996; this study), however, indicate the protobasin formed in response to extension on the west-dipping, low-angle Muddy-Grasshopper fault. Secondly, Flores and M'Gonigle (1991) described a west southwest-deeping basin as a result of Laramide-style uplifts west of the protobasin. However, thick accumulations of protobasin deposits in the Medicine Lodge basin (< 3.4 km), and relatively thin accumulations of the sediment of Bear Creek in the Horse Prairie basin (< 1 km) suggest that the basin deepens towards the Muddy-Grasshopper fault to the east northeast. Finally, dissection of the protobasin by uplift of the Maiden Peak spur occurred in middle Miocene time in the Flores and M'Gonigle (1991) model. However, examination of the Horse Prairie basin-fill in accordance with new provenance and paleocurrent data suggests the Maiden Peak fault, which separates the modern Horse Prairie and Medicine Lodge basins, may have been active during deposition of early Oligocene (?) to early Miocene sediment of Everson Creek, resulting in dissection of the protobasin as early as early Oligocene time.

Maiden Peak Basin

Superposed on the western half of the Medicine Lodge/Horse Prairie protobasin and Lemhi Pass fault is an Oligocene to early Miocene east-tilted half-graben, which appears to have been controlled by subsidence along the west-dipping Maiden Peak fault

system at its eastern margin during deposition of the sediment of Everson Creek. The depocenter that accumulated sediment during activity on the west-dipping Maiden Peak fault system is here referred to as the Maiden Peak basin (Fig. 19). The synrift Oligocene to early Miocene sediment of Everson Creek constitutes 1.4 m of the 1.6 km of Maiden Peak basin-fill deposits. Sedimentological data suggesting deposition of the sediment of Everson Creek during active subsidence of the Maiden Peak basin include: 1) coarse hanging wall-derived boulder gravels at the base of the sediment (unit Tg2, Plate 1), 2) multiple lenses of megabreccia (unit Tmb, Plate 1), interpreted to be ancient mass wasting deposits derived from the hanging wall, 3) scattered, footwall-derived gneissic clasts high in the sediment of Everson Creek (samples 11, 12, Fig. 10), 4) an angular unconformity within the sediment (between Tg2 and Tss, Plate 1; Fig. 6; Fig. 7), 5) abundant clasts, recycled from underlying Tertiary basin-fill, imply tilting during deposition of the sediment of Everson Creek (Fig. 8), and 6) paleocurrent and provenance data from the top of the sediment show flow from both the hanging wall and footwall into a south-flowing axial drainage system (Fig. 10).

The north-trending Maiden Peak basin has been modified little since its inception in the Oligocene. The location of the axial drainage closely approximates the location and orientation of the current Horse Prairie Creek, except for a reversal in flow direction and a slight shift toward the center of the basin. The observed drainage reversal indicates some modification of the Maiden Peak basin after its formation, but the changes appear to have been minor.

Passive Neogene Infilling of the Maiden Peak Basin

The lithology, orientation, and provenance of the middle Miocene sediment of Bannock Pass suggest only moderate topographic relief during its deposition, and little

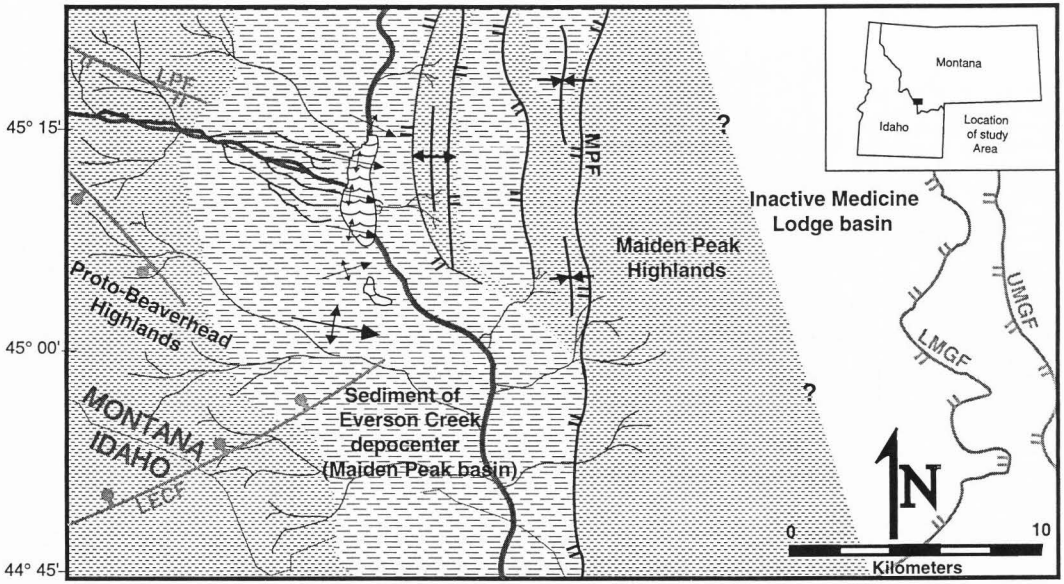

Figure 19. Oligocene to early Miocene paleogeographic map of the Maiden Peak basin. Short horizontal dashes represent highlands; long horizontal dashes represent depocenters based on mapped exposures. Structures in black were active in upper Oligocene to early Miocene time; structures in grey are inactive and shown for reference only. Sediments that accumulated in the fault-bounded basin include gravels, conglomerates, siltstone and sandstone of the sediment of Everson Creek. Map represents a slice in time during the development of a south-flowing axial drainage depicted in interpretations of the paleocurrent data (see Figure 10).

tectonism since. The sediment of Bannock Pass is confined to the southern third of the Maiden Peak half-graben, and is here interpreted as a post-rift deposit. The presence of sediment that is lithologically indistinguishable from the sediment of Bannock Pass in the western Grasshopper basin and along Bloody Dick Creek (S. U. Janecke, unpublished mapping; Fig. 4) suggests that this unit once extended farther north, and was eroded prior to deposition of the younger gravels (Fig. 20).

On the eastern half of the Horse Prairie basin, the sediment of Bannock Pass dips up to 8° to the west, away from the Maiden Peak fault, and contains blocks of gneiss derived from the Maiden Peak spur (M'Gonigle, 1994). In the western half of the basin examined in this study, the unit dips approximately 4° to the east, away from the Beaverhead Mountains, and contains west-derived, Middle Proterozoic quartzite clasts. The projections of the basal contacts of the two dip panels intersect near the axis of the modern Horse Prairie basin (E-E'; Plate 2). The distribution, orientation, provenance data, and fine-grained character suggest that the sediment of Bannock Pass passively infilled an existing topographic basin (Fig. 20), and has only experienced very slight modification by subsequent tectonism. It is unlikely that extension on the Maiden Peak fault continued after deposition of the sediment of Bannock Pass in middle Miocene time because the sediment in the Horse Prairie basin dips away from the fault in its immediate hanging wall. One possible alternative is that the sediment was downdropped symmetrically within a full graben. However, no antithetic faults have been found to the west of the Maiden Peak fault.

Gravel Caps and Quaternary (?) Incision

The only package of sediment preserved in the Horse Prairie basin above the middle Miocene sediment of Bannock Pass is a thin gravel deposit found on high ridges and hills. In the northen half of the Horse Prairie basin, this deposit overlies the sediment of Everson Creek. This gravel cap does not exceed 30 m in thickness, and appears to be

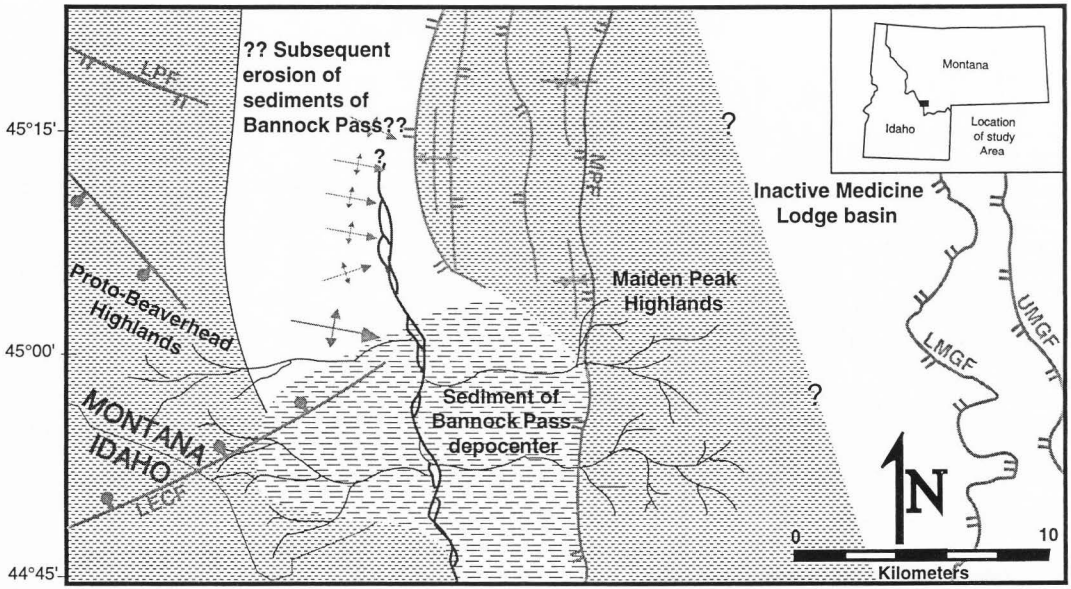

Figure 20. Middle Miocene paleogeographic map of the Horse Prairie/Medicine Lodge region. Short horizontal dashes represent highlands; long horizontal dashes represent depocenters based on mapped exposures. Structures in black were active in middle Miocene time; structures in grey are inactive and shown for reference only. Map represents a slice in time during passive infilling of the Maiden Peak basin by the sediment of Bannock Pass. The original extent of the depocenter and the flow direction of north-south stream system are unknown. Middle Miocene sediments are not preserved in the Medicine Lodge basin.

a stream-laid deposit that grades into the modern Beaverhead Mountains. The unit consistently dips very gently to the east, away from the range front, and contains clasts derived from Tertiary and pre-Tertiary bedrock presently exposed to the west. Similar deposits on the eastern half of the Horse Prairie basin have identical relationships to the Maiden Peak spur (M'Gonigle, 1994). Given these relationships, it appears that the gravel filled the preexisting Maiden Peak basin, much like the sediment of Bannock Pass, until a period of incision which left the stream gravels capping topographically high ridges.

Although any angular discordances between the gravel caps and the underlying sediment of Bannock Pass must be very slight in the southern third of the study area, rejuvenation of the source area or a major decrease in ash input may be indicated by a change from dominantly fine-grained to very coarse-grained deposition. If source rejuvenation is the cause for the changes in sedimentation, the rejuvenation of the source area did not result in denudation of the underlying sediment in the southern third of the basin. The mechanism of source rejuvenation may have been uplift in the footwall of the Beaverhead fault to the west. This uplift could result in renewed topography to the west, deposition of a bajada of well-rounded, coarse clastics, folding of the underlying sediment of Bannock Pass into a very gentle, north-plunging syncline (E-E'; Plate 2), and a minor discordance in dip between the younger gravel deposits and the underlying sediment of Bannock Pass.

Another change in the depositional environment within the Maiden Peak basin occurred sometime after deposition of the gravel caps, and resulted in incision by current stream systems into the basin-fill deposits. This episode of incision left the gravel caps stranded up to 230 m above current river level. The amount of incision is a minimum because it assumes the observed thickness of the gravel deposits is equal to the original thickness, when in fact the original thickness may have been much greater. Possible

causes for incision include: 1) climate change, 2) a decrease in sediment input after Pleistocene glaciation, 3) headward erosion within the Missouri River drainage basin, and 4) uplift in the footwalls of the adjacent Beaverhead and Red Rocks normal faults.

The effects of climate change, changes in sediment input, and uplift in the footwalls of the adjacent Beaverhead and Red Rocks normal faults are difficult to evaluate, but simple headward erosion in the uppermost reaches of the Missouri River drainage basin may be the dominant factor affecting Quaternary (?) incision in the Horse Prairie basin.

CONCLUDING REMARKS

SUMMARY

The Cenozoic extensional history of the Horse Prairie basin is characterized by at least five temporally distinct episodes of normal faulting, and at least three generations of folding related to extension. The Divide Creek and Bloody Dick Creek faults may reflect an episode of Mesozoic or Cenozoic northeast-southwest extension, however, the exact timing and kinematics of these faults remain largely enigmatic. If these pre-volcanic faults reflect crustal thinning, these structures clearly predate other normal faults found in the study area, and may represent widespread gravitational collapse the Sevier fold and thrust belt, possibly coeval with contraction.

The first tightly constrained episode of Cenozoic extension occurs on northwest-dipping, syn-Challis faults. The magnitude of this short-lived episode of northwest-southeast extension is difficult to constrain due to significant middle Eocene paleotopography. Nevertheless, the Horse Prairie basin appears to have experienced middle Eocene, northwest-southeast extension similar to that found to extend the Challis volcanic arc in east-central Idaho (McIntyre et al., 1982; Janecke, 1992, 1995), although extension within the study area appears to have been of lesser magnitude.

In late middle Eocene to early Miocene time, after the decline of Challis volcanism, the Horse Prairie basin experienced a second episode of northeast-southwest extension on the Muddy-Grasshopper, Maiden Peak, and Lemhi Pass fault systems. This event extends the crust in a direction and style similar to the pre-volcanic faults, and may reflect continued gravitational collapse subsequent to a brief interruption during Challis volcanism. The timing, geometry, and location of these late to post-volcanic normal faults support the interpretations of Janecke (1994) with regards to the placement of a narrow (100 ± 25 km) north- to north-northwest-trending rift zone through southwestern Montana. The breakaway zone separating extended hanging wall to the

west from intact footwall to the east is now thought to lie at the crest of the Tendoy Range, 20 km east of the Horse Prairie basin (Perry and M'Gonigle, 1995; Janecke et al., 1996a, 1996b).

This episode of late to post-volcanic extension is responsible for the bulk of the extensional strain in the study area, and preserves the majority of the Tertiary basin-fill deposits. The sediment of Bear Creek, and the equivalent units in the Medicine Lodge basin appear to have been deposited in an east northeast-deepening basin bound on the east by the Muddy-Grasshopper fault system. Subsequently, this "protobasin" was dissected by the Lemhi Pass and Maiden Peak fault systems. A younger angular unconformity-bounded package of sediment, the sediment of Everson Creek, accumulated in a half-graben bounded on the east by the Maiden Peak fault system. The sediment of Bannock Pass passively infilled this basin, representing the third angular unconformity-bounded sequence. The superposition of these depocenters resulted in the development of a structurally and stratigraphically complex half-graben.

Two fold trains found within the Paleogene basin-fill deposits can be attributed to extension on the Lemhi Pass and Maiden Peak fault systems. In the hanging wall of the Lemhi Pass fault, Challis volcanic rocks and the sediments of Bear Creek are folded into a series of northeast-plunging folds oriented at a relatively high angle to the fault. The exact mechanism for folding is uncertain, but a combination of mechanisms seems likely. Five to 10 km to the east and southeast, the sediment of Everson Creek is folded into a series of gentle east southeast-plunging anticlines and synclines in the hanging wall of the Maiden Peak fault. These folds are oriented at a relatively high angle to the Maiden Peak fault, but should be considered oblique folds. The mechanism of folding is unknown, and requires more detailed study of the fault plane, and more detailed characterization of the orientation of footwall and hanging-wall rocks.

Paleogene normal faults and extension-related folds dominate the extensional evolution of the Horse Prairie basin, but are overprinted by two generations of Neogene normal faulting also extend the area. Another period of northwest-southeast extension interrupted the persistent northeast-southwest extension direction in the middle Miocene. The result of middle Miocene extension is a subtle angular unconformity between the sediment of Everson Creek and the sediment of Bannock Pass. This angular unconformity may correlate with the regional mid-Tertiary unconformity, which is thought to represent the initiation of "Basin and Range" extension in the region (e.g. Fields et al., 1985). In the Horse Prairie basin, however, this mid-Tertiary unconformity may simply reflect the waning phases of Paleogene extension.

Northwest-striking faults, which locally remain seismically active in the region, offset the Little Eightmile Creek fault of the first phase of "Basin and Range" extension, and represent the fifth and final episode of extension in the study area. The second phase of "Basin and Range" extension follows the persistent northeast-southwest extension direction, but appears to be too far removed in time to reflect continued gravitational collapse. This youngest phase of deformation is not widespread within the study area, but may correlate with the Beaverhead fault to the southwest, and to other northwest-striking, seismically active faults in the region (Stickney and Bartholomew, 1987; Crone and Haller, 1991; Janecke, 1992). Several workers have attributed seismically active normal faults in southwest Montana and east central Idaho to the passage of the Yellowstone hot spot (Rodgers et al., 1990; Anders et al., 1993; Sears, 1995), but this mechanism is not sufficient to account for the time-space patterns of extension in the entire Basin and Range Province.

REGIONAL IMPLICATIONS

The data collected and compiled in this study can be used to address a number of important issues relevant to Cenozoic extension within the Basin and Range Province. I

briefly discuss a number of these topics, including: Cenozoic evolution of the Rocky Mountain Basin and Range Province, the effects of preexisting structures on subsequent extension, the relationship between magmatism and extension, half-graben evolution and sedimentation patterns, and the significance of folding during extension.

Cenozoic Evolution and the Role of Inheritance

Although much of the Basin and Range Province has experienced more than one episode of extension, multiple temporally and geometrically distinct events like those found in this study have yet to be documented. Southwest of the study area, Janecke (1992) discussed two episodes of Paleogene extension in addition to Basin and Range extension in east central Idaho. Northeast of the study area, Fritz and Sears (1993) documented two episodes of Neogene extension, a middle Miocene event, and a younger event that postdates eruption of a 6 Ma basalt flow, but did not present evidence of Paleogene extension. These data suggest the Horse Prairie basin is either unique in its Cenozoic tectonic evolution, or that evidence of the events described in this study have not been recognized by previous workers. Given the long and complex geologic history of the study area, and the possibility of major structural boundaries in the vicinity (e.g. southeast margin of the Belt basin, eastern margin of Sevier-style deformation, western margin of Laramide-style deformation, eastern margin of a Paleogene rift zone), it seems unlikely that a common tectonic evolution would be shared by all basins within the Rocky Mountain Basin and Range Province. I prefer the interpretation that the Horse Prairie basin is unique, and that a similar Cenozoic evolution may only be found in basins that have inherited a similar pre-Cenozoic evolution.

The precise role of inheritance is difficult to define within the study area, although the orientation of pre-Cenozoic structures appears to have influenced the orientation of subsequent normal faults. Reactivation of preexisting structures has been documented

throughout western Montana. Kellogg et al. (1995) hypothesized the reactivation of the Hilgard thrust system by the Neogene Madison normal fault system in the northern Madison Range. Similar relationships have been hypothesized in the Beaverhead, Ruby River, Gallatin, and Medicine Lodge valleys (Schmidt et al., 1984, 1993; Janecke et al., 1996a). Harlan et al. (1996) identified five episodes of deformation characterized by northeast-dipping structural elements in southwest Montana. In addition, Schmidt (1996) described northwest-dipping structures that have been recurrently active since the early Proterozoic. Northwest- and northeast-striking normal faults recur multiple times throughout the Cenozoic, suggesting a possible correlation to the pre-Cenozoic northwest- and northeast-trending structural elements. Although the Bloody Dick Creek and Little Eightmile Creek faults are the only structures in the study area shown to have been reactivated, inheritance seems to have been an important process involved in the development of the Horse Prairie half-graben.

Magmatism and Extension

The cause-and-effect relationships and the relative timing of magmatism and extension remain a controversial topic. Several workers have hypothesized that extension is a prerequisite for Cenozoic calc-alkaline magmatism in the western U.S. (Leeman and Harry, 1993; Hawkesworth et al., 1995; Hooper et al., 1995). Others propose that magmatism caused extension (Anderson, 1971; Lister and Baldwin, 1993), or that locally there is no relationship between extension and magmatism (Best and Christiansen, 1991; Axen et al., 1993). Data collected in this study can be used to evaluate the applicability of these hypotheses to the Horse Prairie basin, as well as providing insight into the relationship between magmatism and extension throughout the province.

In the Horse Prairie basin, magmatism and extension clearly overlap in time and space (Fig. 21). In detail, however, a direct correlation between magmatism and extension can only be found locally. If the Divide Creek and Bloody Dick Creek faults

represent crustal thinning, then local magmatism does not appear to have been a cause or an effect of extension. These pre-volcanic faults may reactivate Mesozoic thrust faults, extend the crust opposite to the shortening direction in the Sevier Orogeny, and lie within or close to structural culminations in the fold and thrust belt (Skipp, 1987, 1988; Tysdal, 1996a, 1996b; Tysdal and Moye, 1996; Janecke et al., *in review*; this study). These data suggest that the initial phases of extension in the region can be attributed to gravitational collapse of previously thickened crust, and that no correlation exists between local magmatism and extension. The effects of regional magmatism (emplacement of the Idaho Batholith to the north and northwest of the study area, ~100-58 Ma; Lund and Snee, 1988; Desmarais, 1983) are difficult to discern, but the distance between normal faults of this generation and the batholith (> 125 km) suggests a weak correlation at best.

In contrast, the second episode of extension appears to have a strong correlation with local and regional magmatism (Fig. 21). The extension direction for middle Eocene normal faults is orthogonal to the middle Eocene convergence vector for the Farallon and North American plates, and is parallel to the axis of the Challis volcanic arc, suggesting that these syn-volcanic normal faults reflect extension of the arc (Janecke, 1992, 1995). The relative timing and cause-and-effect relationships between magmatism and extension, however, are unclear. Syn-volcanic faults are an anomaly among Paleogene normal faults within the study area, both in their magnitude and extension direction, and appear to represent a short-lived interruption in a protracted episode of Paleogene gravitational collapse.

Late to post-volcanic faults, like pre-volcanic normal faults, do not appear to be driven by magmatism because they are not coeval with local or regional magmatic activity (Fig. 21). This generation of normal faults also extends the crust in a northeast-southwest to east-west direction, and is likely the result of continued gravitational collapse, because they generally parallel Mesozoic thrust faults in the region. The

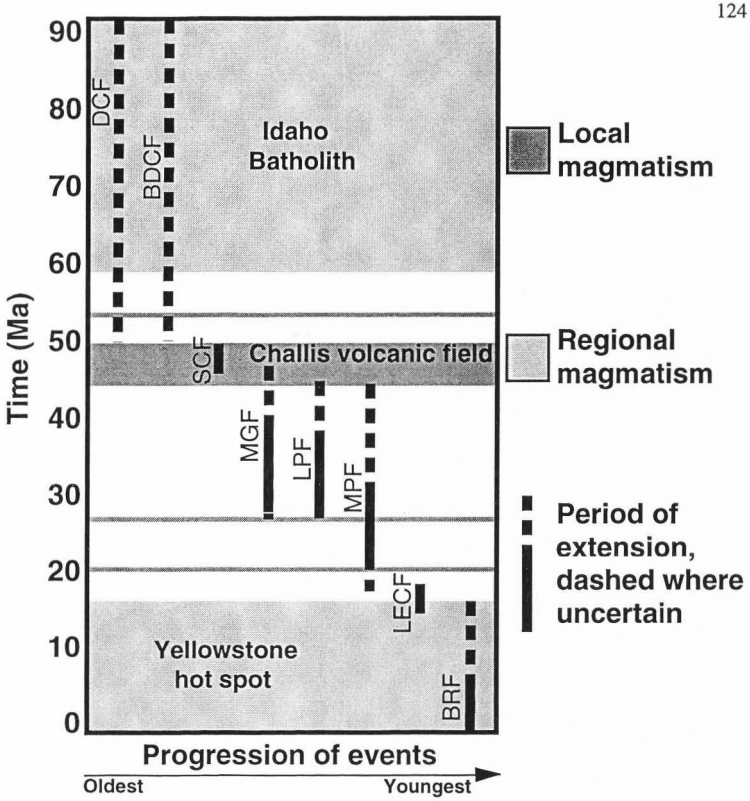

Figure 21. Graph comparing extensional episodes and magmatism in the Horse Prairie basin and surrounding region. Regional magmatism from 90-58 Ma refers to intrusion of the Idaho batholith > 125 km to the north northwest (Lund and Snee, 1988; Desmarais, 1983); regional magmatism also occurred along the Yellowstone hot spot track southwest, south, and southeast of the study area (~17-0 Ma). Local magmatism refers to magmatism in the Horse Prairie, Medicine Lodge, and Grasshopper basins and intervening ranges. Extensional episodes include slip on the Divide Creek (DCF), Bloody Dick Creek (BDCF), syn-Challis (SCF), Muddy-Grasshopper (MGF), Lemhi Pass (LPF), Maiden Peak (MPF), Little Eightmile Creek (LECF), and "Basin and Range" (BRF) normal faults. Note that extension is not focused during times of local or regional magmatism.

initiation of this episode of extension is difficult to constrain, but may coincide with the waning phases of Challis volcanism (Fig. 21). Thermal weakening due to Challis volcanism may have triggered extension, but extension long outlasted magmatism, and is not coeval with local or regional magmatism throughout most of its history.

The relationship between magmatism and extension for "Basin and Range" extension is ambiguous. Middle Miocene extension is not coeval with local magmatism, but a correlation with regional magmatism (Yellowstone hot spot, > 300 km to the SW) is permitted by the data (Fig. 21). As previously mentioned, the mechanism for middle Miocene extension is uncertain, but effects of the initiation of the Yellowstone hot spot may be the driving force. If this model is correct, extension may have been driven by regional magmatism; however, further study is required to test this hypothesis. Younger Basin and Range normal faults in the Horse Prairie basin appear to be associated with regional magmatism, but no magmatism of this age was found within the study area. Magmatism associated with the passage of the Yellowstone hot spot may be the driving mechanism for much of the youngest normal faulting in the area, but correlations between magmatism and middle Miocene and younger extension throughout the Basin and Range Province remain controversial.

In summary, most of the extensional strain in the study area accumulated in the Paleogene, on pre- and late to post-volcanic normal faults. This protracted period of extension does not correlate well with local or regional magmatism, and most likely reflects gravitational collapse of the Sevier fold and thrust belt. Although regional and local magmatism may have locally driven extension in the study area, the initiation and bulk of extension in the region was not the product of, nor a prerequisite to magmatism.

Sequential Evolution of a Detachment Fault System

Structural and sedimentological data from late to post-volcanic normal faults and from the sediments of Bear Creek and Everson Creek contain striking similarities with typical two-dimensional models for half-graben evolution. Gibbs (1987) proposed a generic model for the evolution of faults and sedimentary wedges above a stepped extensional fault (Fig. 22). This model is analogous to an east-west cross section through the Muddy-Grasshopper, Maiden Peak, and Lemhi Pass fault systems (Fig. 2). The model proposed by Gibbs (1987) describes a number of relationships found within the Horse Prairie and Medicine Lodge supradetachment basins. Gibbs (1987) shows the development of a low-angle detachment fault, and collapse of the footwall during initial phases of extension. Similarly, Janecke et al. (1996a) interpreted the Muddy-Grasshopper fault as a low-angle breakaway fault for late to post-volcanic extension, and presented evidence for collapse of the footwall early in the development of the extensional system. In addition, Gibbs (1987) showed evidence for a large normal fault that soles into a ramp in the detachment during collapse of the hanging wall (shortcut fault; Fig. 22). Reflection seismic data across the northern extension of the Maiden Peak fault system in the Grasshopper basin appear to show such a ramp in the Muddy-Grasshopper fault (Janecke et al., 1996a). Additional collapse of the hanging wall is achieved by slip on the Lemhi Pass fault and by the three splays of the Maiden Peak fault system.

Other relationships found in the Gibbs (1987) model are supported by data collected in this study. The occurrence of multiple angular unconformities and buried fault blocks is supported by the orientation of the Challis volcanic rocks and the sediments of Bear Creek and Everson Creek, and by cross-cutting relationships found in the Horse Prairie basin. Additionally, extension-related folds similar to those depicted in the model are found throughout the Medicine Lodge and Horse Prairie basins. However,

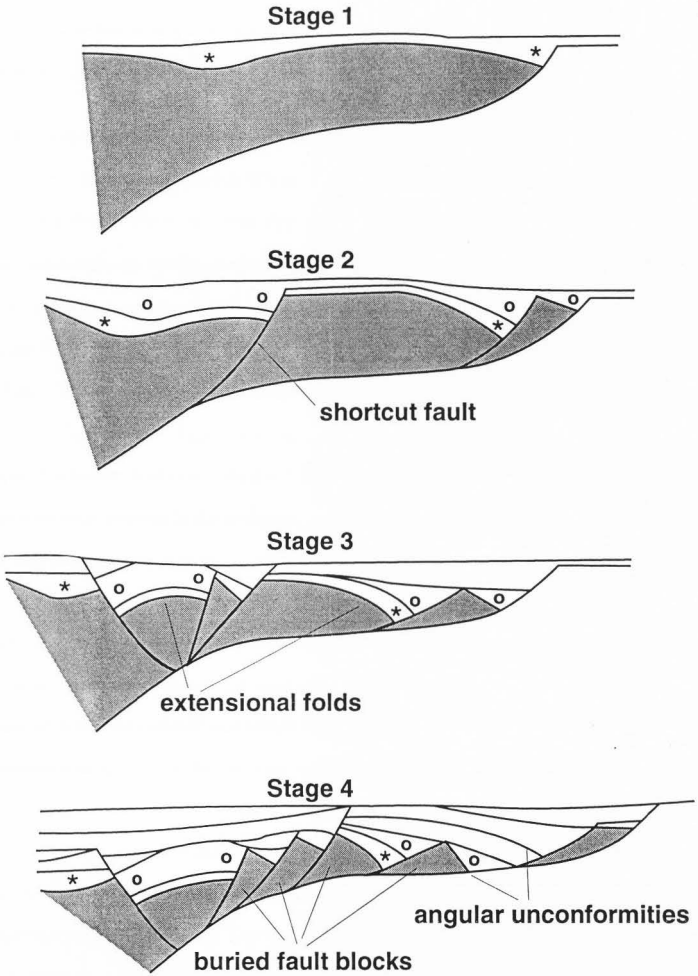

Figure 22. Sequential evolution of a stepped detachment fault system. Circles and asterisks mark the sequential positions of basin-fill deposited in the first two stages of development. Footwall collapse and a shortcut fault develop in stage 2, followed by additional collapse of the footwall and hanging wall, and extensional folding in stages 3 and 4. Modified from Gibbs (1987).

a two-dimensional model is inadequate to describe the three-dimensional deformation found within the study area.

Half-Graben Sedimentation Patterns

Sedimentation patterns within the sediment of Everson Creek, which was deposited during slip on the west-dipping Maiden Peak fault system, show evidence for long axial drainage systems and a persistence of detritus shed from the hanging wall into a depocenter adjacent to the Maiden Peak fault system. The Maiden Peak fault system is located in the hanging wall of a low-angle west-dipping detachment, and dips between 20° and 40° to the west. The Maiden Peak basin, which accumulated the sediment of Everson Creek in the Oligocene to early Miocene, should therefore be considered a supradetachment basin according to the definition of Fillmore et al. (1994). However, sedimentation patterns in the sediment of Everson Creek do not agree with typical models for sedimentation patterns in supradetachment basins.

Friedmann and Burbank (1995) proposed a model describing sedimentation patterns, structural characteristics, and magmatism associated with two arid intracontinental extensional end-members: supradetachment basins and rift basins. In terms of structural and sedimentological attributes, supradetachment basins are typically characterized by: 1) basin-bounding normal faults active at low-angles, 2) extension values often exceeding 100 percent, 3) long transverse footwall drainages, 4) depocenters 10 to 20 km from the breakaway, 5) 1 to 3 km of basin-fill, 6) substantial unconformities, and 7) mass wasting comprising 30 to 50 percent of the basin-fill (Fig. 23; Friedmann and Burbank, 1995). In contrast, rift basins are characterized by: 1) steep basin-bounding faults (45° to 60°), 2) extension values between 10 and 25 percent, 3) axial and hanging wall drainages, 4) asymmetric subsidence, and 5) 6 to 10 km of basin-fill (Fig. 23; Friedmann and Burbank, 1995).

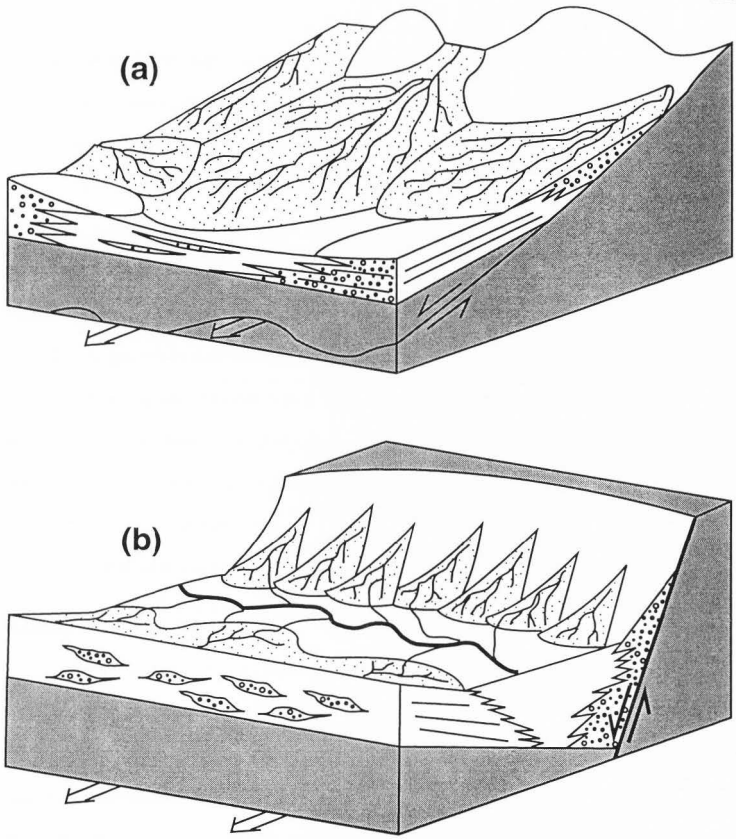

Figure 23. Two end-member models for intracontinental extension. (a) Closed arid terrestrial supradetachment basin. Note low-angle nonplanar detachment, distance between depocenter and breakaway, mass wasting deposits, and long drainages from the footwall. (b) Closed arid terrestrial rift basin. Note fault geometry, asymmetric subsidence, thick accumulations of basin-fill, axial and hangingwall drainages, and small drainages from the footwall. Modified from Friedmann and Burbank (1995).

In terms of structural attributes, data collected in the Maiden Peak basin match those predicted by the supradetachment model. The Maiden Peak fault system is low-angle, and has accommodated significant amounts of dip-slip separation (> 11 km). Alternatively, sedimentological characteristics of the Maiden Peak basin agree with those predicted by the rift model. Evidence of axial and hanging wall drainages is abundant within the sediment of Everson Creek, but sediment shed from the footwall does not appear until very high in the section close to the Maiden Peak fault. In addition, the mass wasting deposits that occur in the sediment of Everson Creek are uncommon, and in much lesser quantities than predicted by the supradetachment model. This discrepancy may in part be explained by climatic differences between the Horse Prairie basin and the arid models of Friedmann and Burbank (1995). The data collected in this study suggest the Horse Prairie basin does not fit the end-member models of Friedmann and Burbank (1995), and that the rift and supradetachment models may not adequately characterize basins in extended terranes.

Folding in Extension

Extension-related folds have been described by numerous workers throughout the Basin and Range Province (Fig. 24). The significance and complexity of extensional folds are underappreciated, despite their common occurrence. This study suggests that transverse and oblique folds are common structures, and that the resulting three-dimensional strain is a common occurrence as well. Estimates of preextension crustal geometries will differ if plane-strain extension is assumed in an area that has experienced three-dimensional strain. Extension-related folds can also have significant effects on basin geometry, and on the distribution of units involved in folding. In addition, folding within syntectonic sediments can influence sediment dispersal patterns. As a result, bed thickness may change over short distances, and changes in facies patterns can occur abruptly.

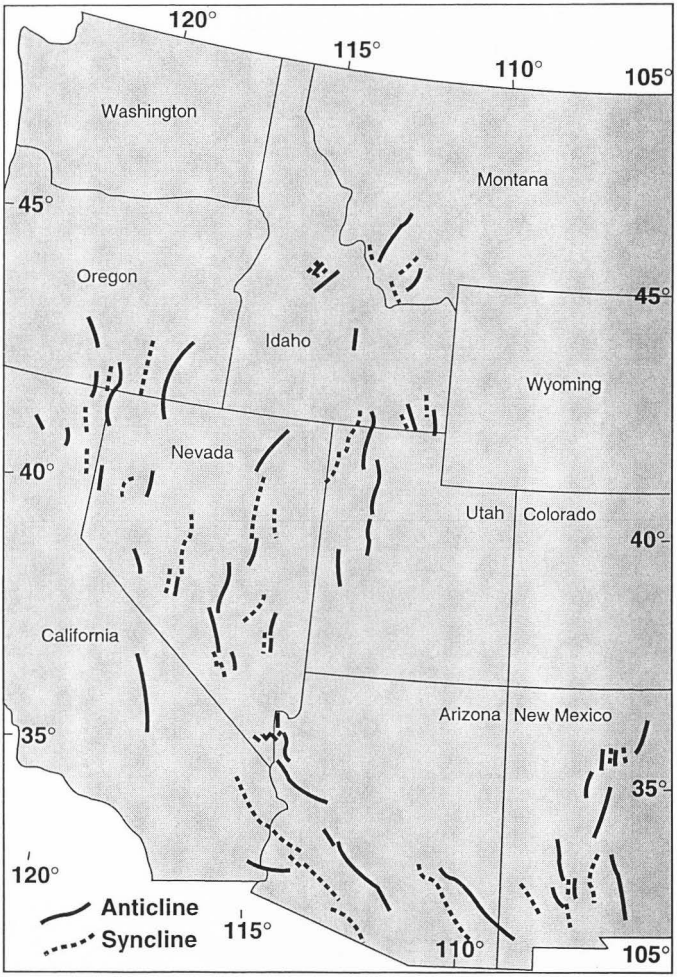

Figure 24. Map of extensional folds documented throughout the Basin and Range Province at accommodation zones. Modified from Stewart et al. (*in review*).

Detailed structural analysis of extensional folds, and of rocks in the hanging wall and footwall of the associated normal fault, is needed to provide a robust interpretation of the mechanisms responsible for extension-related folds. Additional work is needed within the Horse Prairie basin, and throughout the Basin and Range Province, to accurately determine the significance of folding in extensional settings.

REFERENCES CITED

Allen, K. D., and Hahn, G. A., 1994, Geology of the Sunbeam and Grouse Creek gold-silver deposits, Yankee Fork mining district, Eocene Challis volcanic field, Idaho; a volcanic dome- and volcaniclastic-hosted epithermal system: Economic Geology, v. 89, p. 1964-1982.

Anders, M. H., Hopper, J. R., Abad, R., and Spiegelman, M., 1993a, Lower crustal flow; the origin of late Cenozoic extension north of the eastern Snake River Plain: Geological Society of America Abstracts with Programs, v. 25, no. 5, p. 2.

Anders, M. H., Spiegelman, M., Rodgers, D. W., and Hagstrum, J. T., 1993b, The growth of fault-bounded tilt blocks: Tectonics, v. 12, no. 6, p. 1451-1459.

Anderson, J. J., 1971, Geology of the southwestern high plateaus of Utah: Bear Valley Formation, an Oligocene-Miocene volcanic arenite: Geological Society of America Bulletin, v. 82, p. 1179-1205.

Applegate, D. R., and Hodges, K. V., 1995, Mesozoic and Cenozoic extension recorded by metamorphic rocks in the Funeral Mountains, California: Geological Society of America Bulletin, v. 107, p. 1063-1076.

Atwater, T., 1970, Implications of plate tectonics for the Cenozoic tectonic evolution of western North America: Geological Society of America Bulletin, v. 81, p. 3513-3536.

Axen, G.J., Taylor, W.J., and Bartley, J.M., 1993, Space-time patterns and tectonic controls of Tertiary extension and magmatism in the Great Basin of the western United States: Geological Society of America Bulletin, v. 105, no. 1, p. 56-76.

Best, M. G., and Christiansen, E. H., 1991, Limited extension during peak Tertiary volcanism, Great Basin of Nevada and Utah: Journal of Geophysical Research, v. 96, no. B8, p. 13,509-13,528.

Burchfield, B. C., and Royden, L. H., 1985, North-south extension within the convergent Himalayan region: Geology, v. 13, p. 679-682.

Camilleri, P. A., and Chamberlain, K. R., 1997, Mesozoic tectonics and metamorphism in the Pequop Mountains and Wood Hills region, northeast Nevada: Implications for the architecture and evolution of the Sevier orogen: Geology, v. 109, p. 107-126.

Christiansen, R. L., and McKee, E. H., 1978, Late Cenozoic volcanic and tectonic evolution of the Great Basin and Columbia intermontane regions, *in* Smith, R. B., and Eaton, G. P., eds., Cenozoic tectonics and regional geophysics of the western Cordillera: Geological Society of America Memoir 152, p. 283-312.

Christiansen, R. L., and Yeats, R. S., 1992, Post-Laramide geology of the U.S. Cordilleran region, *in* Burchfield, B. C., Lipman, P. W., and Zoback, M. L., eds., The geology of North America, Volume G3: The Cordilleran orogen: Conterminous United States: Boulder, Colorado, Geological Society of America, p. 261-406.

Coney, P. J., and Harms, T., 1984, Cordilleran metamorphic core complexes; Cenozoic extensional relics of Mesozoic compression: Geology, v. 12, p. 550-554.

Connor, J. J., and Evans, D. V., 1986, Geologic map of the Leesburg Quadrangle, Lemhi County, Idaho: U.S. Geological Survey MF 1880, scale 1:62,500.

Constenius, K. N., 1981, Stratigraphy, sedimentation, and tectonic history of the Kishenehn Basin, northwestern Monatana [Masters thesis]: Laramie, University of Wyoming, 116 p.

Constenius, K. N., 1982, Relationship between the Kishenehn Basin and the Flathead normal fault system and Lewis thrust salient, *in* Powers, R. B., ed., Geologic studies of the Cordilleran thrust belt, Volume 1: Rocky Mountain Association of Geologists, p. 817-830.

Constenius, K. N., 1988, Structural configuration of the Kishenehn Basin delineated by geophysical methods, northwestern Montana and southeastern British Columbia: Mountain Geologist, v. 25, p.13-28.

Constenius, K. N., 1995, Extensional structures superposed on the Charleton-Nebo allochthon, central Utah: Geological Society of America Abstracts with Programs, v. 27, p.6.

Constenius, K. N., 1996, Late Paleogene extensional collapse of the Cordilleran foreland fold and thrust belt: Geological Society of America Bulletin, v. 108, p.20-39.

Coppinger, W., 1974, Stratigraphic and structural study of Belt Supergroup and associated rocks in a portion of the Beaverhead Mountains, southwest Montana, and east-central Idaho [Ph.D. dissertation]: Oxford, Miami University, 224 p.

Crone, A. J., and Haller, K. M., 1991, Segmentation and coseismic behavior of Basin and Range normal faults: Examples from east-central Idaho and southwestern Montana, U.S.A.: Journal of Structural Geology, v. 13, p. 151-164.

Davis, G. A., 1979, Problems of intraplate extensional tectonics, western United States, with special emphasis on the Great Basin, *in* Troxel, B. W., and Goode, H. D., eds., Basin and Range symposium and Great Basin field conference: Rocky Mountain Association of Geologists, p. 41-54.

Desmarais, N. R., 1983, Geology and geochronology of the Chief Joseph plutonic-metamorphic complex, Idaho-Montana [Ph.D. dissertation]: Seattle, University of Washington, 150 p.

Dokka, R. K., and Ross, T. M., 1995, Collapse of southwestern North America and the evolution of early Miocene detachment faults, metamorphic core complexes, the Sierra Nevada orocline, and the San Andreas fault system: Geology, v. 23, p. 1075-1078.

Dubois, D. P., 1982, Tectonic framework of basement thrust terrane, northern Tendoy Range, southwestern Montana, *in* Powers, R.B., ed., Geologic studies of the Cordilleran thrust belt, Volume 1: Rocky Mountain Association of Geologists, p. 145-158.

Dunlap, D. G., 1982, Tertiary geology of the Muddy Creek basin, Beaverhead County, Montana [Masters thesis]: Missoula, The University of Montana 133 p.

Ekren, E. B., 1988, Stratigraphic and structural relations of the Hoodoo Quartzite and Yellowjacket Formation of Middle Proterozoic age from Hoodoo Creek eastward to Mount Taylor, central Idaho: U.S. Geological Survey Bulletin 1570, 17 p.

Evans, K. V., and Zartman, R. E., 1990, U-Th-Pb and Rb-Sr geochronology of middle Proterozoic granite and augen gneiss, Salmon River Mountains, east-central Idaho: Geological Society of America Bulletin, v. 102, p. 63-73.

Fields, R. W., 1972, Geology of the Tertiary intermontane basins of western Montana: Geological Society of America Abstracts with Programs, v. 4, no. 6, p. 376.

Fields, R. W., Tabrum, A. R., Rasmussen, D. L., and Nichols, R., 1985, Cenozoic rocks of the intermontane basins of western Montana and eastern Idaho, *in* Flores, R. M., and Kaplan, S. S., eds., Cenozoic paleogeography of the west central U.S.: Denver, Colorado, Rocky Mountain Section, Society of Economic Paleontologists and Mineralogists, p. 9-36.

Fillmore, R. P., Walker, J. D., Bartley, J. M., and Glazner, A. F., 1994, Development of three genetically related basins associated with detachment-style faulting; predicted characteristics and an example from the central Mojave Desert, California: Geology, v. 22, p. 1087-1090.

Flores, R. M., and M'Gonigle, J. W., 1991, Oligocene-Miocene lacustrine rudite-dominated alluvial-fan delta, southwest Montana, U.S.A.: *in* Dabrie, C.J., ed., II fan-delta workshop, special issue, Universidad Complutense de Madrid, p. 241-278.

Friedmann, S. J., and Burbank, D. W., 1995, Rift basins and supradetachment basins: Intracontinental extensional end-members: Basin Research, v. 7, p. 109-127.

Fritz, W.J., and Sears, J.W., 1993, Tectonics of the Yellowstone hot spot wake in southwestern Montana: Geology, v. 21, p. 427-430.

Gans, P. B., Mahood, G. A., and Schermer, E., 1989, Synextensional magmatism in the Basin and Range Province; a case study from the eastern Great Basin: Geological Society of America Special Paper 233, 53 p.

Gibbs, A., 1987, Development of extension and mixed-mode sedimentary basins, *in* Coward, M. P., Dewey, J. F. and Hancock, P. L., eds., Continental extensional tectonics: Geological Society Special Publication No. 28, p. 19-33.

Glazner, A. F., and Bartley, J. M., 1984, Timing and tectonic setting of Tertiary low-angle normal faulting and associated magmatism in the southwestern United States: Tectonics, v. 3, p. 385-396.

Hait, M. H., Jr., and M'Gonigle, J. W., 1988, Implications of Cenozoic extension to interpretations of Tertiary Basin paleogeography and thrust belt paleotectonics: Geological Society of America Abstracts with Programs, v. 20, p. 108.

Haley, J. C., Dyman, T. S., Perry W. J. Jr., and Obradovich, J. D., 1995, The origin and significance of "Pyrenean-type" syntectonic unconformities in upper Cretaceous synorogenic sediments of southwestern Montana: Geological Society of America Abstracts with Programs, v. 27, no. 4, p. 12.

Hanneman, D. L., 1989, Cenozoic basin evolution in a part of southwest Montana [Ph.D. dissertation]: Missoula, University of Montana, 347 p.

Hanneman, D. L., and Wideman, C. J., 1991, Sequence stratigraphy of Cenozoic continental rocks, southwestern Montana: Geological Society of America Bulletin, v. 103, p. 1335-1345.

Hansen, P. M., 1983, Structure and stratigraphy of the Lemhi Pass area, Beaverhead Range, southwest Montana and east-central Idaho [Masters thesis]: University Park, Pennsylvania State University, 112 p.

Harlan, S. S., Schmidt, C. J., and Geissman, J. W., 1996, Nature and timing of recurrent movement on NW-trending faults in SW Montana: Middle (?) Proterozoic to Neogene history: Geological Society of America Abstracts with Programs, v. 28, no. 7, p. 509.

Hawkesworth, C., Turner, S., Gallagher, K., Hunter, A., Bradshaw, T., and Rogers, N., 1995, Calc-alkaline magmatism, lithospheric thinning, and extension in the Basin and Range: Journal of Geophysical Research, v. 100, no. B7, p. 10,271-10,286.

Hodges, K. V., and Walker, J. D., 1992, Extension in the Cretaceous Sevier orogen, North American Cordillera: Geological Society of America Bulletin, v. 104, p. 560-569.

Hooper, P. R., Bailey, D. G., and Holder, G. A. M., 1995, Tertiary calc-alkaline magmatism associated with lithospheric extension in the Pacific Northwest: Journal of Geophysical Research, v. 100, p. 10,303-10,319.

Horton, B. K., 1995, Facies associations and sediment source areas of the upper Cretaceous Knob Mountain conglomerate, Beaverhead Group, Montana and Idaho: Geological Society of America Abstracts with Programs, v. 27, no. 4, p. 14.

Huerta, A. D., and Rodgers, D. W., 1996, Kinematic and dynamic analysis of a low-angle strike-slip fault: The Lake Creek fault of south central Idaho: Journal of Structural Geology, v. 18, p. 585-593.

Janecke, S.U., 1992, Kinematics and timing of three superposed extensional systems, east-central Idaho: Evidence for an Eocene tectonic transition: Tectonics, v. 11, p. 1121-1138.

Janecke, S.U., 1994, Sedimentation and paleogeography of an Eocene to Oligocene rift zone, Idaho and Montana: Geological Society of America Bulletin, v. 106, p.1083-1095.

Janecke, S. U., 1995, Eocene to Oligocene half grabens of east-central Idaho: Structure, stratigraphy, age and tectonics: Northwest Geology, v. 24, p. 159-199.

Janecke, S. U., Blankenau, J. J., and VanDenburg, C. J., 1996c, Extension-related folds: Their classification and significance: Geological Society of America Abstracts with Programs, v. 28, no. 7, p. 115.

Janecke, S. U., Geissman, J. W., and Bruhn, R. L., 1991, Localized rotation during Paleogene extension in east central Idaho: Paleomagnetic and geologic evidence: Tectonics, v. 10, p. 403-432.

Janecke, S. U., M'Gonigle, J. W., McIntosh, W. C., VanDenburg, C. J., Perry, W. J. Jr., Good, S. C., and Nichols, R., 1996b, Sedimentation patterns in the Muddy Creek, Medicine Lodge/Horse Prairie and Grasshopper supra-detachment basins, MT: Geological Society of America Abstracts with Programs, v. 28, no. 7, p. 444.

Janecke, S. U., Perry, W. J. Jr., and M'Gonigle, J. W., 1996a, Scale-dependent reactivation of pre-existing structures by an Eocene-Oligocene detachment fault, southwestern Montana: Geological Society of America Abstracts with Programs, v. 28, no. 5, p. 78.

Kellogg, K. S., Schmidt, C. J., and Young, S. W., 1995, Basement and cover-rock deformation during Laramide contraction in the northern Madison Range (Montana) and its influence on Cenozoic basin formation: American Association of Petroleum Geologists Bulletin, v. 79, no. 8, p. 1117-1137.

Kuenzi, W. D., and Fields, R. W., 1971, Tertiary stratigraphy, structure and geologic history, Jefferson basin, Montana: Geological Society of America Bulletin, v. 82, p. 3374-3394.

Landis, C. A., Jr., 1963, Geology of the Graphite Mountain-Tepee Mountain area, Montana-Idaho [Masters thesis]: University Park, Pennsylvania State University, 153 p.

Landreth, J. O., 1964, Geology of the Rattlesnake Creek area, Lemhi county, Idaho [Masters thesis]: Moscow, University of Idaho.

Leeman, W. P., and Harry, D. L., 1993, A binary source model for extension-related magmatism in the Great Basin, western North America: Science, 262, p. 1550-1554.

Lister, G. S., and Baldwin, S. L., 1993, Plutonism and the origin of metamorphic core complexes: Geology, v. 21, p. 607-610.

Lucchitta, B.K., 1966, Structure of the Hawley Creek area, Idaho-Montana [Ph.D. dissertation]: University Park, Pennsylvania State University, 203 p.

Lund, K., and Snee, L. W., 1988, Metamorphism, structural development, and age of the continent-island arc juncture in west-central Idaho, in Ernst, W. G., ed., Metamorphism and crustal evolution of the western United States, Rubey Vol. 7: Englewood Cliffs, New Jersey, Prentice-Hall, p. 296-331.

MacKenzie, W. O., 1949, Geology and ore deposits of a section of the Beaverhead Mountains east of Salmon, Idaho [Masters thesis]: Moscow, University of Idaho, 53 p.

McIntyre, D. H., Ekren, E. D., and Hardyman, R. F., 1982, Stratigraphic and structural framework of the Challis volcanic rocks in the eastern half of the Challis 1° x 2° quadrangle, Idaho, *in* Bonnichsen, B., and Breckenridge, R. M., eds., Cenozoic geology of Idaho: Idaho Bureau of Mines and Geology Bulletin 26, p. 3-22.

McMechan, R. D., 1981, Stratigraphy, sedimentology, structure and tectonic implications of the Oligocene Kishenehn Formation, Flathead Valley graben, southeastern British Columbia [Ph.D. dissertation]: Kingston, Ontario, Queen's University, 327 p.

McMechan, R. D., and Price, R. A., 1980, Reappraisal of a reported unconformity in the Paleogene (Oligocene) Kishenehn Formation: Implications for Cenozoic tectonics in the Flathead Valley graben, southeastern British Columbia: Bulletin of Canadian Petroleum Geology, v. 28, p. 37-45.

M'Gonigle, J.W., 1993, Geologic map of the Medicine Lodge Peak quadrangle, Beaverhead County, southwest Montana: U.S. Geological Survey Quadrangle Map GQ-1724, scale 1:24,000.

M'Gonigle, J.W., 1994, Geologic map of the Deadman Pass quadrangle, Beaverhead County, southwest Montana: U.S. Geological Survey Quadrangle Map GQ-1753, scale 1:24,000.

M'Gonigle, J. W., and Dalrymple, G. B., 1993, $^{40}Ar/^{39}Ar$ ages of Challis volcanic rocks and the initiation of Tertiary sedimentary basins in southwestern Montana: Mountain Geologist, v. 30, p. 112-118.

M'Gonigle, J. W., and Dalrymple, G. B., 1996, $^{40}Ar/^{39}Ar$ ages of some Challis Volcanic Group rocks and the initiation of Tertiary sedimentary basins in southwestern Montana: U.S. Geological Survey Bulletin 2132, 17 p.

M'Gonigle, J. W., and Hait, M. H., Jr., 1997, Geologic map of the Jeff Davis Peak and the eastern part of the Everson Creek quadrangle, Beaverhead County, southwest Montana: U.S. Geological Survey Quadrangle Map GQ-2604, scale 1:24,000.

M'Gonigle, J. W., Kirschbaum, M. A., and Weaver, J. N., 1991, Geologic map of the Hansen Ranch quadrangle, Beaverhead County, southwest Montana: U.S. Geological Survey Quadrangle Map GQ-1704, scale 1:24,000.

Miller, D. M., 1990, Mesozoic and Cenozoic Tectonic evolution of the Northeastern Great Basin, *in* Shaddrick, D. R., Kizis, J. A., Jr., and Hunsaker, E. L., III, eds., Geology and ore deposits of the northeastern Great Basin, Geological Society of Nevada, Field Trip No. 5, p. 43-73.

Perry, W. J. Jr., Dyman, T.S., and Sando, W.J., 1989, Southwestern Montana recess of Cordilerran thrust belt, *in* French, D.E., and Grabb, R.F. eds., Montana Geological Society 1989 field conference guidebook: Montana Centennial Edition, v. 1, p. 261-270.

Perry, W. J. Jr., and M'Gonigle, J. W., 1995, Neogene extensional events, northern Tendoy Mountains and adjacent Medicine Lodge basin, southwest Montana: Geological Society of America Abstracts with Programs, v. 27, no. 4, p. 51.

Perry, W. J. Jr., and Sando, W. J., 1983, Sequential deformation in the thrust belt of southwestern Montana, *in* Powers, R. B., ed., Geologic studies of the Cordilleran thrust belt, 1982: Denver, Colorado, Rocky Mountain Association of Geologists, v. 1, p. 137-144.

Pezzopane, S. K., and Weldon, R. J., 1993, Tectonic role of active faulting in central Oregon: Tectonics, v. 12, no. 5, p. 1140-1169.

Pierce, K. L., and Morgan, L. A., 1992, The track of the Yellowstone hot spot: Volcanism, faulting, and uplift, *in* Link, P. K., Kuntz, M. A., and Platt, L. B., eds., Regional geology of eastern Idaho and western Wyoming: Geological Society of America Memoir 179, p. 1-53.

Piety, L. A., Sullivan, J. T., and Anders, M. H., 1992, Segmentation and paleoseismicity of the Grand Valley fault, southeastern Idaho and western Wyoming, *in* Link, P. K., Kuntz, M. A., and Platt, L. B., eds., Regional geology of eastern Idaho and western Wyoming: Geological Society of America Memoir 179, p. 1-53.

Rasmussen, D. L., 1973, Extension of the middle Tertiary unconformity in western Montana: Northwest Geology, v. 2, p. 27-35.

Rasmussen, D. L., 1977, Geology and mammalian paleontology of the Oligocene-Miocene Cabbage Patch Formation, central-western Montana [Ph.D. dissertation]: Lawrence, University of Kansas, 794 p.

Reynolds, 1979, Character and extent of Basin-Range faulting, western Montana and east-central Idaho, *in* Troxel, B. W., and Goode, H. D., eds., Basin and Range symposium and Great Basin field conference: Rocky Mountain Association of Geologists, p. 305-312.

Rodgers, D. W., and Hackett, W. R., and Ore, H. T., 1990, Extension of the Yellowstone Plateau, eastern Snake River Plain and Owyhee Plateau: Geology, v. 18, p. 1138-1141.

Royden, L. H., and Burchfield, B. C., 1987, Thin-skinned north-south extension within the convergent Himalayan region; Gravitational collapse of a Miocene topographic front, *in* Coward, M. P., Dewey, J. F., and Hancock, P. L., eds., Continental extensional tectonics: Geological Society of London Special Publication 28, p. 611-619.

Ruppel, E. T., 1975, Precambrian Y sedimentary rocks in east-central Idaho, Chap. A *of* Precambrian and Lower Ordovician rocks in east-central Idaho: U.S. Geological Survey Professsional Paper 889, p. 1-23.

Ruppel, E. T., and Lopez, D. A., 1984, The thrust belt in southwest Montana and east-central Idaho: U.S. Geological Survey Professional Paper 1278, 41 p.

Ruppel, E. T., O'Neill, J. M., and Lopez, D. A., 1993, Geologic map of the Dillon 1° x 2° quadrangle, Idaho and Montana: U.S. Geological Survey Miscellaneous Investigations Series Map I-1803-H.

Schlische, R. W., 1995, Geometry and origin of fault-related folds in extensional settings: American Association of Petroleum Geologists Bulletin, v. 79, p. 1661-1678.

Schmidt, C. J., 1996, Neogene inversion of Cretaceous rift basins and reversion of Carboniferous uplifts in the Pampean Ranges, Argentina, with implications for reactivation in the Laramide Rocky Mountains: Geological Society of America Abstracts with Programs, v. 28, no. 7, p. 112.

Schmidt, C. J., Sheedlo, M., and Werkema, M., 1984, Control of range-boundary normal faults by earlier structure, southwestern Montana: Geological Society of America Abstracts with Programs, v. 16, no. 4, p. 253.

Schmidt, C. J., Evans, J. P., Harlan, S. S., Weberg, E. D., Brown, F. S., Batatian, D., Derr, D. N., Malizzi, L., McDowell, R. J., Nelson, G. C., Parke, M., and Genovese, P. W., 1993, Mechanical behavior of basement rocks during movement of the Scarface thrust, central Madison Range, Montana, *in* C. J. Schmidt, R. Chase, and E. A. Erslev, eds., Laramide basement deformation in the Rocky Mountain foreland of the western United States: Boulder, Colorado, Geological Society of America Special Paper 280, p. 89-105.

Schmidt, K. L., Lewis, R. S., Burmester, R. F., and Lang, R. A., 1994, Reconnaissance geologic map of the Shoup and Horse Creek area, Lemhi and Idaho Counties, Idaho: Idaho Geological Survey Technical Report 94-3, scale 1:50,000, 13 p.

Scholten, R., 1982, Continental subduction in the northern U.S. Rockies--A model for back-arc thrusting in the western Cordillera, *in* Powers, R. B., eds., Geologic Studies of the Corilleran thrust belt: Rocky Mountain Association of Geologists, v. 1, p. 123-136.

Scholten, R., Keeman, K. A., and Kupsch, W. O., 1955, Geology of the Lima region, southwestern Montana and adjacent Idaho: Geological Society of America Bulletin, v. 66, no. 4, p. 345-404, scale 1:125,000.

Scholten, R. and Ramspott, L. D., 1968, Tectonic mechanisms indicated by structural framework of central Beaverhead Mountains, Idaho-Montana: Geological Society of America Special Paper 104, 71 p., map scale 1:125,000.

Sears, J. W., 1995, Middle Miocene rift system in SW Montana: Implications for the initial outbreak of the Yellowstone hot spot: Geologic history of the Dillon area, southwestern Montana: Northwest Geology, v. 25, p. 43-46.

Sears, J. W., Hurlow, H., Fritz, W. J., and Thomas, R. C., 1995, Late Cenozoic disruption of Miocene grabens on the shoulder of the Yellowstone hot spot track in southwest Montana: Field guide from Lima to Alder, Montana: Northwest Geology, v. 24, p. 201-219.

Sharp, W. N., and Cavender, W. S., 1962, Geology and thorium-bearing deposits of the Lemhi Pass area, Lemhi County, Idaho, and Beaverhead County, Montana: U.S. Geological Survey Bulletin 1126, 76 p.

Skipp, B., 1984, Geologic map and cross sections of the Italian Peak and Italian Peak Middle Roadless areas, Beaverhead County, Montana, and Clark and Lemhi Counties, Idaho: U.S. Geological Survey Miscellaneous Field Studies Map MF-1061-B, scale 1:62,500.

Skipp, B., 1985, Contraction and extension faults in the southern Beaverhead Mountains, Idaho and Montana: U.S. Geological Survey Open-file report 85-545, 170 p.

Skipp, B., 1987, Basement thrust sheets in the Clearwater orogenic zone, central Idaho and western Montana: Geology, v. 15, p. 220-224.

Skipp, B., 1988, Cordilleran thrust belt and faulted foreland in the Beaverhead Mountains, Idaho and Montana, *in* Schmidt, C. J., and Perry, W. J., Jr., eds., Interaction of the Rocky Mountain foreland and Cordilleran thrust belt: Geological Society of America Memoir 171, p. 237-266.

Soregaroli, A. E., 1961, Geology of the McKim Creek area, Lemhi County, Idaho [Masters thesis]: Moscow, University of Idaho, 53 p.

Staatz, M. H., 1972, Geology and description of the thorium-bearing veins, Lemhi Pass quadrangle, Idaho and Montana: U.S. Geological Survey Bulletin 1351, 94 p.

Staatz, M. H., 1973, Geologic map of the Goat Mountain quadrangle, Lemhi County, Idaho and Beaverhead County, Montana: U.S. Geological Survey Quadrangle Map GQ-1097, scale 1:24,000.

Staatz, M. H., 1979, Geology and mineral resources of the Lemhi Pass thorium district, Idaho and Montana: U.S. Geological Survey Professional Paper 1049-A, 90 p.

Stickney, M. C., and Bartholomew, M. J., 1987, Seismicity and Quaternary faulting of the northern Basin and Range Province, Montana and Idaho: Bulletin of the Seismological Society of America, v. 77, p. 1602-1625.

Taylor, W. J., and Bartley, J. M., 1992, Prevolcanic extensional Seaman breakaway fault and its geologic implications for eastern Nevada and western Utah: Geological Society of America Bulletin, v. 104, p. 255-266.

Thomas, R. C., 1995, Tectonic significance of Paleogene sandstone deposits in southwestern Montana: Field guide from Lima to Alder, Montana: Northwest Geology, v. 24, p. 237-244.

Thomas, R. C., Sears, J. W., Ripley, A. A., and Berg, R. B., 1995, Tertiary extensional history of southwestern Montana: Field trip guide for the Sweetwater and upper Ruby valleys, Montana: Northwest Geology, v. 25, p. 5-25.

Thompson, G. T., Fields, R. W., and Alt, David, 1981, Tertiary paleoclimates, sedimentary patterns and uranium distrubution in southwestern Montana: Montana Geological Society, Southwest Montana Field Conference Guidebook, p. 105-109.

Tietbohl, D., 1981, Structure and stratigraphy of the Hayden Creek area, Lemhi Range, east-central Idaho [Masters thesis]: University Park, Pennsylvania State University, 121 p.

Tietbohl, D., 1986, Middle Proterozoic diamictite beds in the Lemhi Range, east-central Idaho, *in* Roberts, S. M., ed., Belt Supergroup; a guide to Proterozoic rocks of western Montana and adjacent areas: Montana Bureau of Mines and Geology Special Publication 94, p. 197-207.

Tucker, D. R., 1975, Stratigraphy and structure of Precambrian Y (Belt?) metasedimentary and associated rocks, Goldstone Mountain quadrangle, Lemhi County, Idaho, and Beaverhead County, Montana [Ph.D. dissertation]: Oxford, Florida, Miami University, 221 p.

Tysdal, R. G., 1996a, Geologic map of the Lem Peak quadrangle, Lemhi County, Idaho: U.S. Geological Survey Quadrangle Map GQ-1777, scale 1:24,000.

Tysdal, R. G., 1996b, Geologic map of adjacent areas in the Hayden Creek and Mogg Mountain quadrangles, Lemhi County, Idaho: U.S. Geological Survey Miscellaneous Inverstigations Series Map I-2563, scale 1:24,000.

Tysdal, R. G., and Moye, F. J., 1996, Geologic map of the Allison Creek quadrangle, Lemhi County, Idaho: U.S. Geological Survey Quadrangle Map GQ-1778, scale 1:24,000.

VanDenburg, C. J., Janecke, S. U., and Nichols, R., 1996, Multiple episodes of Tertiary extension in the west-central Horse Prairie basin, southwestern Montana: Geological Society of America Abstracts with Programs, v. 28, no. 5, p. 120.

Wells, M. L., 1997, Alternating contraction and extension in the hinterlands of orogenic belts: An example from the Raft River Mountains, Utah: Geology, v. 109, p. 107-126.

Werkema, M. A., and Young, S. W., 1983, Overlapping styles of deformation, northern Madison Range, Montana: Geological Society of America Abstracts with Programs, v. 15, no. 5, p. 296.

Wernicke, B., 1992, Cenozoic extensional tectonics of the U.S. Cordillera, *in* Burchfield, B. C., Lipman, P. W., and Zoback, M. L., eds., The geology of North America, Volume G3: The Cordilleran orogen: Conterminous United States: Boulder, Colorado, Geological Society of America, p. 553-581.

Wernicke, B., Christiansen, R. L., England, P. C., and Sonder, L. J., 1987, Tectonomagmatic evolution of Cenozoic extension in the North American Cordillera, *in* Coward, M. P., Dewey, J. F., and Hancock, P. L., eds., Continental extensional tectonics: Geological Society of London Special Publication 28, p. 203-221.

Winston, D., and Link, P. K., 1993, Middle Proterozoic rocks of Montana, Idaho and eastern Washington: The Belt Supergroup, *in* Reed, J. C., Jr., Bickford, M. E., Houston, R. S., Link, P. K., Rankin, D. W., Sims, P. K., and Van Schmus, W. R., eds., Precambrian: Conterminous U. S.: Geological Society of America The Geology of North America C-2, p. 487-517.

Wust, S. L., 1986, Regional correlation of extension directions in Cordilleran metamorphic core complexes: Geology, v. 14, p. 828-830.

Young, S. W., 1985, Structural history of the Jordan Creek area, northern Madison Range, Madison County, Montana [Masters thesis]: Austin, University of Texas, 113 p.

APPENDIX

TABLE 3. PEBBLE TO BOULDER COUNT DATA FROM CENOZOIC BASIN-FILL DEPOSITS.

Sample number	Rock unit	Max clast size (cm)	Rounding (1-3)	% Y	% Tcv	% Ts	% Ag	% TKi	% Pz	% other
1*	Ts2	10	3	19	2	79				
2*	Ts2	10	3	4	2	94				
3	Ts2	8	3	85	10	5				
4*	Tss	15	3	43	52					5
5*	Ts2	10	3	10	4	86				
6*	Tss	15	2-3	66	26	4		4		
7	Tcg1	35	3	100						
8	Tcg2	300	3	92	4			4		
9	Tg1	40	3	31	69					
10	Tg1	40	3	78	22					
11	Tg1	75	3	46	54					
12	Tg1	20	3	25	75					
13*	Tg1	20	3	14	86					
14	Tg1	200	2-3	6	90	4				
15*	Tg1	40	3	62	38					
16	Tg2	20	3	69	29	2				
17*	Ts2	6	3	17	13	70				
18*	Ts2	15	3	40	23	37				
19*	Ts2	8	3	13	11	76				
20*	Ts2	15	3	16	5	79				
21*	Ts2	15	2	63	26	11				
22	Tg2	30	3	96	4					
23	Tg2	25	3	68	32					
24*	Ts2	8	2-3	22	33	45				
25*	Tss	15	2-3	18	42	40				
26*	Ts2	20	3	8	4	88				
27	Tg2	3	3	72	26					2
28	Tg2	15	2-3	70	30					
29	QTgo	50	3	56	40					4
30	QTgy	200	3	63	27					
31*	Ts2	10	3	19	13	68				
32	QTgo	>100	3	70	28			1		1
33	Ts2	50	3	50	46	4				
34	Tg2	10	3	62	38					
35	Tg2	25	2-3	70	30					
36	Tg2	15	3	68	32					
37*	Tss	8	2-3	38	16	46				
38	QTgo	50	3	51	48					1
39*	Ts2	4	3	6	2	92				
40	QTgo	50	3	58	40	2				
41*	Ts2	10	3	17	9	74				
42*	Ts2	8	3	5	4	91				
43	Ts2	8	3	72	28					
44*	Tg2	>100	1-2	56	40					4
45	Tg2	50	3	50	50					
46	Ts2	5	2-3	76	24					
47	QTgo	100	3	62	36			2		
48*	Ts2	8	2	34	48	18				
49*	Ts2	10	3			100				
50*	Ts2	4	3	16	20	64				
51	QTgy	50	3	54	35	10		1		
52	Ts2	5	2	64	36					

53*	Ts2	4	2	36	50	14				
54*	Ts2	3	1-2	48	44	8				
55	Ts2	6	2-3	82	18					
56	QTgy	30	3	57	13	2	28			
57	Ts2	40	2-3	47	13		40			
58*	Ts2	12	2	60	28		12			
59	QTgy	3	3	61	39					
60*	Ts2	3	2-3	39	43	18				
61*	Ts2	5	3	7	38	55				
62*	Ts2	6	2-3	55	36	9				
63*	Ts2	5	3	2	4	94				
64	Ts2 ?	50	2-3	65	35					
65	Ts2 ?	50	3	55	42		3			
66	Ts2	25	3	63	37					
67*	Ts1	200	1-2	44	38	18				
68	Tg1	100	1-3	67	27	6				
69*	Ts2	4	2	45	49					6
70*	Ts2	6	2-3	62	38					
71*	Ts2	6	1-2	18	44	38				
72*	Ts2	4	2-3	43	48	9				
73*	Ts1	3	2-3	5	45	50				
74*	Ts1	2	2	19	60	21				
75*	Ts1	5	1-2	4	77	19				
76*	Ts2	10	3	35	24	41				
77*	Ts2	5	3	18	9	73				
78*	Ts2	7	3	19	26	55				
79*	Ts1	8	1	9	70	21				
80	Tg1	100	1-2	52	44	4				
81*	Ts1	6	1	39	53	8				
82*	Ts1	8	1	7	29	64				
83*	Ts2	4	2	52	39	9				
84*	Ts2	10	2	46	40	14				
85*	Ts2	4	1-2	25	36	39				
86	Tg2	100	1-2	44	42	14				
87	QTgo	50	1-2	39	57	4				
88	QTgo	100	1-2	19	77	4				
89	Ts3a	30	1-2	19	42	36		4		
90	Ts1	50	1-2	30	54	16				
91	Ts1	50	1-2	29	55	16				
92	QTgo	>25	1-2	55	33	12				
93	Ts3b	40	2	71	13			16		
94	Ts3a	50	1-2	75	17	4		4		

Notes: Sample numbers correspond to sample numbers of Plate 1. Asterisks show localities with cemented exposures. Rounding of clasts is designated (1) for subangular, (2) for subrounded, and (3) for well rounded. Y=Middle Proterozoic quarzite, Tcv=Challis volcanic rock, Ts=recycled Tertiary sediment, Ag=Archean gneiss, Tki=intrusive rock, Pz=Paleozoic rock, other=unidentifiable clast type.

Plate 1. Geologic map of the Horse Prairie half-graben, southwest Montana

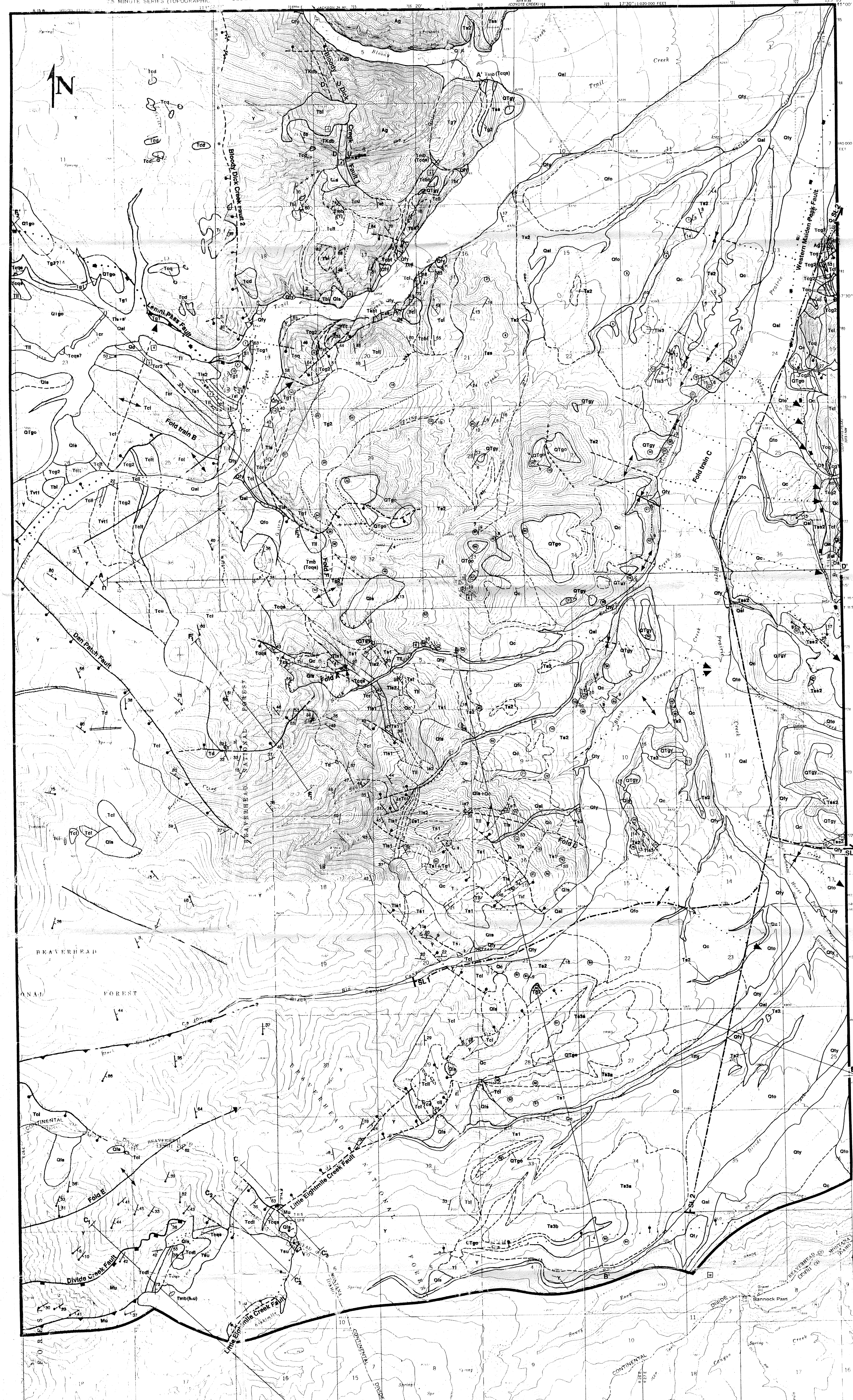

CORRELATION OF MAP UNITS

Quaternary: Qal, Qfy, Qty, Qfo, Qto, Qls, Qc
Unconformity
QTgy, QTgo
Angular Unconformity

Middle Miocene: Ts3b, Ts3a — Sediment of Bannock Pass
Angular Unconformity

Late Eocene - Early Miocene: Tss2, Tls3, Ts2, sh, ss, Tg2, Tmb, Tsu — Sediment of Everson Creek (Local Angular Unconformity)
Angular Unconformity

Middle - Late Eocene: Tli, Ti; Ts1, Tg1, Tls2, ss, Tls1 — Sediment of Bear Creek
Angular? Unconformity

Middle Eocene: Tcqs
Angular? Unconformity

Middle Eocene: Td, Tcl, Tcc, Tcli, Tbi; TKdb; Tcr, Tcs, Tcl, Tcbt, Tclt, Tcg2, Tcq, Tcg1, Tcdl, Tcu — Challis volcanic rocks (Local Angular Unconformity)
Angular Unconformity

Mississippian: Mu
Lower Ordovician: Os
Fault
Middle Proterozoic: Y
Fault
Archean: Ag

DESCRIPTION OF MAP UNITS

Qal Holocene and upper? Pleistocene alluvium (0-20 m).

Qls Holocene and Pleistocene landslide deposits, hachures indicate location of head scarp (0-50 m).

Qc Holocene and Pleistocene colluvium (0-5 m).

Qfy Holocene and upper? Pleistocene younger alluvial-fan deposits (0-15 m).

Qty Holocene and upper? Pleistocene younger terrace deposits (0-10 m).

Qfo Holocene and Pleistocene older alluvial-fan deposits (0-20 m).

Qto Holocene and Pleistocene older terrace deposits (0-10 m).

QTgy Pleistocene to Pliocene? younger ridge-capping gravel (0-15 m).

QTgo Pleistocene to Pliocene? older ridge-capping gravel (0-30 m).

Sediment of Bannock Pass (middle Miocene)

Ts3 Tan, thinly-bedded siltstone and fine sandstone with thin conglomerate lenses; locally contains debris flows and is typically extensively burrowed - **Ts3b** (lighter upper unit 0-70 m), **Ts3a** (darker lower unit 0-90 m). Appears to have passively infilled a preexisting basin.

Sediment of Everson Creek (late Eocene? - early Miocene)

Ts2 Late Eocene? to early middle Miocene - Dominantly white to light tan, massive to thinly-bedded tuffaceous siltstone, fine to coarse sandstone, interbedded pebble conglomerate and coarse gravel (0-950 m).

Tls3 Limestone unit - Thin, localized limestone and calcareous sandstone (0-12 m).

sh Shale unit - White to tan wood-bearing shale (0-3 m).

ss/ Tss2 Sandstone unit - Arkosic sandstone and conglomerate; (local two-mica-bearing sandstone; 0-200 m).

Tg2 Middle gravel unit - Well rounded, quartzite-clast gravel confined to a paleovalley (0-270 m).

Tmb Megabreccia unit - Possible rock avalanche deposits (0-35 m).

Tsu Middle Eocene? to Miocene? sediment undifferentiated - Likely deposited during extension on the Little Eightmile Creek fault (0-1000 m).

Sediment of Bear Creek (middle Eocene - Oligocene?)

Ts1 Dominantly pebble to boulder gravel with interbedded fine sandstone and lacustrine limestone (0-1000 m).

Tg1 Older gravel unit - Coarse, far-travelled, volcaniclastic and quartzite-clast gravel (0-390 m).

Tls2 Lacustrine limestone unit - Laterally continuous, gastropod-bearing limestone (typically silicified; 0-40 m).

ss Sandstone unit (0-5 m).

Tls1 Lacustrine limestone unit - Laterally continuous, gastropod-bearing limestone (typically silicified; 0-50 m).

Challis Volcanic Group (middle Eocene)

Tcqs Sanidine-quartz welded tuff - White, tan, or orange, densely welded, rhyolitic ash flow tuff. Appears to be confined to a paleovalley. 46.0 ± 0.39 Ma (M'Gonigle and Dalrymple, 1993; 0-3.5 m).

Tcdl Dacite lava interbedded with unit Tcqs (0-560 m).

Tcr Tuff of Curtis Ranch - White to greenish-white or yellow, biotite-bearing ash flow (Tcr) and air fall (Tcr2) tuff (0-105 m).

Tcs Volcaniclastic sandstone and conglomerate (0-50 m).

Tcl Lava flow - Dark colored aphanitic flows and flow breccias with thin intercalated tuffs and small lahar deposits (0-1100 m).

Tclt Lithic-rich tuff - Brown, tan, white, pink, or orange welded ash flow tuff containing abundant rhyolite lithics with minor amounts of dark grey quartzite lithics in an ash matrix (0-1250 m).

Tcbt Biotite tuff - White to yellow, air fall and ash-flow tuff containing abundant biotite crystals and pumice shards in an ash matrix (0-670 m).

Tcg2 Conglomerate - Poorly sorted, well-rounded pebbles, cobbles and boulders up to 3 meters in diameter interbedded with unit Tcq and confined to an east flowing paleovalley (0-30 m).

Tvt1 Ash flow tuff - Lithic-rich ash flow tuff found between units Tcq and the vitric tuff of Lemhi Pass in the Lemhi Pass quadrangle (S. U. Janecke, unpublished mapping; Staatz, 1979; 0-150 m)

Tcq Quartzite-bearing rhyolite tuff - White, pink, or light grey tuff containing abundant black quartzite lithics. 48.64 ± 0.33 Ma (M'Gonigle and Dalrymple, 1993, 0-440 m).

Tcg1 Basal conglomerate - Well-rounded pebbles and cobbles in a coarse sand and white tuffaceous matrix. Quartzite clasts dominate, with tuffaceous pebbles locally present in minor amounts (0-45 m).

Tcu Challis undifferentiated - Poorly exposed and/or highly variable volcanic rocks.

Pre-Tertiary rocks

Mu Mississippian limestone undifferentiated (0-470 m).

Os Ordovician Summerhouse Formation - Light grey to white quartzites (0-10 m).

Y Middle Proterozoic sandstone and quartzite - This unit is undifferentiated, and most likely contains portions of the Lemhi and Missoula Groups (< 12000 m; Hansen, 1983).

Ag Archean gneiss - granitic gneiss and metasedimentary rocks.

Intrusions

Tbi Basaltic intrusion - Dark grey to black, aphanitic to porphyritic olivine(?) pyroxene basalt. 47.3 ± 0.2 Ma ($^{40}Ar/^{39}Ar$ matrix concentrate; S. U. Janecke and W. C. Mcintosh, unpublished data, 1996)

Td Diorite - Greenish-grey, medium-grained porphyritic biotite, augite, hornblende diorite.

Tli /Tcli Extrusion / intrusion (Eocene? to Oligocene?) - Typically brecciated and intense weathered, grey, dark grey, or hematitic red andesitic flows or shallow intrusions

Ti /Tci Intrusion (age unknown) - Grey, dark grey, or hematitic red andesitic intrusions.

Tcd Quartz latite (age unknown) - Pink to purplish-brown, light grey, or brown, porphyritic quartz latite.

Tkdb Diabase (age unknown) - dark to light green, fine-crystalline diabase.

Contact, dashed where uncertain, dotted where concealed

Bedding traces

Normal fault, dashed where uncertain, dotted where concealed. Bar and ball on downthrownside.

Low-angle normal fault, dashed where uncertain, dotted where concealed. Block on downthrown side.

Low-angle oblique normal fault, dashed where uncertain, dotted where concealed. Block on downthrown side. Arrows show relative horizontal movement.

Thrust fault, dashed where uncertain, dotted where concealed. Triangles on upthrown side.

Lineament

Anticline; axial arrow indicates plunge direction.

Syncline; axial arrow indicates plunge direction.

34 Strike and direction of dip of bedding

34 Strike and direction of dip of bedding compiled from previous workers (see index for sources).

34 Strike and direction of dip of bedding determined by three-poi solutions.

(1) Sample site for provenance data collection. Numbers correspond to sample site numbers in appendix.

[1] Sample site for $^{40}Ar/^{39}Ar$ geochronology

A——A' Cross-section locations

Seismic profile locations

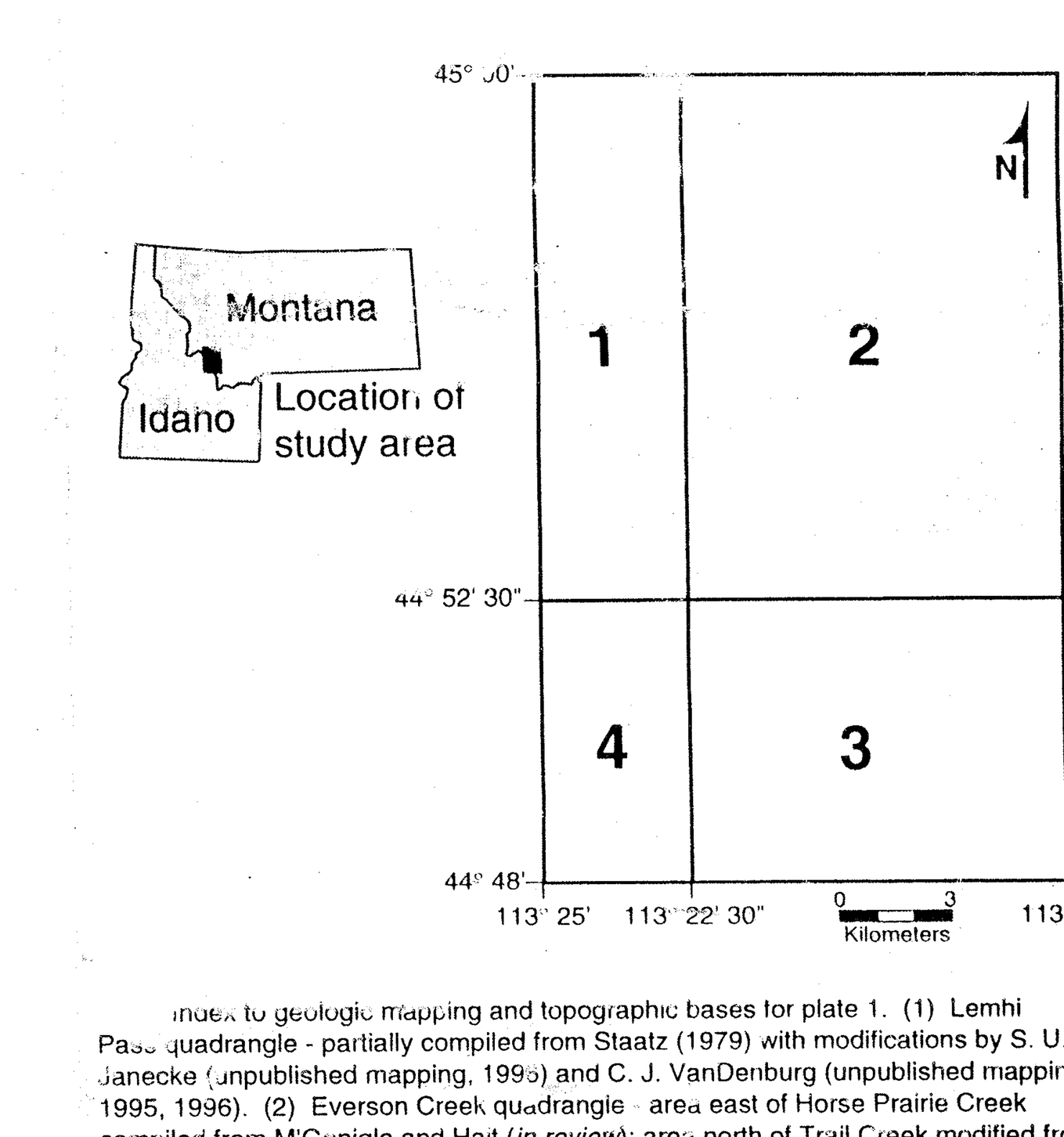

Index to geologic mapping and topographic bases for plate 1. (1) Lemhi Pass quadrangle - partially compiled from Staatz (1979) with modifications by S. U. Janecke (unpublished mapping, 1995) and C. J. VanDenburg (unpublished mappin 1995, 1996). (2) Everson Creek quadrangle - area east of Horse Prairie Creek compiled from M'Gonigle and Hait (*in review*); area north of Trail Creek modified fr Hansen (1983); remainder of quadrangle mapped by C. J. VanDenburg (unpublish mapping, 1995, 1996) and S. U. Janecke (Unpublished mapping, 1995, 1996). (3) Bannock Pass quadrangle - mapped by C. J. VanDenburg (unpublished mappi 1995, 1996). (4) Goat Mountain quadrangle - partially compiled from Staatz (1973 with modifications by C. J. VanDenburg (unpublished mapping, 1995, 1996).

Sample	Rock unit	Age	Method	Source
1	Tbi	47.3 ± 0.4 Ma	$^{40}Ar/^{39}Ar$ whole rock	S. U. Janecke and W. C. McIntosh, unpublished data, 1996
2	TKdb	200-600 (?) Ma (very disturbed spectrum)	$^{40}Ar/^{39}Ar$ whole rock	S. U. Janecke and W. C. McIntosh, unpublished data, 1997
3	Tclt		$^{40}Ar/^{39}Ar$ whole rock	work in progress
4	Tcbt		$^{40}Ar/^{39}Ar$ whole rock	work in progress
5	Tcr	47.53 ± 0.6 Ma	$^{40}Ar/^{39}Ar$ single crystal, sanidine	S. U. Janecke and W. C. McIntosh, unpublished data, 1997
6	Tli	45.7 (?) Ma (total gas age from a disturbed spectrum)	$^{40}Ar/^{39}Ar$ whole rock	S. U. Janecke and W. C. McIntosh, unpublished data, 1997
7	Tls1	52-36.6 Ma	invertebrate fauna (mollusks)	Steve Good, written comm., 1996
8	Ts2	30-19 Ma	vertebrate fauna	Ralph Nichols, written comm., 1996 Fields et al., 1985
9	Ts2	22.8 Ma	tephra correlation	S. U. Janecke, Michael Perkins, and Sarna-Wojocki, unpublished data, 1
[illegible]	Ts2		$^{40}Ar/^{39}Ar$ whole rock	work in progress
11	Ts2	19-16.4	vertebrate fauna	Ralph Nichols, written comm., 1996 Fields et al., 1985
12	Ts3b	16.4-11.7 Ma	vertebrate fauna	Ralph Nichols, written comm., 1996 Fields et al., 1985

Plate 2. Geologic cross-sections

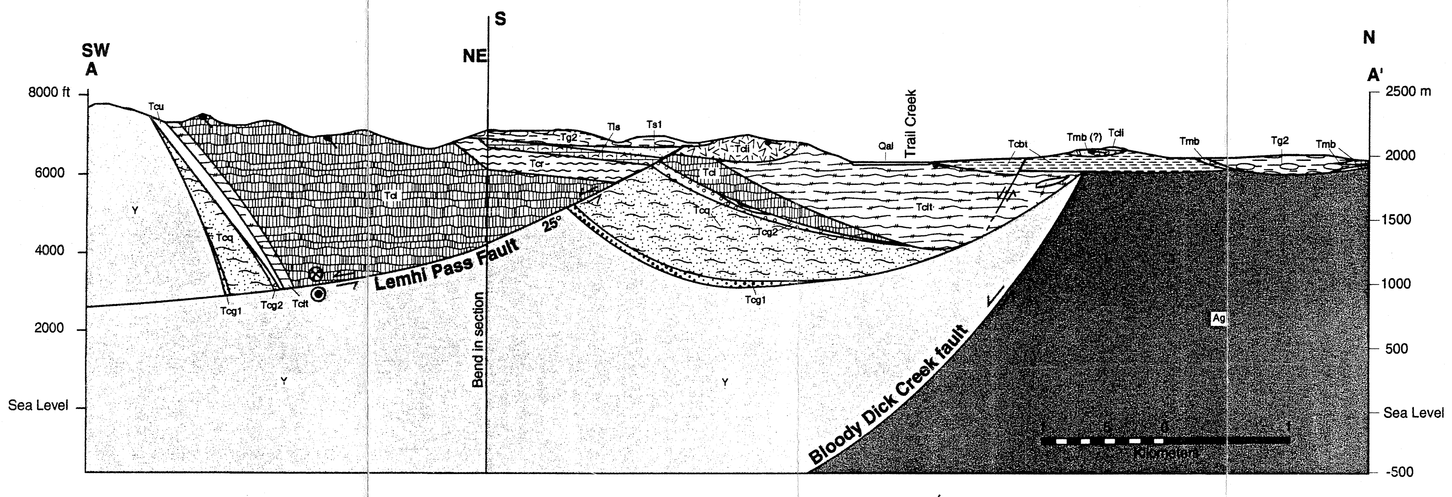

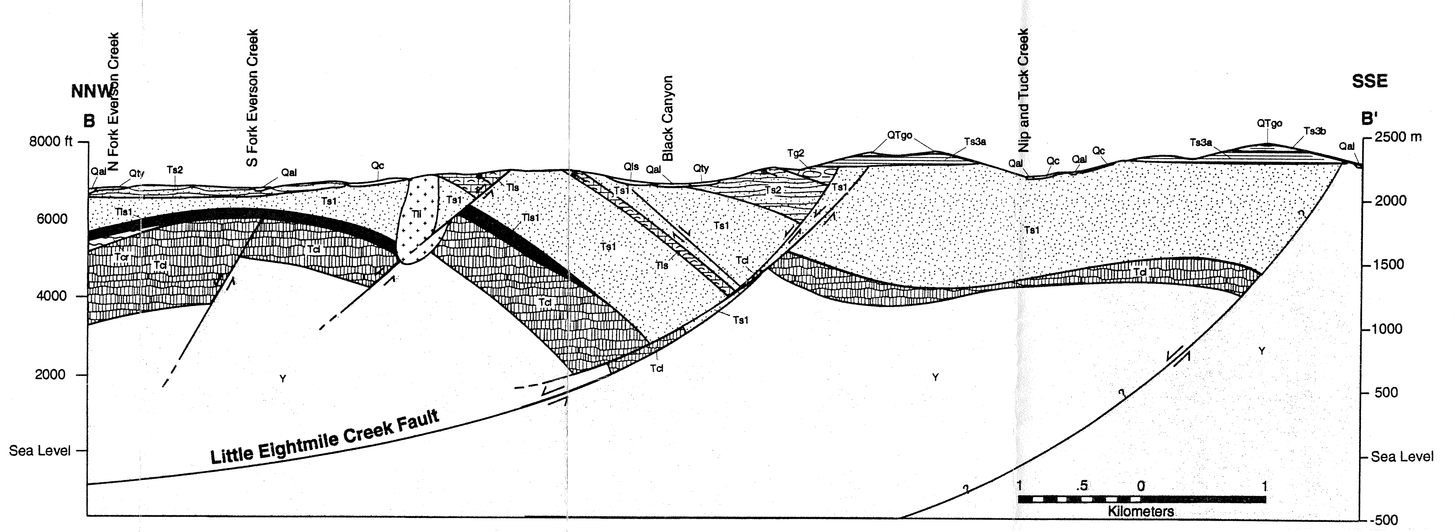

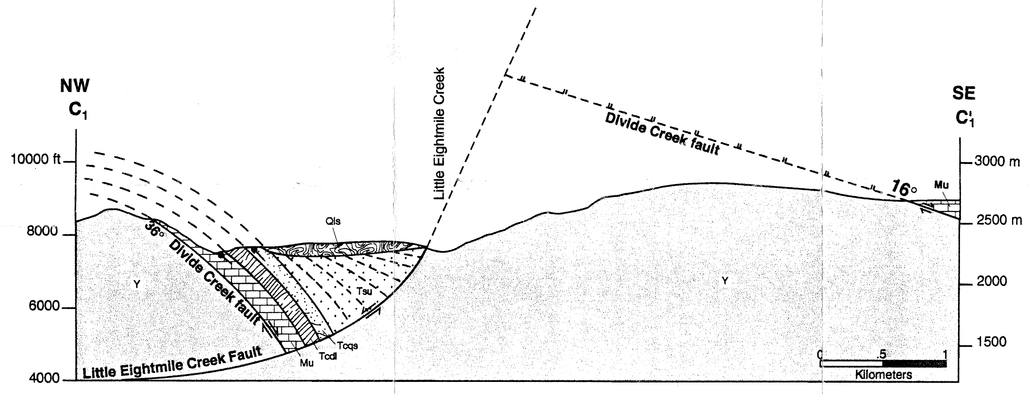

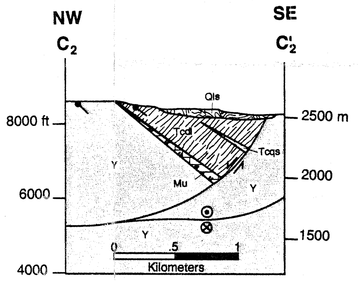

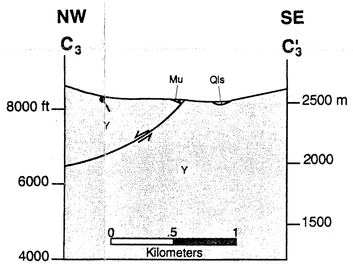

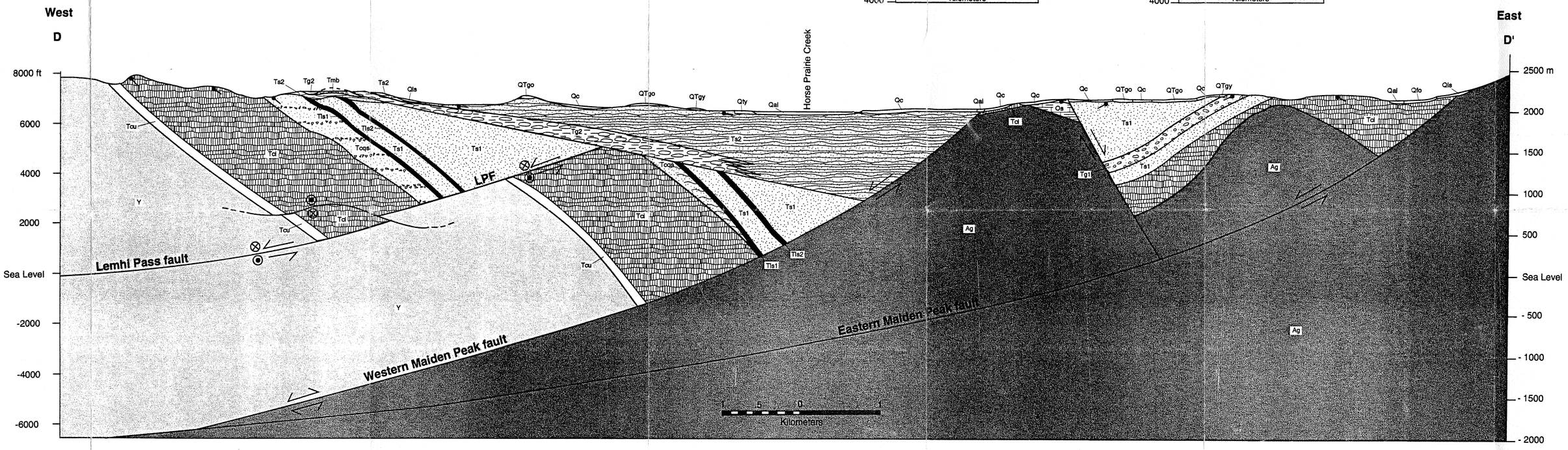

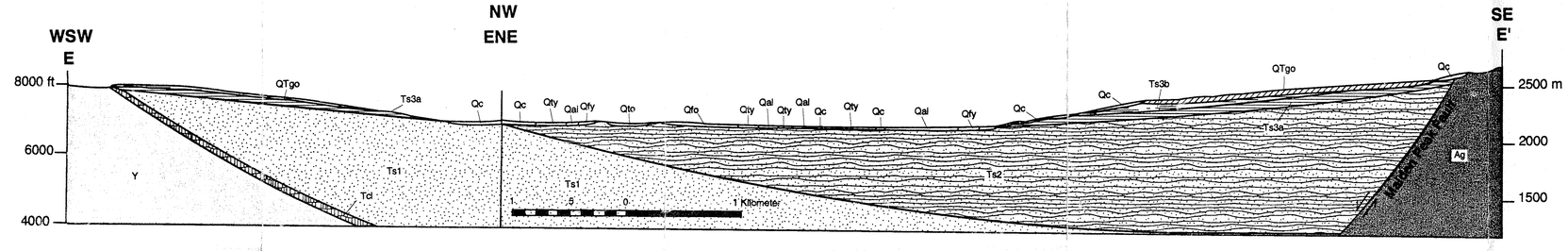

Qal - alluvium
Qc - colluvium
Qfy - younger alluvial fan deposit
Qty - younger alluvial terrace deposit
Qfo - older alluvial fan deposit
Qto - older alluvial terrace deposit
Qls - landslide
QTgy - younger ridge-capping gravel
QTgo - older ridge-capping gravel
Tbi - basaltic intrusion
Tii - extrusion / intrusion within Tertiary sediment
Ti / Tci - intermediate intrusive rock
Tcli - extrusion / intrusion within Challis volcanic rocks
Ts3b - upper unit of the sediment of Bannock Pass
Ts3a - lower unit of the sediment of Bannock Pass
Ts2 - sediment of Everson Creek
Tls3 - upper limestone unit
Tss - sandstone unit
Tg2 - gravel unit
Tmb - megabreccia unit
Tsu - sediment undifferentiated
Ts1 - sediment of Bear Creek
Tg1 - gravel unit

Tls - freshwater limestone undifferentiated
Tls2 - middle limestone unit
Tls1 - lower limestone unit
Tcqs - sanidine-quartz welded tuff
Tcdl - dacite lava flow
Tcr - tuff of Curtis Ranch
Tcs - volcaniclastic sandstone and conglomerate
Tcl - lava flow
Tcbt - biotite tuff
Tclt - lithic-rich tuff
Tcg2 - conglomerate
Tcq - quartzite-bearing rhyolite tuff
Tcg1 - basal conglomerate
Tcu - Challis volcanic rocks undifferentiated
Mu - Mississippian limestone undifferentiated
Os - Ordovician Summerhouse Formation
Y- Middle Proterozoic quartzite and siltite
Ag - Archean gneiss

Fault - '⊗' indicates movement into the plane of cross-section; '⊙' indicates movement out of the plane of cross-section
Fault - arrows indicate relative vertical movement
Contact - dashed where projected above the ground surface

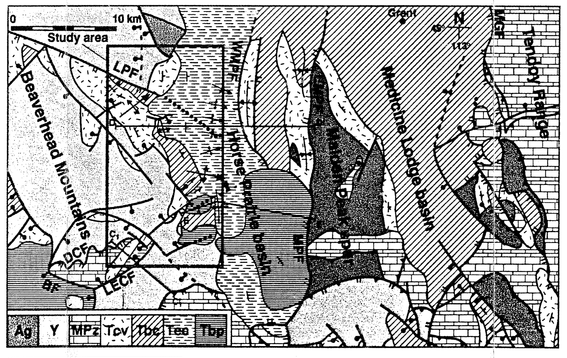

1) B. U. Janecke, unpublished mapping
2) Hansen (1983)
3) J. W. M'Gonigle and W. J. Perry, Jr., unpublished mapping
4) Staatz (1979)
5) This study, see map index, Plate 1
6) M'Gonigle and Hait (in press)
7) M'Gonigle et al. (1991)
8) Dubois (1982)
9) Staatz (1973)
10) M'Gonigle (1994)
11) M'Gonigle (1993)
12) Dunlap (1962)
13) C. J. VanDenburg, unpublished mapping
14) Skipp (1988)
15) Lucchitta (1966)
16) Landis (1963)

Generalized geologic map showing location of cross-section lines extending beyond study area (C-C', D-D', E-E'), and sources for data used in cross-section construction.